

**ISOLATION, IDENTIFICATION, AND QUANTITATION OF BIOMOLECULES  
USING HIGH PERFORMANCE LIQUID CHROMATOGRAPHY AND MASS  
SPECTROMETRY**

by

LANDON RAY GREENE

A dissertation submitted to the  
Graduate School-New Brunswick  
Rutgers, The State University of New Jersey

In partial fulfillment of the requirements

For the degree of

Doctor of Philosophy

Graduate Program in Chemistry and Chemical Biology

Written under the direction of

Professor Jeehiun K. Lee

And approved by

---

---

---

---

New Brunswick, New Jersey

OCTOBER, 2014

## **ABSTRACT OF THE DISSERTATION**

### **Isolation, Identification, and Quantitation of Biomolecules using High Pressure Liquid Chromatography and Mass Spectrometry**

By LANDON RAY GREENE

Dissertation Director:  
Professor Jeehiun K. Lee

The research performed in this dissertation involved isolation, identification, and quantitation of biomolecules using high pressure liquid chromatography and mass spectrometry.

NanoRNAs, 2 – 4 nucleotide RNA oligomers, have been shown to prime transcription initiation in vivo. However, the particular oligonucleotides and absolute abundance could not be determined without the use of specific and sensitive analytical techniques. The goal of this research was to develop an analytical procedure to isolate, identify, and quantify nanoRNAs, in vivo, in *Escherichia coli* cells. A sequence of experiments was performed. A high performance pressure liquid chromatography (a.k.a. high pressure liquid chromatography) method was developed to isolate nanoRNA oligomers. This method was coupled with tandem mass spectrometry for detection. The combined HPLC-MS/MS method identified nanoRNAs in *E. coli* cell cultures. Experiments were performed to optimize the extraction of RNA oligomers from cell cultures to improve quantitation. An optimized extraction procedure and solid phase

extraction method were developed which provided reproducible and quantitative analysis of nanoRNAs. The analysis of 5', 3'-hydroxyl uridine-adenosine and 5', 3'-hydroxyl uridine-adenosine-uridine was performed in *E. coli* cells. The results supported the qualitative hypothesis concerning the presence of these nanoRNAs. However, the absolute quantitation of nanoRNAs had significant error.

Other research in this dissertation involved proteins. A novel monoclonal antibody, Das-1, was generated during ulcerative colitis research. This antibody has been used as a biomarker of various pre-cancerous and cancerous conditions of the gastrointestinal tract. However, the properties and structure of the specific antigen of mAb Das-1, a colonic epithelial protein (CEP), are unknown. The goal was to develop an isolation procedure to purify CEP. A three step procedure was developed. First, a size exclusion method was used to provide purification of CEP based on size. Second, a strong anion exchange method separated CEP based on overall surface charge. Finally, a hydrophobic interaction chromatography method provided purification based on hydrophobicity. The sequential purification of CEP using the three step procedure developed was tracked using several immunoassays. The results demonstrated significant purification of CEP.

## **DEDICATION**

To my parents, Lance and Marie; my wife, Jessica; and my daughter, Cora.

## **ACKNOWLEDGEMENTS**

I would like to acknowledge my advisor, Dr. Jeehiun K. Lee, for her support and guidance over these years. I would also like to thank Dr. Gene Hall and Dr. Karsten Krogh-Jespersen for serving as mentors. Another thank you goes to Dr. Brian Buckley from Environmental & Occupational Health Sciences Institute, for serving on my committee and for allowing the use of precious instrumentation in these studies.

I would like to thank my collaborators for working patiently with me on very interesting research projects: Dr. Kiron M. Das, MD, Dr. Xin Geng, MD, Dr. Bryce E. Nickels, and Dr. Seth Goldman.

I would like to thank the following previous and current members of the Lee group: Min Liu, Mu Chen, Kai Wang, Anna Michelson, Sisi Zhang, Yuan Tian, Hao Zeng, Julianne Davis and Yijie Niu for their friendship and help.

I am very grateful to my parents, brothers and family for their unconditional support and love.

# TABLE OF CONTENTS

ABSTRACT OF THE DISSERTATION .....	ii
DEDICATION .....	iv
ACKNOWLEDGEMENTS .....	v
TABLE OF CONTENTS .....	vi
LIST OF FIGURES .....	viii
LIST OF TABLES .....	xii
Chapter 1. Introduction .....	1
1.1 Overview .....	1
1.1.1 Identification and Quantitation of NanoRNAs in Bacteria Cells .....	1
1.1.2 Isolation of Colonic Epithelial Protein from Human Colon Cells. ....	6
1.2 Instruments .....	9
1.2.1 High Pressure Liquid Chromatography .....	9
1.2.2 Electrospray Ionization Mass Spectrometry .....	11
1.2.3 Quadrupole Ion Trap Mass Spectrometers .....	13
1.3 Methodology .....	15
1.3.1 High Pressure Liquid Chromatography Separations .....	15
1.3.2 HPLC Tandem Mass Spectrometry .....	22
Chapter 2. Development of an HPLC Method for the Separation of NanoRNAs .....	25
2.1 Introduction .....	25
2.2 Experimental .....	27
2.3 Results and Discussion .....	28
2.3.1 Evaluation of HPLC Stationary Phases .....	28
2.3.2 Evaluation of HPLC Mobile Phase Conditions. ....	32
2.3.3 Optimized HPLC Conditions .....	35
2.4 Conclusion .....	36
Chapter 3. Identification of NanoRNAs in <i>Escherichia coli</i> Cells using HPLC Tandem MS	37
3.1 Introduction .....	37
3.2 Experimental .....	39
3.3 Results and Discussion .....	41
3.3.1 Mass Spectrometer Fragmentation Patterns of RNA Oligonucleotides .....	41
3.3.2 Analysis of NanoRNAs in <i>Escherichia coli</i> Cells .....	46
3.4 Conclusion .....	50

Chapter 4.	Selection of <i>Escherichia coli</i> Cell Extraction Procedures and Sample Preparation Conditions for Routine Analysis.....	51
4.1	Introduction.....	51
4.2	Experimental.....	52
4.3	Results and Discussion .....	54
4.3.1	E. coli Cell Culture NanoRNA Extraction Selection.....	54
4.3.2	Development of a Solid Phase Extraction Method.....	59
4.3.3	SPE Recovery of NanoRNAs from E. coli Cell Cultures.....	63
4.4	Conclusions.....	67
Chapter 5.	Validation of a HPLC-MS/MS Method for Quantitative Analysis of NanoRNAs in <i>Escherichia coli</i> Cell Cultures.....	69
5.1	Introduction.....	69
5.2	Experimental.....	70
5.3	Results and Discussion .....	72
5.3.1	HPLC-MS/MS Method Validation Experiments.....	72
5.3.2	Preliminary Quantitative E. coli Cell Culture Analysis.....	77
5.3.3	Quantitative Analysis of NanoRNAs in E. coli Cell Cultures .....	82
5.4	Conclusions.....	89
Chapter 6.	Development of a Protocol for the Isolation, Purification and Identification of a Colonic Epithelial Protein.....	91
6.1	Introduction.....	91
6.2	Experimental.....	92
6.3	Results and Discussion .....	94
6.3.1	Size Exclusion/Gel Filtration Isolation .....	94
6.3.2	Strong Anion Exchange Isolation .....	96
6.3.3	Hydrophobic Interaction Chromatography Isolation .....	102
6.4	Conclusion .....	105
REFERENCES	.....	106

## LIST OF FIGURES

Figure 1: Basic structures of RNA and DNA oligonucleotides.....	2
Figure 2: Transcription in prokaryotic cells (bacteria). ....	3
Figure 3: NanoRNAs prime transcription initiation in vivo <sup>16</sup> . ....	5
Figure 4: Pentamer structure of IgM.....	7
Figure 5: Lesional fluid, from the pancreas, immunoreactivity against mAb Das-1 by ELISA <sup>28</sup> .....	8
Figure 6: High pressure liquid chromatography schematic. ....	10
Figure 7: Electrospray ionization diagram.....	12
Figure 8: Quadrupole ion trap mass spectrometer diagram. ....	13
Figure 9: Chromatographic retention factor diagram and equation.....	16
Figure 10: Chromatographic resolution diagram and equation. ....	17
Figure 11: Chromatographic efficiency diagram and equation. ....	18
Figure 12: Comparison of HILIC to traditional modes of chromatography <sup>61</sup> . ....	19
Figure 13: Oligonucleotide fragmentation nomenclature. ....	23
Figure 14: NanoRNA accumulation in <i>Pseudomonas aeruginosa</i> <sup>87</sup> .....	25
Figure 15: Structures of representative nanoRNAs. ....	26
Figure 16: Separation of nanoRNAs by strong anion exchange chromatography.....	29
Figure 17: Separation of nanoRNAs by reverse-phase ion pairing chromatography. ....	30
Figure 18: Separation of nanoRNAs by HILIC chromatography (pH 2). ....	31
Figure 19: Separation of nanoRNAs by HILIC ion-pairing chromatography (pH 2).....	33
Figure 20: Comparison of nanoRNA separation by HILIC ion-pairing chromatography, pH 2 vs. pH 5. ....	34



Figure 21: Chromatographic overlay of RNA di- & tri-nucleotides separated by HILIC ion-pairing chromatography.....	35
Figure 22: Transcription start site shifting in <i>Escherichia coli</i> <sup>88</sup> . ....	37
Figure 23: Example UV chromatographic of <i>E. coli</i> cell culture lysate using the developed HPLC method.....	38
Figure 24: Mass fragmentation of 5', 3'-hydroxyl uridine-adenosine.....	42
Figure 25: Mass fragmentation of 5', 3'-hydroxyl cytidine-adenosine. ....	43
Figure 26: Mass fragmentation of 5', 3'-hydroxyl guanosine-guanosine.....	43
Figure 27: Mass fragmentation of 5', 3'-hydroxyl uridine-adenosine-uridine .....	44
Figure 28: Mass fragmentation of 5', 3'-hydroxyl uridine-adenosine-adenosine .....	45
Figure 29: Overlay of product ion scan, 880 m/z to 574 m/z (top), and UV chromatogram, 254nm (bottom), for 75 fmoles UAU. ....	46
Figure 30: Comparison of mass chromatographs for wild type and <i>nrnB</i> active <i>E. coli</i> samples.....	48
Figure 31: LC-MS/MS chromatograms of UAU in <i>E. coli</i> cultures, evaluation of various extraction procedures. ....	56
Figure 32: Standard addition linear regression for 'MS-4' extraction cell cultures. ....	57
Figure 33: Standard addition linear regression for MS-1 extraction cell cultures.....	58
Figure 34: LC chromatographs of fractions collected from solid phase extraction of nanoRNAs with the Oasis WAX cartridge. ....	60
Figure 35: LC chromatographs of fractions collected from solid phase extraction of nanoRNAs with the MAX cartridge. ....	61

Figure 36: LC chromatographs of fractions collected from solid phase extraction of nanoRNAs with the C18 cartridge.....	62
Figure 37: Standard addition linear regression for MS-3 extraction in E. coli cultures. ..	66
Figure 38: HPLC-MS/MS analysis of E. coli cell cultures for UAU (prepared in duplicate).....	67
Figure 39: High throughput DNA sequencing, transcription start site shift summary <sup>90</sup> ..	70
Figure 40: Thermo Finnigan LTQ linear regression results. ....	74
Figure 41: Second preliminary analysis standard addition curves for E. coli cell cultures. ....	81
Figure 42: NanoRNA quantitation results of ‘Analysis 1’ stationary phase cultures.....	83
Figure 43: NanoRNA quantitation results, Analysis 1, log vs. stationary phase.....	84
Figure 44: Summarized results: Quantitation of nanoRNAs in E. coli cell cultures. ....	89
Figure 45: Gel filtration chromatographic overlay of protein molecular weight markers and colon cell supernatant.....	95
Figure 46: ELISA analysis of gel filtration fractions from separation of colon cell supernatant. ....	96
Figure 47: HPLC-UV chromatographs, at 280nm, of a strong anion exchange method separating ‘gel filtration fractions’ and colon cell supernatant.....	97
Figure 48: ELISA analysis of strong anion exchange (up to 500mM NaCl) fractions from separation of colon cell supernatant and gel filtration pooled samples. ....	98
Figure 49: HPLC-UV chromatographs, at 280nm, of a strong anion exchange method (up to 1M NaCl) separating alcohol dehydrogenase and colon cell supernatant. ....	99

Figure 50: ELISA analysis of strong anion exchange (up to 1mM NaCl) fractions from separation of colon cell supernatant and gel filtration pooled samples. ....	100
Figure 51: Western blot analysis of the pooled fractions after strong anion exchange analysis (A, B, & C) compared to ‘Before SAX’ and controls.....	101
Figure 52: Silver staining after two isolation steps (A, B, & C) compared to the original colon cell supernatant. ....	102
Figure 53: Overlaid chromatographs of protein markers separated by hydrophobic interaction chromatography, at 280 nm. ....	103
Figure 54: ELISA analysis of hydrophobic interaction chromatography fractions from separation of isolated fraction ‘A’ (CEP after two steps). ....	104

## LIST OF TABLES

Table 1: Parent-to-daughter ion transitions for several nanoRNAs.....	46
Table 2: UAU analysis (standard addition) in E. coli cell cultures: wild type and nrnB..	49
Table 3: E. coli extraction methods for nanoRNAs.....	55
Table 4: Results of UAU analysis in E. coli using various extraction procedures. ....	56
Table 5: Solid phase extraction recovery of nanoRNAs in E. coli cell culture extracts...	65
Table 6: Thermo Finnigan LTQ linearity raw data.....	73
Table 7: Reproducibility and limit-of-detection/limit-of-quantitation analysis for the LTQ system. ....	75
Table 8: Injection repeatability on the LCQ system. ....	76
Table 9: Injection Repeatability on the Qtrap system.....	77
Table 10: Preliminary analysis of E. coli cell cultures (in triplicate). ....	78
Table 11: Second preliminary analysis of various cell cultures (in triplicate). ....	80
Table 12: Summary of ‘Analysis 1’ results. ....	85
Table 13: ‘Analysis 2’ standard addition linear regression R <sup>2</sup> values.....	86
Table 14: Control Injections of ‘Analysis 2’ .....	86
Table 15: Summarized results of ‘Analysis 3’ .....	88
Table 16: Summarize results: Quantitation of nanoRNAs in E. coli cell cultures. ....	88

## Chapter 1. Introduction

### 1.1 Overview

#### *1.1.1 Identification and Quantitation of NanoRNAs in Bacteria Cells*

Ribonucleic acids (RNA) are one of the two types of nucleic acids<sup>1</sup> found in all cells. The other type is deoxyribonucleic acids (DNA) which are differentiated by a 2'-substitution. The role of RNA in the coding, decoding, regulation, and expression of genes in cells is vital. Not only is RNA necessary for life but also has been used for treatment of human diseases<sup>2</sup>. The role of RNA in medicine was deemed so significant Dr. Craig Mello<sup>3</sup> and Dr. Andrew Fire<sup>4</sup> received a Nobel Prize in 2006 for their discovery of RNA interference, gene silencing by double-stranded RNA. The future impact of RNA in medicine and science has led to a surge in research around RNA's roles in cells<sup>5,6</sup>.

RNA's primary structure consists of a series of nucleoside monomer units bound to each other through 3'→5' phosphodiester linkage, Figure 1. Each monomer consists of a five membered D-pentofuranose sugar (β-D-ribose in RNA) connected to a heterocyclic nucleobase by an N-glycosidic bond. The four primary bases of RNA are adenine, cytosine, guanine, or uracil. Adenine and guanine are purines. Cytosine and uracil are pyrimidines. Other RNA monomers with modified nucleobases<sup>7</sup> and 2' substituents are found in cells, but will not be discussed in this research. The 5' and 3' caps of RNA oligonucleotides are typically triphosphates, monophosphates or hydroxyl groups depending on the function of the chain.

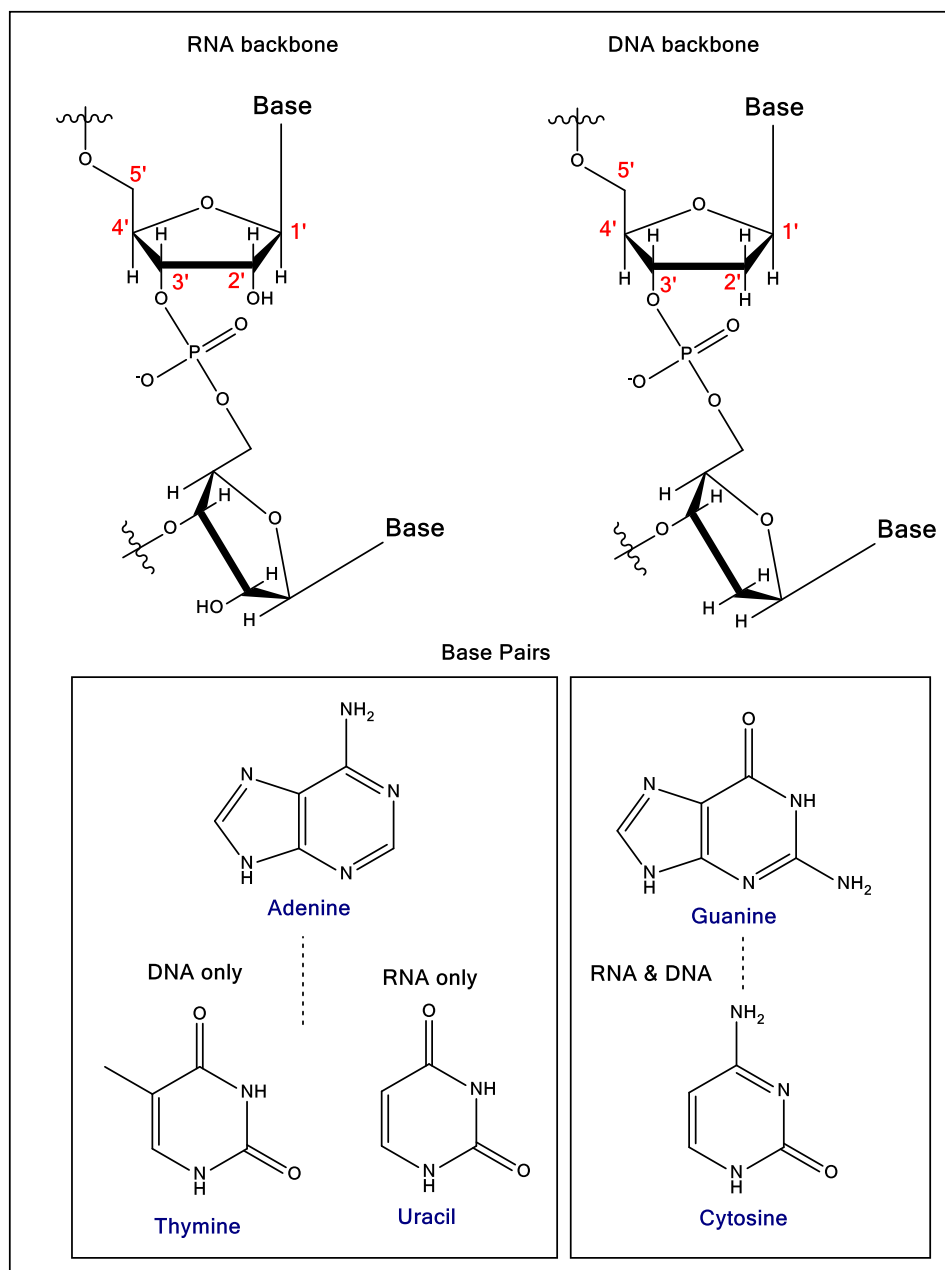


Figure 1: Basic structures of RNA and DNA oligonucleotides.

Based on the role and structure, RNA can be classified into three primary types: ribosomal (rRNA), messenger (mRNA) and transfer RNA (tRNA). However, other types of RNA exist which also play important roles in cells<sup>8,9</sup>. Messenger RNA is transcribed from DNA and then carries that genetic information on to ribosomes where it is used to sequence amino acids. These amino acids are then incorporated into protein synthesis.

The research we present here focused on the transcription process of DNA to mRNA in prokaryotes. Transcription is the synthesis of mRNA by the copying of the template strand of double-stranded DNA. RNA nucleotides are connected one by one to form base pairs with the DNA template strand bases (Figure 2). The direction of RNA synthesis is from 5' to 3' and is the opposite direction of the DNA template strand. This process occurs in four major steps: binding, initiation, elongation and termination.

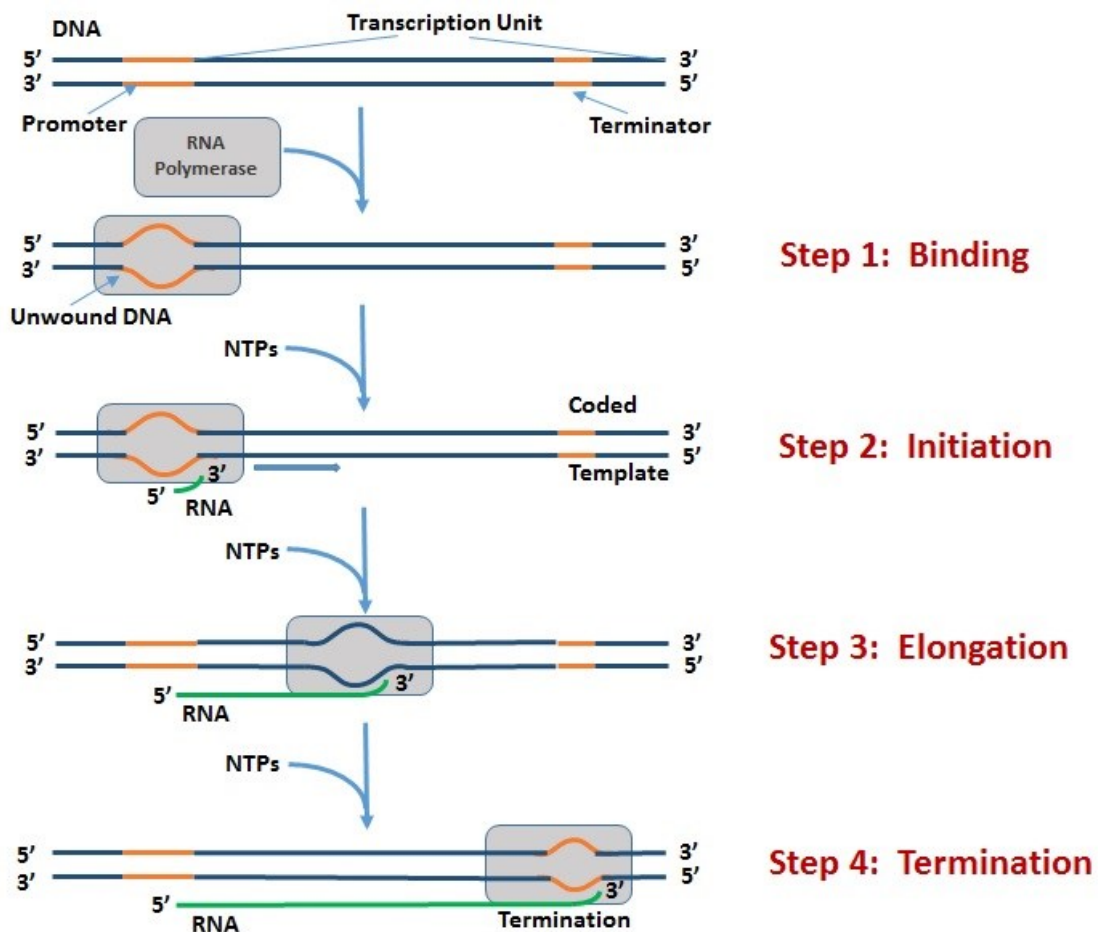


Figure 2: Transcription in prokaryotic cells (bacteria).

Prokaryotic initiation begins with the binding of RNA polymerase to the promoter region in DNA<sup>10</sup>. RNA polymerase which is an enzyme consisting of five polypeptide subunits: 2  $\alpha$  subunits, 1  $\beta$  subunit, 1  $\beta'$  subunit, and 1  $\omega$  subunit associates with a sigma factor (a co-enzyme)<sup>11</sup>. The combined RNA polymerase holoenzyme identifies the appropriate -35 and -10 base pairs downstream of the promoter DNA sequence. Once bound, the RNA polymerase holoenzyme mediates a nucleotide triphosphate to prime transcription. At this point small sequences of RNA may be produced, referred to as an abortive transcript<sup>12</sup>, which are discarded when the size gets around 23 base pairs. Abortive initiation ceases once the holoenzyme distorts in a way to allow propagation and then, step 3, elongation occurs<sup>13</sup>. Elongation starts from the initial NTPs priming the sequence and as the RNA polymerase travels along the template strand complimentary base pairs are matched and the mRNA sequence is synthesized. Termination, step 4, of mRNA synthesis, in prokaryotes, is believed to occur in one of two ways. One theory is a G-C-rich hairpin loop is formed and causes stress on the RNA-DNA hybridization resulting in termination<sup>14</sup>. The other theory is a protein called “Rho” destabilizes the interaction between the template and the mRNA resulting in termination<sup>15</sup>. Following termination the synthesis of mRNA is complete. Research by our collaborators, Dr. Bryce Nickels and Dr. Seth Goldman, have challenged the theory that only NTPs are responsible for priming transcription initiation (step 2, Figure 3<sup>16</sup>) in vivo and proved that it was possible for “nanoRNAs”, ~2 – 4 nucleotide RNAs, to serve as primers to initiate transcription also.

As illustrated in Figure 3, they have been able to prove that by depleting the amount of an oligoribonuclease<sup>17</sup>, Orn, in *Pseudomonas aeruginosa* leads to an



accumulation of nanoRNAs. Using high-throughput sequencing, they were able to show that this nanoRNA accumulation corresponded to an increase in transcription start site

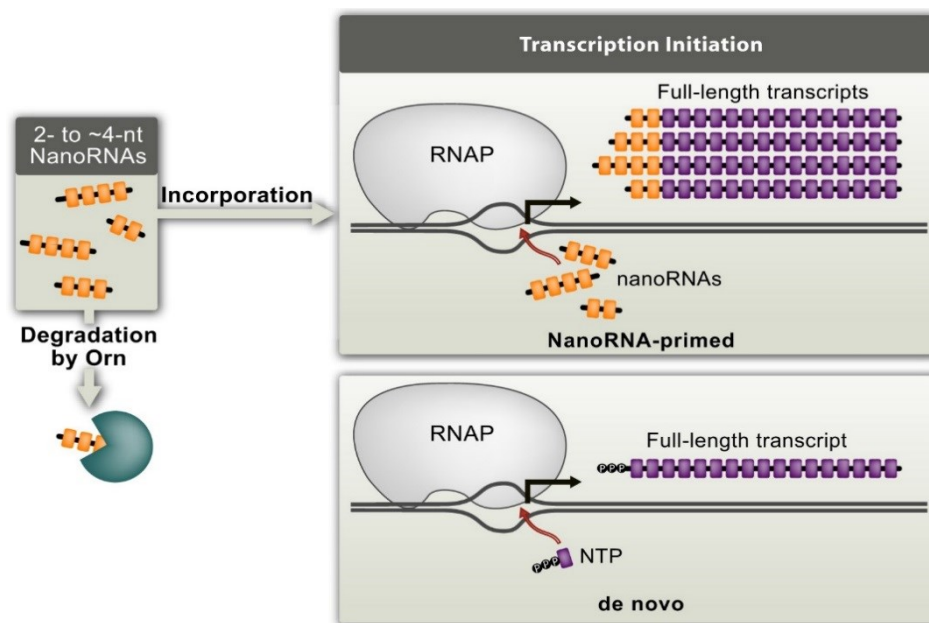


Figure 3: NanoRNAs prime transcription initiation in vivo<sup>16</sup>.

shifting. The transcription start site shifting generated altered full-length transcripts in vivo. This observation led to experiments to evaluate this nanoRNA priming effect on global gene expression in the cells. Using microarray analysis, they were able to compare the global gene expression profile of Orn-depleted cells to the global gene expression profile of non-depleted cells. The results identified 1158 genes (~20% of known genes in *Pseudomonas aeruginosa*) whose expression was altered. This research demonstrated nanoRNAs can prime transcription initiation in vivo and have an effect on global gene expression.

The next step in this research was to determine the absolute abundance of nanoRNA species responsible for the observed priming events. High-throughput sequencing yields a relative abundance for several nanoRNA species; yet, absolute abundance could only be determined by mass spectrometry. The focus of the research

detailed here was the development of a procedure for purifying nanoRNA in bacteria cell samples, isolating specific nanoRNA species using liquid chromatography, and utilizing tandem mass spectrometry to perform absolute quantitation of specific RNA oligomers. In Chapter 2 and Chapter 3, the development of a LC-MS/MS method capable of analyzing various nanoRNAs species is detailed. Then the ability of this method to detect the presence of a RNA oligomer, in vivo, in Escherichia Coli cells is demonstrated. Chapter 4, focuses on the optimization of the sample preparation of Escherichia coli cells for analysis. Finally, Chapter 5 details validation of the LC-MS/MS quantitative ability and highlights some semi-quantitative results achieved in vivo.

### ***1.1.2 Isolation of Colonic Epithelial Protein from Human Colon Cells.***

Proteins are large biological molecules made up of hundreds to thousands of amino acids in a specific sequence. The sequence of amino acids (20 primary types in humans) defines the 3-dimensional structure and function of each protein<sup>18</sup>. Within living organisms, some protein functions include antibody response, catalyzing reactions, replicating genetic material, and transporting molecules<sup>19</sup>. The specific proteins studied in this research are an antibody-antigen pair. Antibodies, also called immunoglobulins, are large Y-shaped proteins which bind preferentially to specific antigens. In mammals, antibodies are differentiated into five isotypes: IgA, IgD, IgE, IgG, and IgM. These isotypes differ in their biological properties, functional locations and response with different antigens. The IgM antibody, the focus of this research, is typically found as a pentamer (also a hexamer) immunoglobulin<sup>20</sup>. The pentamer version consists of five immunoglobulins covalently linked together with disulfide bonds and a J-chain (polypeptide), see Figure 4. The 10 binding sites of IgM give it high avidity. The

specific IgM, mAb-Das 1, used in this research was developed by our collaborator, Kiron Das<sup>21</sup>.

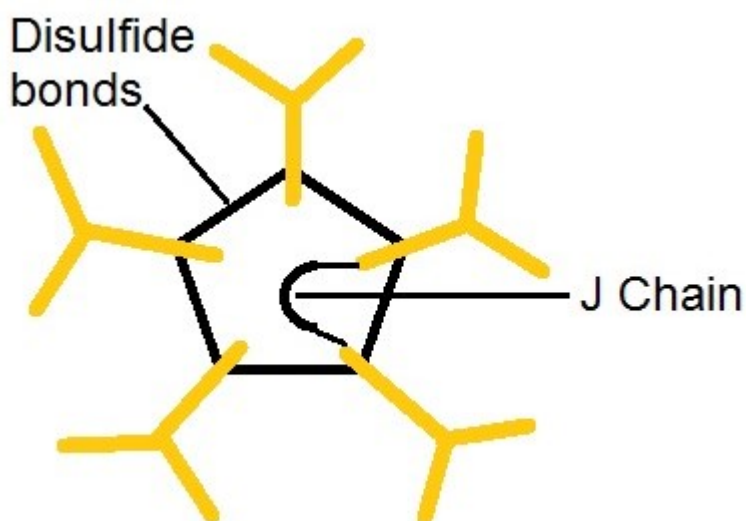


*Figure 4: Pentamer structure of IgM.*

mAb-Das 1 (IgM 7E<sub>12</sub>H<sub>12</sub>) was discovered by performing a hybridoma experiment on a ~40k Da protein found in colon cells of ulcerative colitis patients. Following its discovery this novel antibody has been extensively researched for reactivity with cells of many organs. In particular, mAb-Das 1 reacts specifically with colonic epithelial cells but not with thirteen other epithelial organs<sup>22</sup>. The observed reactivity is attributed to the binding of another antigen in colonic epithelial cells<sup>23</sup>. This colon epithelial antigen, ~200k Da, is called the colon epithelial protein (CEP) as the structure remains unknown<sup>24</sup>. Interestingly, CEP expression is found in fetal tissues of the esophagus, stomach, small bowel and bladder<sup>25</sup>. However, CEP is not found in these organs in adults, only in the colon epithelial cells. More importantly, CEP is expressed in precancerous and cancerous conditions, including Barrett's esophagus<sup>26</sup>/esophageal adenocarcinoma and gastric intestinal metaplasia<sup>27</sup>/gastric adenocarcinoma. More

Figure 5: Lesional fluid, from the pancreas, immunoreactivity against mAb Das-1 by ELISA<sup>28</sup>.

mAb Das-1 reactivity with a specific antigen, CEP, has been established as an important biomarker in various precancerous and cancerous conditions of the gastrointestinal tract. Our goal, in the research presented here, was to isolate and identify CEP. With its identity we could gain further insight into the role CEP has in these precancerous and cancerous conditions. Although CEP is readily found in normal colon epithelial cells, isolating enough to study has been challenging. In Chapter 6, the development of an isolation procedure for this unknown colon epithelial protein will be discussed. This work will show the use of several chromatographic techniques to effectively clean-up the sample and isolate CEP.

## **1.2 Instruments**

### ***1.2.1 High Pressure Liquid Chromatography***

High-performance liquid chromatography (HPLC) is an analytical technique used to separate solubilized compounds<sup>29</sup>. HPLC, like other forms of chromatography, separates compounds based on their difference in relative affinities for the mobile and stationary phases used. Depending on the stationary phase, the mechanism of separation can be based on size, adsorption, partition, affinity or ion exchange<sup>30</sup>. Some typical uses for HPLC include assessing the purity of a substance<sup>31</sup>, tracking chemical reactions<sup>32</sup>, isolating a particular compound<sup>33</sup> and characterizing certain properties of compounds<sup>34</sup>.

The instrumentation consists of a pumping system, an injector, a chromatographic column, stationary and mobile phases, connecting tubing and fittings, a detector and a data collection device (computer, integrator or recorder). A schematic of the typical instrument layout is shown in Figure 6.

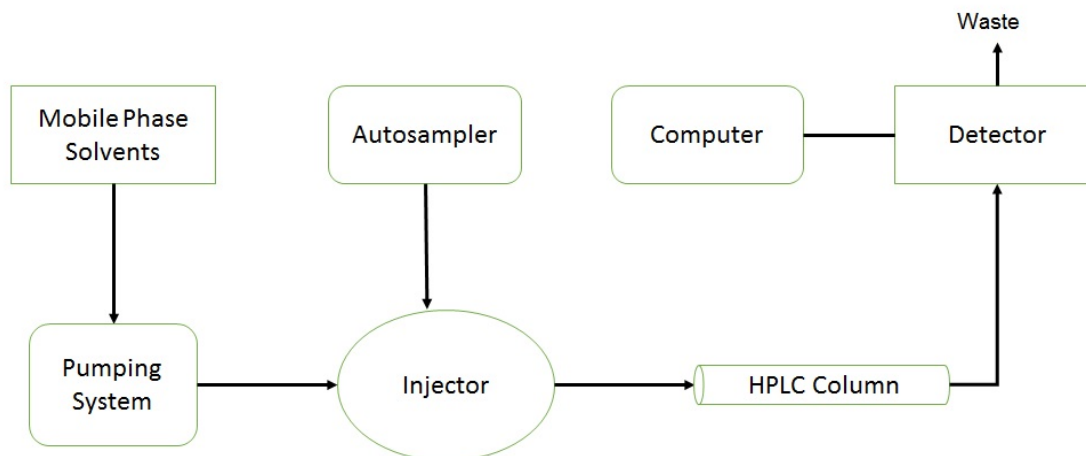


*Figure 6: High pressure liquid chromatography schematic.*

Although every part of the instrumentation can significantly affect a separation, more consideration is given to the column (stationary phase), mobile phase and detector when developing a HPLC method.

The column stationary phase, is typically a polymer or stainless steel tube that may be filled with a variety of packing materials<sup>35</sup>. Both the size of the column and the type of packing material affect the separation. The size is typically between 25 and 300 mm long with an internal diameter between 2 and 10 mm. There are many types of stationary phase packing materials used in HPLC including, but not limited to:

- unmodified silica, alumina or porous graphite (normal-phase chromatography)
- chemically modified supports of polymers, silica, or porous graphite (reversed-phase chromatography)
- resins or polymers with acid or basic groups (ion-exchange chromatography)
- porous silica or polymers (hydrophilic interaction chromatography)

The selection of the chromatography column is specific to the type of molecules which need to be separated or isolated. The main classes of molecules are typically broken down into large (>2000 Da) versus small (<2000 Da) and polar/charged versus non-polar<sup>36</sup>. Although, other classes of molecules can also be separated such as chiral molecules.

The choice of mobile phase(s) is based on the physicochemical properties of the analyte(s), the desired retention behavior, the mode of chromatographic separation and the detector. Mobile phases usually consist of aqueous and/or organic solvents and various types of buffers.

Many types of detectors can be coupled with HPLC in-line or off-line. The most traditional detector is the UV/vis spectrophotometer<sup>37</sup>. However, depending on the information needed and the molecular properties of the analytes various other detectors may be used, such as: fluorescence spectrophotometers<sup>38</sup>, differential refractometers (RI)<sup>39</sup>, electrochemical detectors<sup>40</sup>, evaporative light-scattering detectors (ELSD), charged aerosol detectors (CAD)<sup>41</sup>, and mass spectrometers (MS)<sup>42</sup>. Off-line detection can also be performed by collecting time-based fractions from the HPLC effluent.

### ***1.2.2 Electrospray Ionization Mass Spectrometry***

Electrospray ionization (ESI) is an ionization technique which operates under atmospheric pressure (API)<sup>43</sup>. Electrospray mass spectrometer ion sources are capable of producing charged ions without fragmenting the parent analytes. The ions produced can then be detected by various types of mass analyzers, some examples are: linear quadrupole ion trap, three-dimensional quadrupole ion trap, orbitrap<sup>44</sup>, time-of-flight mass analyzer<sup>45</sup>, and ion cyclotron resonance mass analyzer. In a typical

experiment, a dilute (less than mM) analyte solution is introduced to the source either from a syringe pump or as the eluent flow from HPLC. This flow passes into the electrospray needle, or capillary, at a flow rate of  $\sim 1 - 1000 \mu\text{L}/\text{min}$ . The electrospray needle has a high potential difference (2–6 kV) applied to it relative to the counter electrode (source cone or capillary). This strong electric field produces a ‘Taylor cone’ and begins the spraying of charged droplets from the needle with a surface charge of the same polarity to the charge on the needle<sup>46</sup>. As the charged droplets work through the electric field de-solvation occurs with the assistance of a coaxial nitrogen gas. The process of de-solvation is shown in Figure 7<sup>47</sup>.

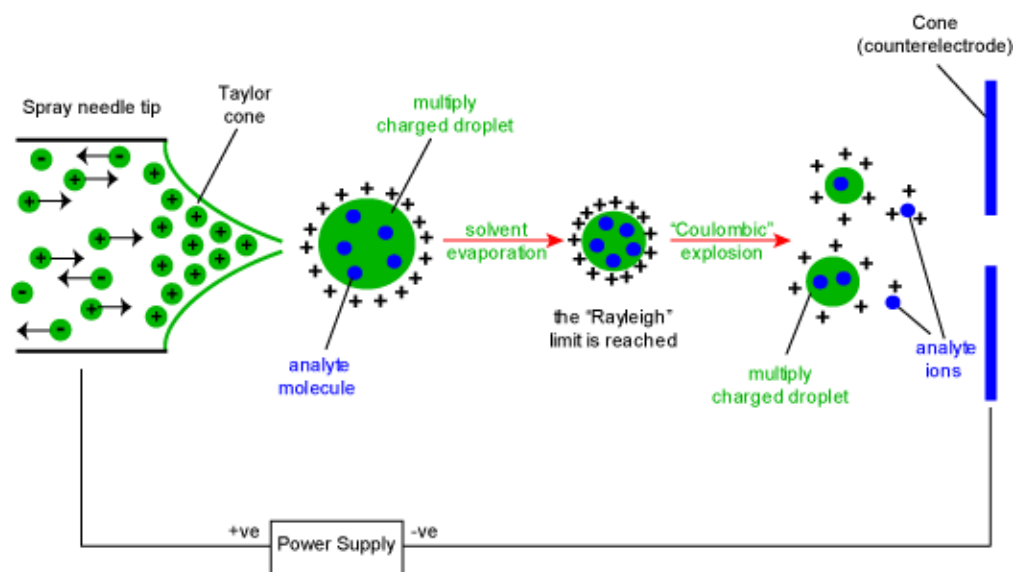


Figure 7: Electrospray ionization diagram.

Heated nitrogen slowly evaporates the charged droplets until the ‘Rayleigh’ limit is reached. This limit is the maximum charge a droplet can hold at a specific volume. Once the limit is reached a “Coulombic” explosion occurs resulting in smaller charged droplets<sup>48</sup>. This process is repeated until the charged species, droplets or analytes, reaches the counter electrode. At which point the mass analyzer, under high vacuum,



collects and further de-solvates the charged analytes. The de-solvation process detailed is not an energetic process, but rather it effectively cools the gaseous ions. When appropriate instrumental conditions are used some of the analyte ions remain intact (no fragmentation) and can be analyzed along with specific fragments. The electrospray ionization process has been used for analysis of many types of molecules including, but not limited to: proteins, peptides<sup>49</sup>, oligonucleotides<sup>50</sup>, polymers and pharmaceuticals<sup>51</sup>.

### 1.2.3 *Quadrupole Ion Trap Mass Spectrometers*

Quadrupole ion trap (QIT) mass spectrometers<sup>52-53</sup> are found in two forms: linear<sup>54</sup> and 3-dimensional<sup>55</sup>. Both varieties are widely used throughout analytical chemistry labs in academia and industry. The basic mechanism behind QIT mass spectrometers is the trapping of ions from a source using a combination of a constant DC and an oscillating AC to generate an electric field. QITs are known for their moderate sensitivity, larger mass range (6000 m/z) and their MS<sup>n</sup> capabilities. Throughout this research several QIT mass spectrometers were used; both linear and 3-dimensional forms.

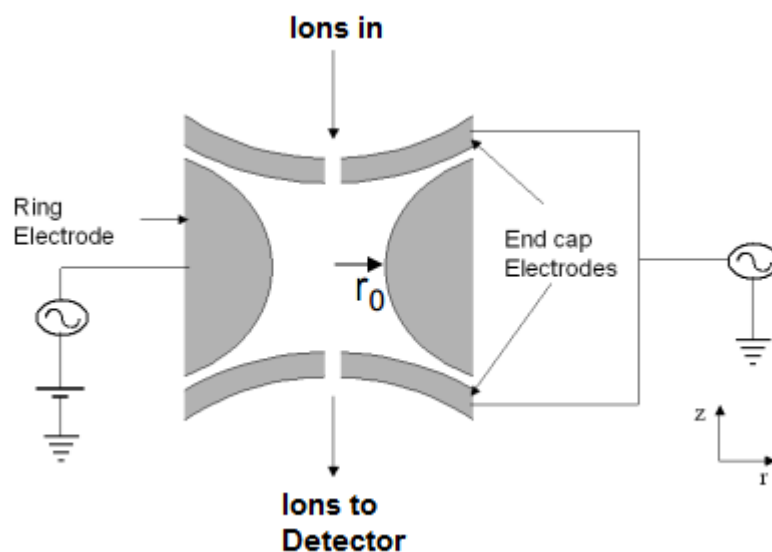


Figure 8: Quadrupole ion trap mass spectrometer diagram.

In Figure 8 is a schematic of the set-up of a 3-dimensional ion trap mass analyzer. Ions produced in the source of the instrument are introduced to the ion trap through the inlet. The inlet is capable of focusing specific ions prior to the trap. As the ions enter the trap they are selected by the action of the three electrodes: the ring electrode and two end cap electrodes. The ions are trapped in the space between these three electrodes by AC (oscillating) and DC (static) electric fields. The resulting oscillating cloud of ions follows a stable trajectory. The specific ion trajectory is dependent on the voltages applied and their individual mass-to-charge ( $m/z$ ) ratios. Ion detection occurs when the potentials are altered to destabilize the ion motions. This results in ejection of the ions through the exit end cap, usually performed in order of increasing  $m/z$ . As the ions are ejected, detection of the ions occurs.

The 3-dimensional quadrupole ion trap mass spectrometer used in this research was the Thermo Finnigan LCQ equipped with an electrospray ionization source. The instrument was directly connected to the effluent of a Waters 2695 Alliance HPLC. This mass spectrometer was used primarily for initial screening. The use of this system was not ideal for quantitative analysis given the set-up of the source to the ion trap. As the spray of the source was aligned with the inlet of the ion trap which caused significant background noise from non-ionized species.

In contrast to the 3-D quadrupole ion trap, the linear ion trap can be used as a selective mass filter (quadrupole), or as an actual trap by creating a potential well for the ions along the axis of the electrodes. The linear ion trap uses a set of quadrupole rods to confine ions radially and a static DC potential end cap electrodes to confine the ions axially. The process of selecting or ejecting ions is similar to that of the 3D ion trap.

Advantages of the linear trap are increased ion storage capacity, faster scan times, and simplicity of construction.

In this research, two linear ion traps were utilized: Thermo Finnigan LTQ and AB Sciex 4000 Qtrap. The LTQ is a traditional linear ion trap. The Qtrap is a hybrid triple quadrupole/linear ion trap. This instrument is set-up like a triple quadrupole mass spectrometer with a quadrupole-collision cell-quadrupole design. However, the last quadrupole can also be utilized as a trap. Both mass spectrometers have superior sensitivity compared to the LCQ. Throughout this research, both instruments were used for RNA oligonucleotide analysis.

### **1.3 Methodology**

The methods used in this research include the high pressure liquid chromatography separations, tandem mass spectrometry analysis, sandwich ELISA and western blot immunoassay.

#### ***1.3.1 High Pressure Liquid Chromatography Separations***

HPLC employs a specific set of conditions (stationary phase and mobile phase) in order to achieve separation of molecules from each other. The degree of separation necessary and information obtained from the separation are typically unique to the application. In this research, HPLC separations were used in multiple situations. An HPLC method was developed in Chapter 2 to retain specific nanoRNA species and separate oligonucleotides of the same size from each other. This method also needed to be compatible with mass spectrometry. In Chapter 6, several different types of HPLC separations were utilized to isolate an unknown colonic epithelial protein(s). In all cases the basic principles of chromatography were used to achieve specific separations of

molecules. The underlying parameters used in assessing these separations were retention, resolution and efficiency.

Retention is the ability of the stationary phase to interact with molecules causing them to be retained on the column<sup>56</sup>. As shown in Figure 9, a retention factor ( $k$ ) can be

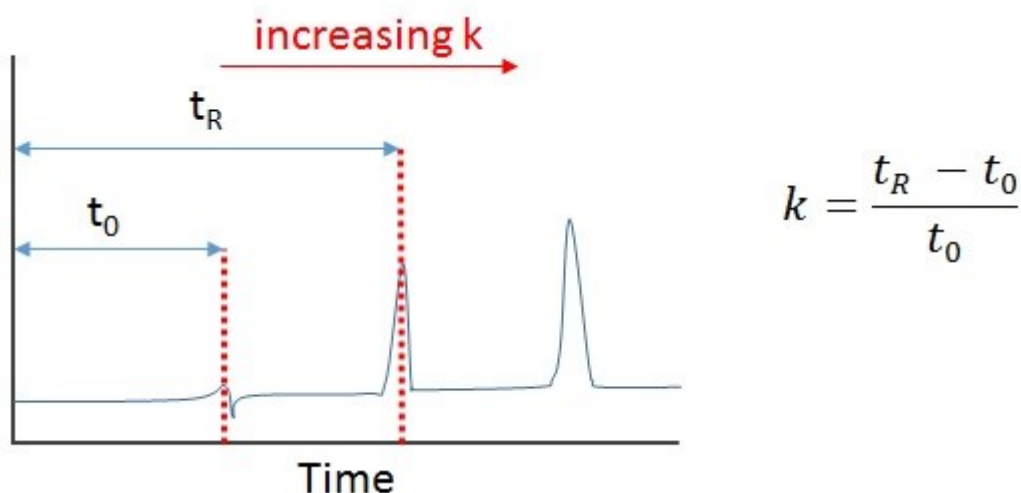


Figure 9: Chromatographic retention factor diagram and equation.

measured using the retention time ( $t_R$ ) and the void time ( $t_0$ ) according to the equation shown. The void time represents the time it takes for 1 column volume of liquid to pass through the column. Hence, a molecule is only retained if its  $t_R$  is greater than the  $t_0$ , or  $k$  is greater than 1. Retention was used throughout this research to determine whether the column was specific for the molecules we were interested in.

The other parameter we utilized in this research was resolution. Resolution is the calculation of the separation of two molecules in chromatography<sup>57</sup>. As shown in Figure 10, the resolution uses the peak widths at the baseline ( $w_b$ ) and retention times ( $t_R$ ) of two

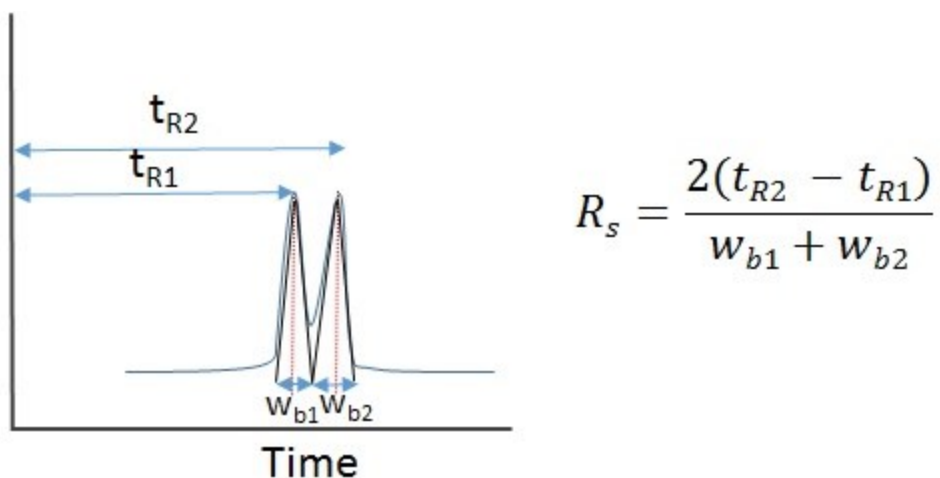


Figure 10: Chromatographic resolution diagram and equation.

peaks to determine the separation. A value of 1 or greater is usually desirable. Values of 2 or greater, typically are baseline resolved<sup>58</sup>. In our research resolution was used to determine separation of similar molecules and interference.

The last parameter used to evaluate the effectiveness of the separations in this research was efficiency. The efficiency of the separation is defined in terms of the theoretical plate number (N). A higher value of N means there is less dispersion of the analyte as it moves through the column resulting in a sharp peak over a narrow peak

width ( $w_b$ )<sup>58</sup>. The equation to calculate efficiency is found in Figure 11.

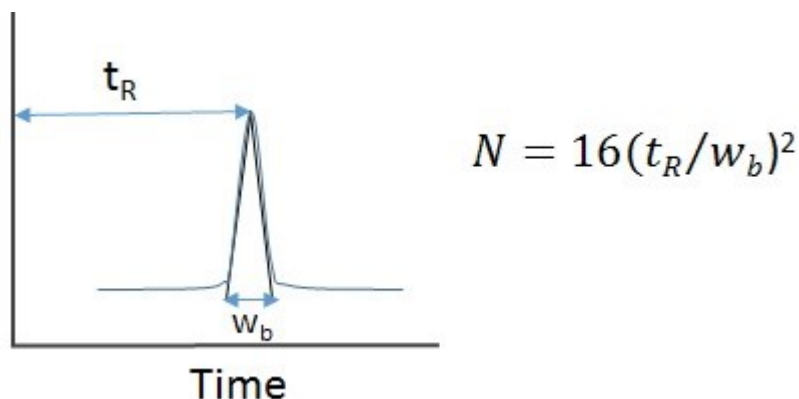


Figure 11: Chromatographic efficiency diagram and equation.

Efficiency is a relative term and was used in this research qualitatively to determine the success of the HPLC methods.

All three parameters were used to create HPLC methods which performed the desired separations in our research. Throughout this research several different HPLC separation techniques, or modes, were utilized. In particular, hydrophilic interaction liquid chromatography, size exclusion chromatography, ion exchange chromatography and hydrophobic interaction chromatography were used.

#### *Hydrophilic Interaction Liquid Chromatography*

Hydrophilic interaction liquid chromatography (HILIC)<sup>59-60</sup> is an emerging mode of HPLC column separation. It has been widely used to effectively separate small polar compounds and small charged compounds. Figure 12<sup>61</sup> shows how HILIC relates to the more traditional modes of chromatography: normal phase liquid chromatography (NP-LC)<sup>62</sup>, reverse phase liquid chromatography (RP-LC)<sup>63</sup> and ion chromatography (IC)<sup>64</sup>.

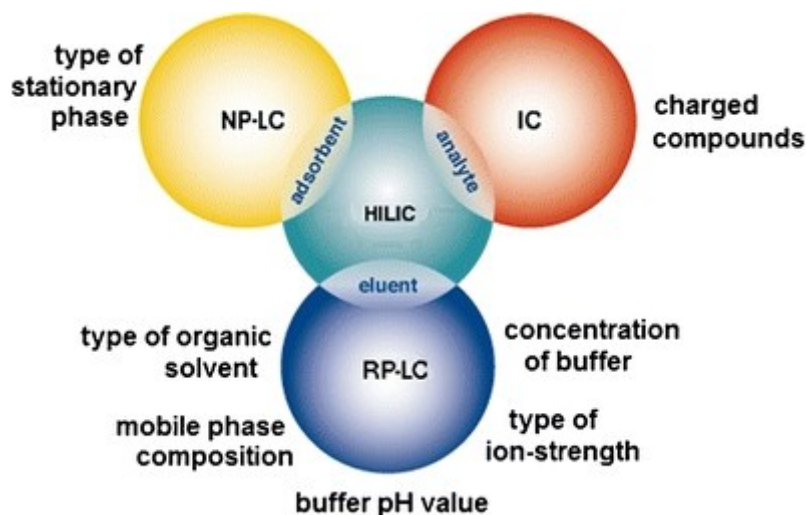


Figure 12: Comparison of HILIC to traditional modes of chromatography<sup>61</sup>.

HILIC separation uses polar, silica based stationary phases which are more traditionally associated with NP-LC. Yet, it uses mobile phases more common to RP-LC mode and can handle charged analytes which were formerly exclusive to ion chromatography. The flow chart below shows mobile phase solvents listed in order of increasing elution strength<sup>65</sup>.

*acetone < isopropanol acetonitrile < ethanol < dioxane < methanol < water*

This trend is opposite to RP-LC. A general HILIC method consists of an initial mobile phase composition of a high content of a water-miscible organic solvent, such as acetonitrile, with a small amount of water then a gradient shift to a high percent aqueous mobile phase composition. By employing this gradient small polar compounds should be retained longer than larger non-polar compounds. The exact mechanism of this separation is not known. Although, it is believed analytes partition between a water-rich layer on the surface of the polar stationary phase and the water-deficient mobile phase, creating a liquid/liquid extraction system<sup>66</sup>.

Our studies utilize HILIC chromatography for the separation of small, charged RNA oligonucleotides. These oligonucleotides are hydrophilic and the use of ion exchange<sup>67-68</sup> or reverse-phase ion pairing chromatography<sup>69</sup> was not desired. Also, HILIC chromatography uses a high organic content which makes this method of separation compatible with mass spectrometry<sup>59</sup>.

#### *Size Exclusion Chromatography/Gel Filtration*

Size exclusion chromatography (SEC), also known as gel filtration, separates molecules based on their size by filtration through a gel<sup>70-71</sup>. The gel consists of spherical beads containing pores of a specific size distribution. Separation occurs when molecules of different sizes are included or excluded from the pores within the matrix. Small molecules diffuse into the pores and their flow through the column is retarded according to their size, while large molecules do not enter the pores and are eluted in the column's void volume. Consequently, molecules are eluted in order of decreasing molecular weight (MW). Unlike other modes of chromatography, molecules do not bind to the chromatography medium so buffer composition does not directly affect resolution. A significant advantage of gel filtration is conditions can be varied to suit the type of sample or the requirements for further purification, analysis or storage without altering the separation<sup>72</sup>.

#### *Ion Exchange Chromatography*

Ion-exchange chromatography separates ions and polar molecules based on their affinity to charged support<sup>73</sup>. In cation exchange chromatography positively charged molecules are attracted to a negatively charged solid support. Conversely, in anion exchange chromatography, negatively charged molecules are attracted to a positively



charged solid support. The adsorption of the molecules to the solid support is driven by the ionic interaction between the oppositely charged ionic groups in the sample molecule and in the functional ligand on the support. The strength of the interaction is determined by the number and location of the charges on the molecule and on the functional group. By increasing the salt concentration (generally by using a linear salt gradient) the molecules with the weakest ionic interactions start to elute from the column first. Molecules that have a stronger ionic interaction require a higher salt concentration and elute later in the gradient. The binding capacities of ion exchange resins are generally quite high. To optimize binding of all charged molecules, the mobile phase is generally a low to medium conductivity (i.e., low to medium salt concentration) solution.

Sometimes pH can be manipulated to enhance resolution in ion exchange chromatography<sup>74</sup>. Generally, the pH of the mobile phase buffer must be between the pI (isoelectric point) or pKa (acid dissociation constant) of the charged molecule and the pKa of the charged group on the solid support. In cation exchange chromatography, raising the pH of the mobile phase buffer will cause the molecule to become less protonated and hence less positively charged. The result is that the protein no longer can form an ionic interaction with the negatively charged solid support, which ultimately results in the molecule to elute from the column. In anion exchange chromatography, lowering the pH of the mobile phase buffer will cause the molecule to become more protonated and hence more positively (and less negatively) charged. The result is that the protein no longer can form an ionic interaction with the positively charged solid support which causes the molecule to elute from the column.

Our research utilized strong anion exchange chromatography (SAX) to provide separation of proteins and nanoRNA oligonucleotides. In both uses, a quaternary ammonium support was used. For the nanoRNA retention, the phosphate backbone of the oligonucleotides was hypothesized to interact with the cationic support<sup>75</sup>. In protein purification, strong anion exchange chromatography was used to discrimination between the overall surface charges of the proteins<sup>76</sup>.

### *Hydrophobic Interaction Chromatography*

The principle of hydrophobic interaction chromatography is complementary to ion exchange and size exclusion chromatography<sup>77-78</sup>. Biomolecules containing hydrophobic and hydrophilic regions are applied to an HIC column in a high-salt buffer. The salt in the buffer reduces the solvation of the solutes. As solvation decreases, hydrophobic regions become exposed and are adsorbed to particle surface. The more hydrophobic the molecule, the less salt is needed to promote binding. A decreasing salt gradient is used to elute samples from the column in order of increasing hydrophobicity<sup>79</sup>.

### **1.3.2 HPLC Tandem Mass Spectrometry**

Tandem mass spectrometry (MS/MS) is a two-stage mass analysis technique<sup>80</sup>. This technique enables the analyst to produce ions in the source, observe the ions in a mass spectrum, fragment desired ions, and analyze the fragment ions produced. Tandem MS experiments are utilized to obtain additional structural information on a particular ionic species. This information can be helpful for several reasons. Tandem MS may be used to provide structure elucidation information. It may also be necessary in order to distinguish between multiple species with similar parent ion masses. Or it may enhance

the sensitivity of the mass analysis by discarding off unwanted ions in the first and/or second dimension.

In our studies, tandem MS was used to provide additional specificity and sensitivity. Tandem MS was used in the analysis of various nanoRNA species. The analysis of RNA oligonucleotides by electrospray ionization tandem MS has been previously reported<sup>81</sup>. In most of these cases the preferred electrospray polarity is negative ion mode<sup>82-83</sup>. This mode, typically, results in more intense signal since the phosphate backbone,  $pK_a \sim 1.5$ <sup>84</sup>, is negatively charged under most conditions evaluated. However, the RNA oligomers we are interested in, 2 – 4 mers, do not show a preference with regards to negative ion mode<sup>85</sup>. Positive ion mode results in a larger parent ion signal for most nanoRNAs studied in this research. The fragmentation of oligonucleotides has also been extensively studied<sup>86</sup>. In this research, previously

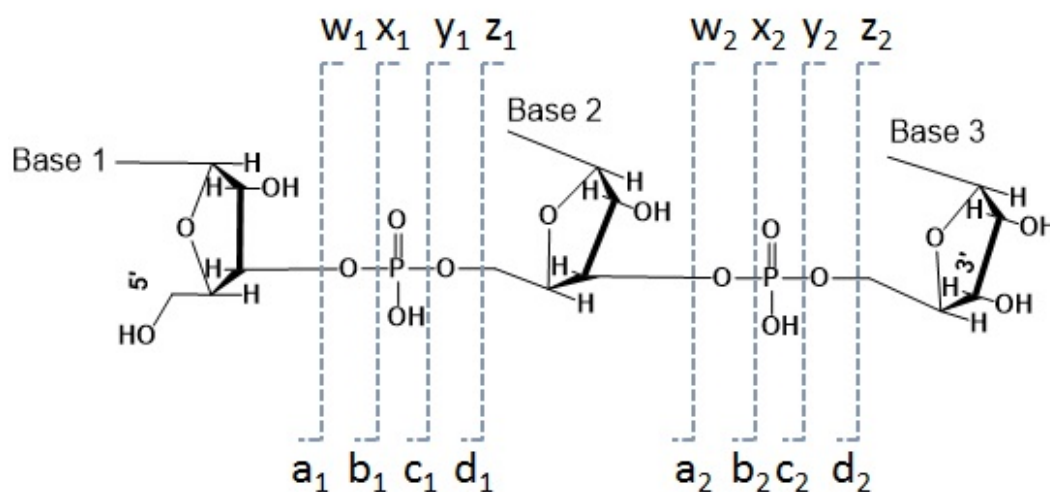


Figure 13: Oligonucleotide fragmentation nomenclature.

developed nomenclature<sup>86</sup> for identification of various fragment ions, as described in Figure 13, will be used.

## Chapter 2. Development of an HPLC Method for the Separation of NanoRNAs

### 2.1 Introduction

As previously discussed in Chapter 1, nanoRNAs can prime transcription initiation, in vivo, in bacterial cells<sup>87</sup>. Shown in Figure 14 are the first results obtained of nanoRNA accumulation, in vivo.

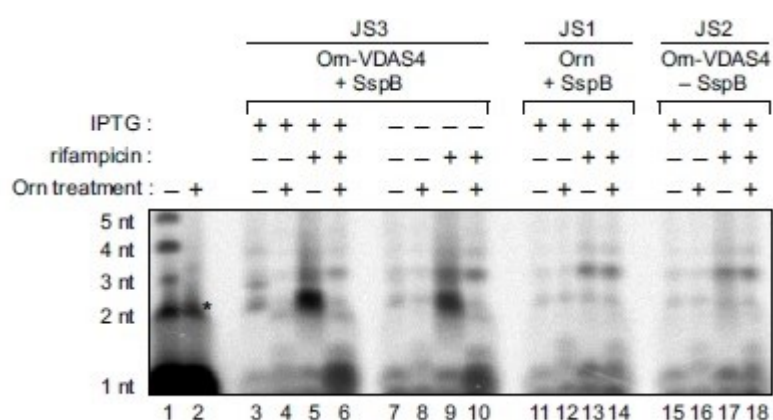
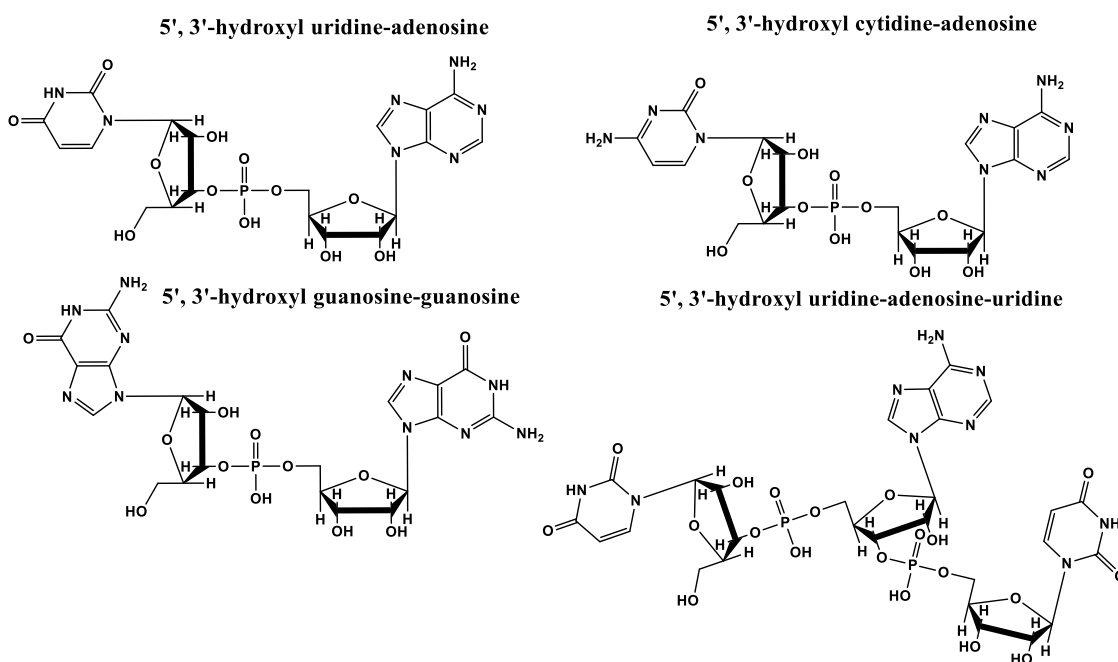


Figure 14: NanoRNA accumulation in *Pseudomonas aeruginosa*<sup>87</sup>

Data displayed in lanes 5 and 9 (JS3) demonstrate by suppressing natural oligoribonuclease activity, Orn<sup>88</sup>, and inhibiting transcription, rifampicin<sup>89</sup>, accumulation of nanoRNAs is possible in *Pseudomonas aeruginosa*. Subsequent orn treatment results in degradation of nanoRNAs (lanes 6 & 10), further demonstrating the presence of nanoRNAs. Accumulation was further supported by negative controls (JS1 & JS2). Not only does the data in Figure 14 demonstrate nanoRNA accumulation, but also defines the size to be primarily 2-3-nucleotides in length. These experimental results initiated the research detailed in this chapter. The goal of this research was to develop a HPLC method capable of isolating nanoRNAs from endogenous material and

providing separation of various di- and tri-nucleotides RNA oligomers from each other. This method also had to be compatible with mass spectrometry in order to achieve the desired sensitivity.

Figure 15 shows the structure of several nanoRNA oligomers which the HPLC method needed to separate.



*Figure 15: Structures of representative nanoRNAs.*

As noticed in Figure 15, the di-nucleotides and tri-nucleotides this research was focused on have a 5'-hydroxyl substituent. This observation was supported by high-throughput sequencing<sup>90</sup>. The primary goal of the HPLC method was to separate di-nucleotide and tri-nucleotide oligomers from each other, larger nanoRNAs, and endogenous material. Oligonucleotides have previously been separated using more established chromatographic methods of ion-pairing reversed phase chromatography<sup>69</sup> or anion-exchange chromatography<sup>67-68</sup>. However, the majority of RNA oligonucleotide

separation methods of these types focus on the separation of 5-mer nucleotide oligomers or larger. Research which does highlight these smaller species focuses more on purification and use of non-optimal conditions for mass spectrometry<sup>91</sup>. Another chromatographic method, HILIC, has emerged as a method of choice for mass spectrometry compatibility and separation of small polar or charged analytes<sup>59-61</sup>. Given our project challenges we hypothesized HILIC chromatography to be the optimal separation method. Not only should HILIC retain these di-nucleotides and tri-nucleotides species, but it also should not retain larger endogenous material such as proteins. The common mobile phases utilized in HILIC separations allows the method to be easily coupled with in-line electrospray mass spectrometry.

In this research, the separation methods of ion-pairing, anion exchange and HILIC chromatography were evaluated for analysis of several di-nucleotide and tri-nucleotides RNA oligomers. The HILIC chromatographic method mobile phase conditions were also optimized.

## **2.2 Experimental**

All solvents used were HPLC grade. Water, formic acid (98.0%), triethylammonium acetate (~1.0 M in water), tris(hydroxymethyl)aminomethane (TRIS, 99.8%), sodium chloride, methanol and acetonitrile used were purchased from Sigma-Aldrich (USA). All mobile phases were prepared as described using a Fisher Scientific Accumet 950 pH meter, calibrated at time of use, to capture the pH. The RNA oligonucleotides: 5',3'-hydroxyl uridine-adenosine (UA), 5',3'-hydroxyl cytidine-uridine (CU), 5',3'-hydroxyl guanosine-guanosine (GG), 5',3'-hydroxyl cytidine-guanosine (CG), 5',3'-hydroxyl cytidine-adenosine (CA), 5',3'-hydroxyl uridine-adenosine-uridine

(UAU), 5',3'-hydroxyl uridine-adenosine-adenosine (UAA), 5',3'-hydroxyl cytidine-adenosine-uridine (CAU), 5',3'-hydroxyl guanosine-adenosine-uridine (GAU), 5',3'-hydroxyl uridine-adenosine-cytidine and 5',3'-hydroxyl uridine-adenosine-uridine-cytosine (UAUC) were received from our collaborator, Dr. Bryce Nickels, at a concentration of ~1mM. These samples were diluted to ~100uM for analysis in 50% acetonitrile in water.

For the experiments, a Waters Alliance 2695 HPLC equipped with a Waters 2996 Photodiode Array detector was used at a wavelength of 254 nm. This instrument was controlled by MassLynx software. The HPLC method parameters were as described below.

## **2.3 Results and Discussion**

### ***2.3.1 Evaluation of HPLC Stationary Phases.***

Developing the HPLC method involved evaluating three different stationary phases. The three types, strong anion exchange, reverse phase (ion pairing) and hydrophilic interaction chromatography (HILIC), were compared by analyzing three nanoRNA oligomers. The three RNA oligomers chosen were 5', 3'-hydroxyl uridine-adenosine (UA), 5', 3'-hydroxyl uridine-adenosine-uridine (UAU), and 3'-hydroxyl uridine-adenosine-uridine-cytosine (UAUC). Both UA and UAU needed to be separated enough to be analyzed by mass spectrometry. While UAUC represented larger oligonucleotides. The goal was to separate larger oligonucleotides from the di- & tri-nucleotide oligomers due to specificity concerns in mass spectrometry.



The strong anion exchange method evaluated used a Dionex DNA Pac PA200 (2mm x 250 mm) column under 100% aqueous conditions buffered to pH 7 in 25mM Tris-HCl. The analytes were eluted using an increasing sodium chloride gradient (from 2

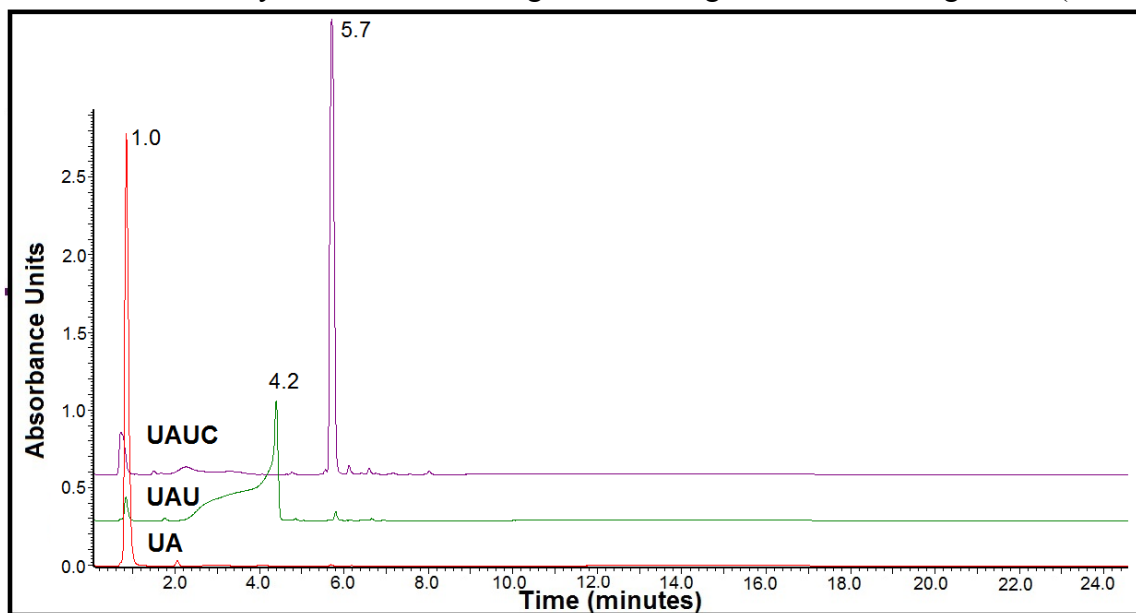


*Figure 16: Separation of nanoRNAs by strong anion exchange chromatography.*

-25 minutes, 0 – 1M sodium chloride) at 0.6 mL/min. Figure 16 displays the overlaid chromatographs, at 254 nm, of the three RNA oligomers using this method. The chromatographs show UAUC was well retained, eluting at 5.7 minutes. However, UAU and UA retention was a major concern. As previously discussed, the retention mechanism in SAX is an electrostatic interaction between our analytes and the quaternary ammonium groups on the stationary phase particle surface<sup>73</sup>. It was hypothesized the charged phosphate groups,  $pK_a \sim 1.5$ <sup>84</sup>, on oligonucleotides interact with the charged particle surface. As observed in Figure 16, the order of retention does support the hypothesis: UAUC does have more retention than UAU. However, the results show UA does not retain at all, it eluted in the void volume (0- ~2 minutes), and UAU had an irregular peak shape. Both these observations may result from an insufficient electrostatic interaction with the column under these conditions. Another major concern

with this method was the mass spectrometer compatibility. The use of sodium chloride could cause salt buildup in the mass spectrometer. This analysis led us to believe that reverse phase (ion pairing) or HILIC chromatography might give provide better results.

Next, a reverse phase (ion pairing) chromatography method was evaluated. This method used a Waters XBridge OST C18 (4.6 mm x 50 mm) reverse phase column with 100 mM triethylammonium acetate (pH 7) used as the ion pairing reagent. A shallow methanol gradient (10 – 20%, from 2-25 minutes), Figure 17, resulted in the optimal

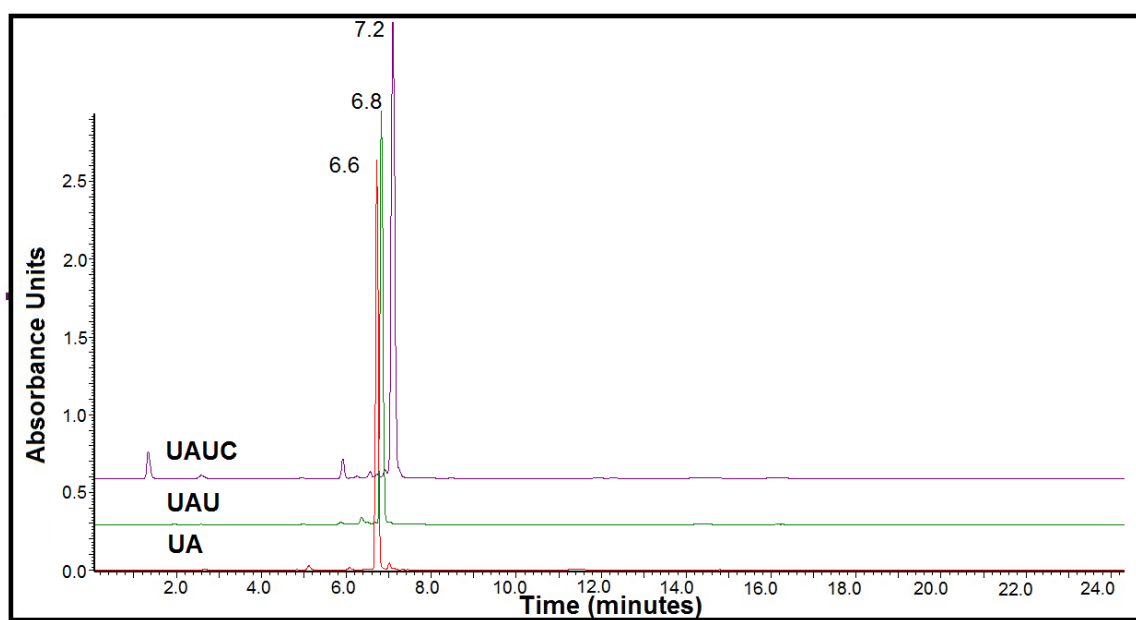


*Figure 17: Separation of nanoRNAs by reverse-phase ion pairing chromatography.*

separation on this column. All RNA oligomers were well retained. They eluted in size order: UA, UAU, and UAUC. This elution was predicted. Assuming the triethylamine (ion pairing reagent) has an electrostatic interaction with the phosphate groups in the RNA backbone, molecules with more phosphate groups should have more ion pairing interactions<sup>56</sup>. The hydrophobicity of the RNA oligomers should increase proportionately with the number of ion pairing interactions and/or the size of the resulting complex. As mentioned in Chapter 1, reverse phase chromatography is based on

hydrophobicity<sup>56</sup>. The greater hydrophobicity of the molecule, the more retention a molecule should have. This was the trend observed. However, the resolution was not sufficient for our purposes. The RNA oligomers our research was most concerned with are di- and tri-nucleotides. In this method UA and UAU are not baseline resolved, resolution ( $R_s$ ) was  $< 1$ .

Given the concerns of the previously evaluated methods, the three RNA oligomers were analyzed using a HILIC method. The method used a Waters Atlantis HILIC silica column (2.1 mm x 150 mm) buffered to pH 2 with 1% formic acid. The analytes were eluted using a decreasing acetonitrile gradient (90 – 65%, from 2-20

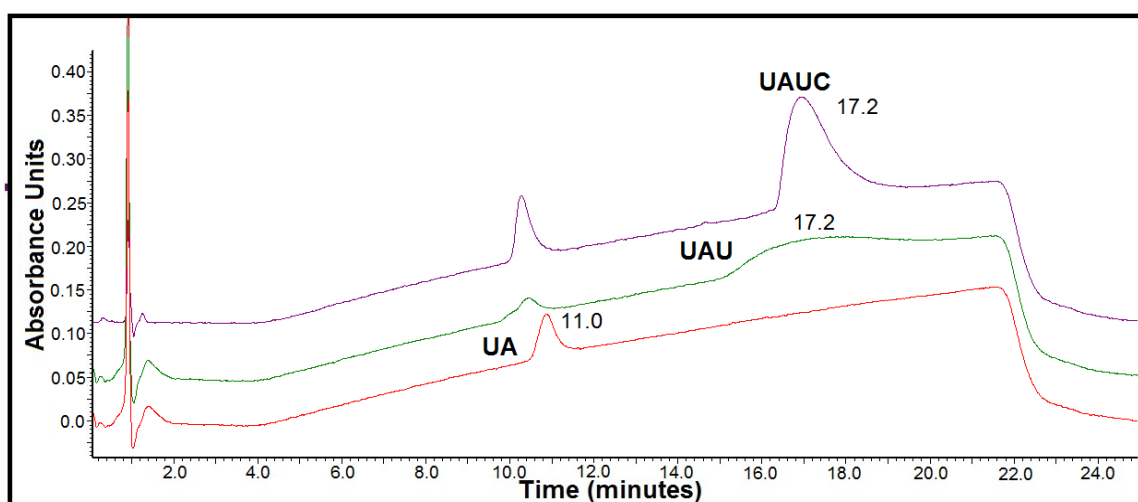


*Figure 18: Separation of nanoRNAs by HILIC chromatography (pH 2).*

minutes). As displayed in Figure 18, the HILIC method retains all three oligomers. The order of the elution for the RNA oligomers was not as expected. HILIC chromatography was hypothesized to perform separation by a liquid-liquid partition mechanism<sup>66</sup> between a water layer on the particle surface and the mobile phase. More hydrophilic molecules should elute later, as the mobile phase aqueous content is increased. The hydrophilicity of the oligomers appeared to be very similar and it was hypothesized the size would

dictate the elution (larger molecules retain less). However, the opposite elution order was observed. One explanation for this could be the increase in the number of charged groups does change the hydrophilicity significantly. The other explanation would be there were some electrostatic interactions between the charged phosphate backbone and the silica surface. So larger oligonucleotides have more sites for interaction causing increased retention. Although the elution order was unexpected the HILIC method provided baseline separation of UA and UAU, resolution of ~2. However, UAU and UAUC were not fully resolved and their peak shapes were very broad, span over 2+ minutes.

Following the evaluation of three chromatographic methods, HILIC separation provided the most adequate separation of the RNA oligomers UA, UAU, and UAUC. Not only does HILIC retain all three molecules, but it also separated the di- & tri-nucleotides tested. The strong anion exchange method also separated these RNA oligomers. However, the SAX method utilized sodium chloride which is not compatible with mass spectrometry. Reverse-phase (ion pairing) did not baseline separate UA and UAU.

### ***2.3.2 Evaluation of HPLC Mobile Phase Conditions.***

The HILIC chromatographic method gave the most promising separation. However, the peak shape and resolution for UAU and UAUC were not sufficient. To improve the resolution and peak shape the mobile phase was optimized. The mobile phase solvents used, water/acetonitrile mixtures, are the optimal solvents in HILIC separation so this was not evaluated. Manipulation of the gradient also would not greatly improve resolution or peak shape. To improve peak shape and resolution, changing the buffer and pH of the aqueous mobile phase were evaluated.

The method used to generate the chromatographs in Figure 18 started with a 10/90 split of 1% formic acid/acetonitrile and increased the aqueous mobile phase to 35% from 2 – 20 minutes. The RNA oligomers were retained and partially resolved; yet, the peak shape was inadequate. The peak shape using the ion pairing reagent, Figure 17, was very sharp, so it was hypothesized the addition of ion pairing reagent to the HILIC method would sharpen the peaks. Figure 19 displays an overlaid chromatograph of UA,

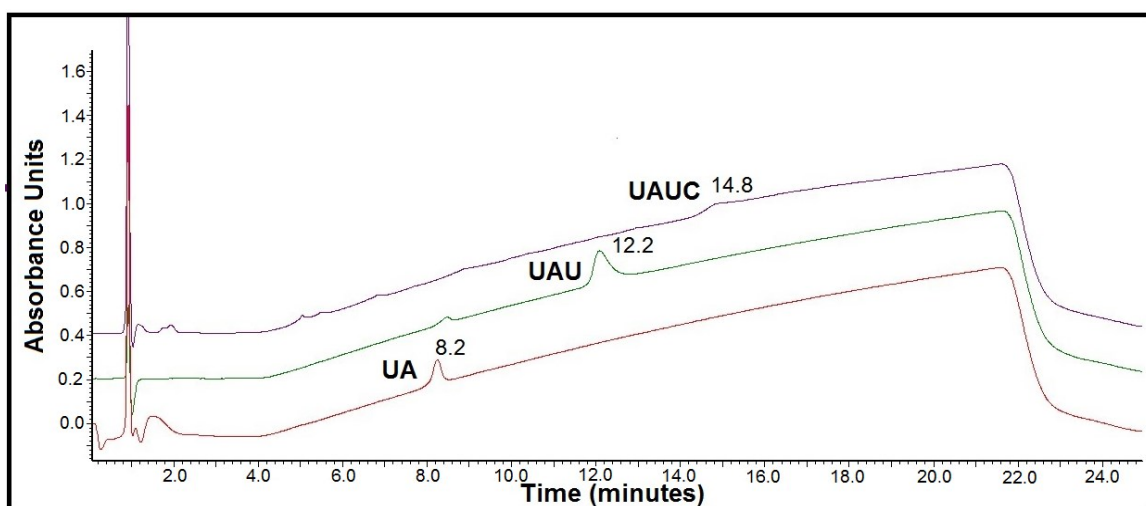


*Figure 19: Separation of nanoRNAs by HILIC ion-pairing chromatography (pH 2).*

UAU and UAUC with a 25 mM triethylammonium formate (pH 2) aqueous mobile phase. As observed, the peak shape of UAU significantly improved, from a previous peak width of ~5 minutes (figure 18) to 1 minute. Baseline resolution between all three oligomers was also achieved. The resolution between UA and UAU increased to 4 from ~2. Consequently, some retention was lost. For example, UA shifted from 11.1 minutes previously to 8.2 minutes. However, it was not of concern. The only other minor concern not addressed was the UAUC peak shape. The addition of ion pairing reagent did not improve UAUC's peak shape.

Next, the pH of the ion pairing reagent in the aqueous mobile phase was evaluated. A 25 mM triethylammonium formate buffer was evaluated at pH 5 and compared to the previous study at pH 2. Figure 20 compares a mixture of UA, UAU and UAUC at pH 5 versus pH 2. The peak shape of UAUC was not significantly better. Also, the resolution between UA and UAU decreased from a resolution of 4 (pH 2) to 2

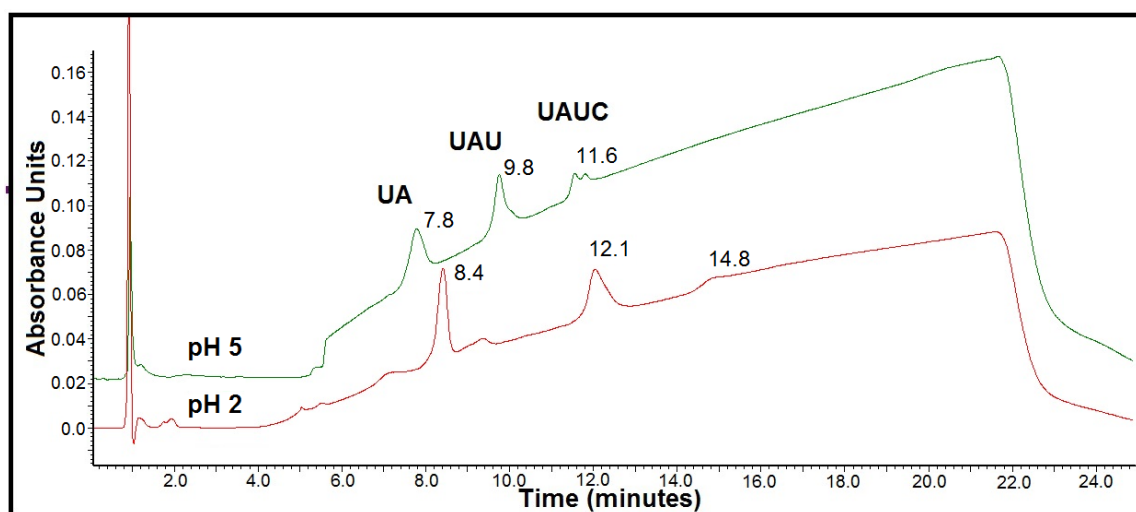


Figure 20: Comparison of nanoRNA separation by HILIC ion-pairing chromatography, pH 2 vs. pH 5.

(pH 5). This comparison demonstrates that 25 mM triethylammonium formate buffered to pH 2 was preferred over pH 5.

Evaluation of the mobile phase conditions yielded a method capable of resolving UA, UAU, and UAUC from each other. This method also eluted UA and UAU with a sufficient peak shape to perform analysis using mass spectrometry detection. Although UAUC peak shape was poor, UAUC was resolved from UA and UAU.

### 2.3.3 Optimized HPLC Conditions

Through evaluating several stationary phase chemistries and mobile phase conditions a HPLC method was developed which met our goals. Next, we performed analysis of several RNA di-nucleotide and tri-nucleotide oligomers using the method developed. This analysis demonstrated the resolving power of the method.

As shown in Figure 21, five RNA di-nucleotide oligomers were analyzed: 5',3'-hydroxyl uridine-adenosine (UA), 5',3'-hydroxyl cytidine-uridine (CU), 5',3'-hydroxyl guanosine-guanosine (GG), 5',3'-hydroxyl cytidine-guanosine (CG), and 5',3'-hydroxyl cytidine-adenosine (CA). All five of these oligomers were baseline separated with a resolution between each other of at least 1. The five RNA tri-nucleotide oligomers analyzed were 5', 3'-hydroxyl uridine-adenosine-uridine (UAU), 5', 3'-hydroxyl uridine-adenosine-adenosine (UAA), 5', 3'-hydroxyl cytidine-adenosine-uridine (CAU), 5', 3'-hydroxyl guanosine-adenosine-uridine (GAU), and 5', 3'-hydroxyl uridine-adenosine-

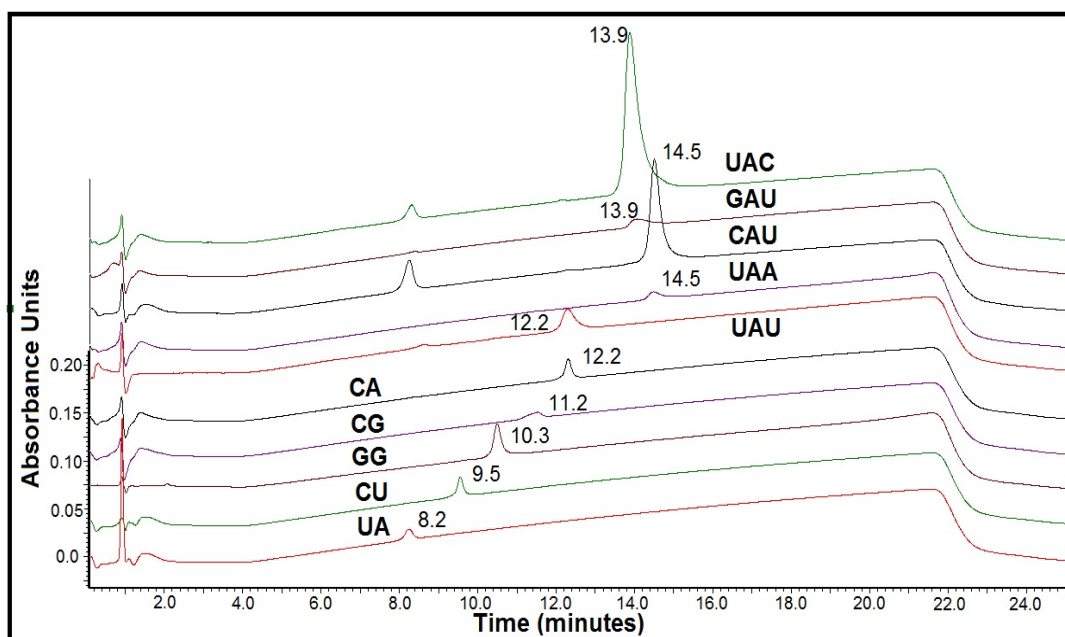


Figure 21: Chromatographic overlay of RNA di- & tri-nucleotides separated by HILIC ion-pairing chromatography.

cytidine. These oligomers were not completely resolved from each other. Only UAU was resolved from the other tri-nucleotide RNA oligomers, retaining at 12.2 minutes. UAU was the primary tri-nucleotide oligomer we targeted. The other four tri-nucleotide oligomers all interfere with each other. The only interference between di- and tri-nucleotide oligomers was between CA and UAU. This co-elution needed to be taken into account when developing the mass spectrometry method.

## **2.4 Conclusion**

We developed a suitable HPLC method for analyzing various di- and tri-nucleotide RNA oligomers. The method uses HILIC ion pairing chromatography to effectively retain and separate three oligomers of interest. Also, the optimized method conditions made it compatible with mass spectrometry. Evaluation of other di- and tri-nucleotide oligomers demonstrated baseline resolution of five di-nucleotides and isolation of the di-nucleotides from the tri-nucleotides. The only exception was the co-elution of CA and UAU which will be addressed in Chapter 3 through detection specificity.



## Chapter 3. Identification of NanoRNAs in *Escherichia coli* Cells using HPLC Tandem MS

### 3.1 Introduction

Previously, it was discussed how our collaborators observed RNA transcription initiation priming by nanoRNAs, *in vivo*<sup>87</sup>. Next, their goal was to determine whether nanoRNA mediated priming occurred in *Escherichia coli* under physiological growth conditions. Using high-throughput DNA sequencing, they performed experiments under various growth conditions to observe transcription start site shifting<sup>88</sup>. Transcription start site shifting is a result of nanoRNA mediated priming. Figure 22 shows a comparison of two *Escherichia coli* cell growth phases, exponential and stationary.

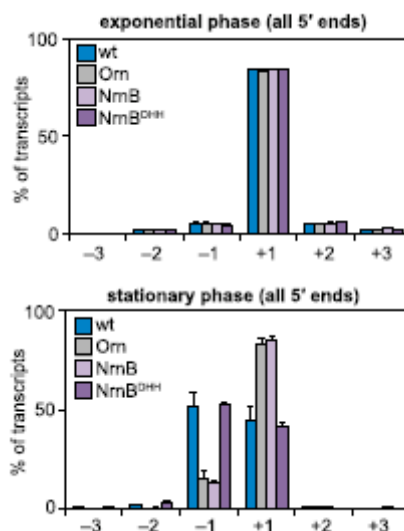


Figure 22: Transcription start site shifting in *Escherichia coli*<sup>88</sup>.

A transcript primed by a nucleotide triphosphate would begin at '+1'. If transcripts were primed by a di-nucleotide nanoRNA, the start site was shifted to '-1'. NanoRNAses, *nrrnB*<sup>92</sup> and *orn*, were used as negative controls in this experiment. The presence of these

nanoRNAses have shown to degrade the nanoRNAs and effectively knock-out nanoRNA mediated priming. Also, a catalytically inactive version of *nrnB*, *nrnB*<sup>DHH 93</sup>, was used as another positive control. As hypothesized, the wild type *E. coli* strain (wt), during stationary phase growth, shows significant nanoRNA mediated priming. These results not only confirmed our collaborators hypothesis but also provided the motivation for the research detailed in this chapter.

In Chapter 2, a mass spectrometer compatible HPLC method was developed. This method demonstrated the capability of isolating several 5', 3'-hydroxyl di-nucleotide and tri-nucleotide RNA oligomers from each other. The next step was to develop a sensitive and specific method to detect the nanoRNAs in an *Escherichia coli*

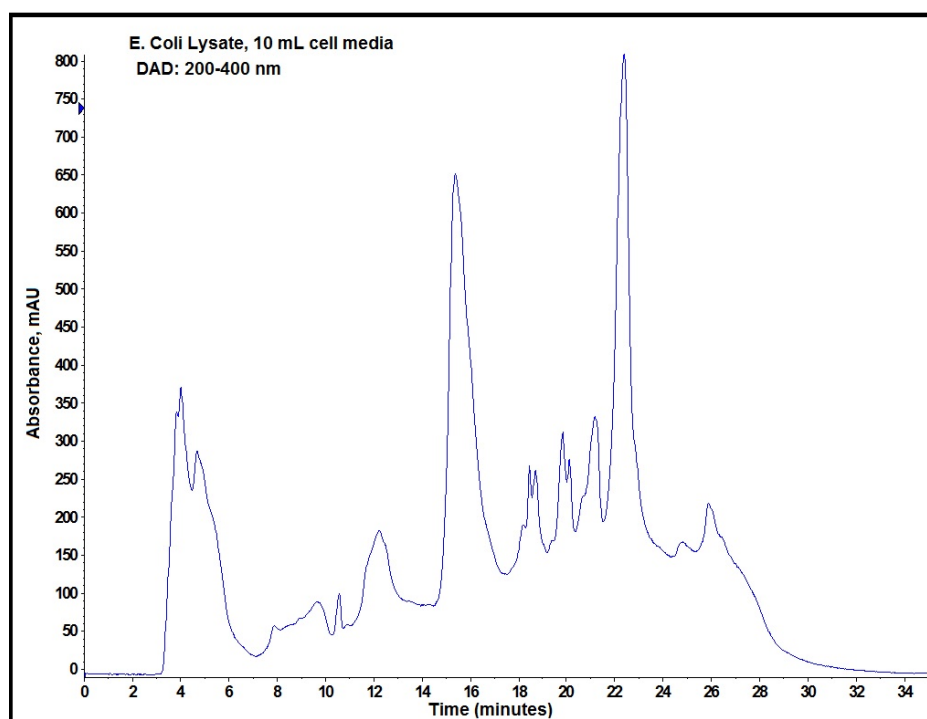


Figure 23: Example UV chromatographic of *E. coli* cell culture lysate using the developed HPLC method.

cell matrix. NanoRNA structures have an intense UV-VIS chromophore. Although the complexity of the cell samples did not make UV-VIS detection a possibility. As

displayed in the chromatograph (Figure 23), the nanoRNAs would not be resolved from other endogenous material if the concentration was high enough to observe a UV-VIS signal. Similarly, fluorescence detection<sup>94</sup> was also not an option. As we had already anticipated<sup>95</sup>, detection by mass spectrometry was necessary for the desired sensitivity and specificity. Previously, HPLC-MS was attempted in *E. coli* cells using a data-dependent scan which searched for specific parent ion masses,  $M+1$  for each (positive electrospray). However, these studies were inconclusive and it was determined the additional specificity of HPLC-MS/MS was necessary to identify any nanoRNAs in the *E. coli* sample matrix.

In this research, the MS electrospray positive fragmentation patterns of RNA 5', 3'-hydroxyl di- & tri-nucleotides were evaluated. Then, a HPLC-MS/MS method was developed to track the presence of specific nanoRNAs using the experimentally determined primary fragmentation pathways. The sensitivity level of the method was then evaluated for 5', 3'-hydroxyl uridine-adenosine-uridine. Lastly, the method was utilized to observe the presence of this nanoRNA in *E. coli* samples.

### 3.2 Experimental

All solvents used were HPLC grade. Water, formic acid (98.0%), triethylammonium acetate (~1.0 M in water), and acetonitrile used were purchased from Sigma-Aldrich (USA). All mobile phases were prepared as described using a Fisher Scientific Accumet 950 pH meter, calibrated at time of use, to capture the pH. The RNA oligonucleotides: 5', 3'-hydroxyl uridine-adenosine (UA), 5', 3'-hydroxyl guanosine-guanosine (GG), 5', 3'-hydroxyl cytidine-adenosine (CA), 5', 3'-hydroxyl uridine-

adenosine-uridine (UAU), and 5', 3'-hydroxyl uridine-adenosine-adenosine (UAA) were received from our collaborator, Dr. Bryce Nickels, at a concentration of ~1mM.

For MS fragmentation analysis, the specified nanoRNA oligomers were diluted to ~1μM for analysis in 1% formic acid in water/acetonitrile (50/50) for MS analysis. The experiments were performed by infusing the nanoRNA (200 μL/min) into a HPLC effluent of 25 mM triethylammonium formate (pH 2): Acetonitrile (25:75) at a flow rate of 300 μL/min. Fragmentation experiments were performed on an Agilent 1100 HPLC connected to an AB Sciex 4000 Qtrap mass spectrometer. Mass spectrometer conditions were optimized for each particular nanoRNA to yield a representative fragmentation pattern in product ion mode (collision energy ~25-35)

*Escherichia coli* cell lysates, prepared by our collaborator Dr. Seth Goldman, were received as a 5mL aqueous solution. These samples were generated from single colonies (MG1655) containing PlacUV5(-1T) reporter plasmid pBEN 493 and either empty expression vector (pPSV38) or NrnB-vsvg expression vector (pSG239) which were inoculated into 5 mL of LB containing gentamycin and rolled overnight at 37°C. These cultures were then diluted 1:100 into LB medium containing antibiotics and 1 mM IPTG. 25 mL aliquots of the diluted cultures were then shaken for 23 hours at 37°C. These cultures were then pelleted, by centrifugation, twice to get rid of the media. Then subsequently extracted using 10% formic acid and precipitated with ammonium acetate. The precipitate was re-suspended in 5mL of water which was lyophilized. The weight of the resulting cell lysate was recorded and the samples were prepared to contain ~20μm/μL of cell lysate in either 1% formic acid in water/acetonitrile (50/50) or 75 fmoles/μL of UAU in 1% formic acid in water/acetonitrile (50/50).

High pressure liquid chromatography mass spectrometry analysis was performed on the prepared cell lysates. All separations were performed on an Agilent 1100 HPLC connected to an AB Sciex 4000 Qtrap mass spectrometer. The liquid chromatography method used a Waters Altantis HILIC silica 3  $\mu\text{m}$  column, 2.1 mm x 150 mm. The samples were separated using a gradient mobile phase consisting of acetonitrile (A) and 25 mM triethylammonium formate buffered to pH 2 in water (B). The gradient condition was: 0–2 min, 10% B; 2–20 min, 10–35% B; 20–21 min, 35–10% B; 21–35 min, 10% B. The effluent was analyzed using in-line mass spectrometry which was equipped with an electrospray ionization interface (ESI). Peaks were detected by positive ionization mode of MS/MS detection. Mass spectrometry analysis was carried out using selected reaction monitoring (SRM) mode with an isolation width set at 2. The transition monitored was for the parent ion at 880.0  $m/z$  ( $M+1$ ) fragmenting to 574  $m/z$  by collision induced dissociation. ESI-MS conditions were as follows: drying gas  $\text{N}_2$ ; gas 1 flow rate of 40 arbitrary units; gas 2 flow rate of 20 arbitrary units; temperature, 400  $^\circ\text{C}$ ; spray voltage, 5500V; and collision energy, 37. All instruments and data were controlled and captured using Analyst software v 1.5.2.

### **3.3 Results and Discussion**

#### ***3.3.1 Mass Spectrometer Fragmentation Patterns of RNA Oligonucleotides.***

As previously discussed in Chapter 1, electrospray ionization in positive ion mode was preferred over negative ion mode for nanoRNA analysis. To determine the major fragmentation patterns of several RNA oligomers ‘product ion’ scanning in positive

electrospray ionization mode was utilized. In these experiments, the parent ion ( $M+1$ ) was selected (trapped) in the ion trap, subjected to collision induced dissociation, and the resulting fragmented ions were detected. This analysis was performed on di-nucleotide and tri-nucleotide RNA oligomers which we were most interested in.

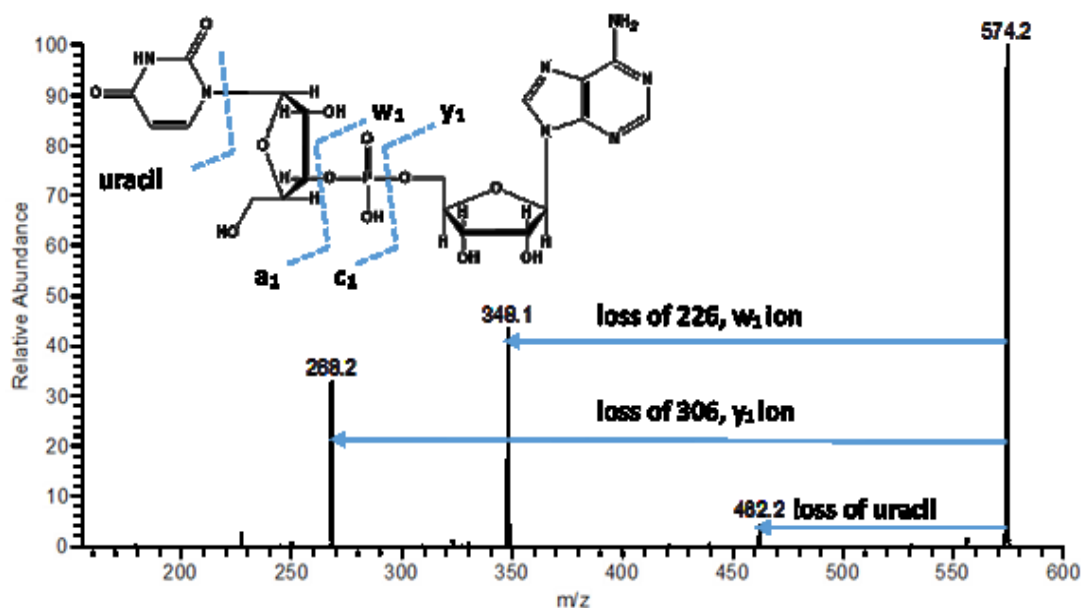


Figure 24: Mass fragmentation of 5', 3'-hydroxyl uridine-adenosine.

In Figure 24, the product ion mass spectrum of 5', 3'-hydroxyl uridine-adenosine (UA) is shown. Fragmentation of UA resulted in two major daughter ions:  $w_1$  and  $y_1$  ions. The fragmentation to the  $w_1$ , 348  $m/z$ , was slightly preferred. Some neutral loss of the base, uracil (112  $m/z$ ), was also observed but to a lesser degree. These fragments were expected to be pre-dominant based off of previous research<sup>96-97</sup>. The mass spectrum of 5',3'-hydroxyl cytidine-adenosine (CA), in Figure 25, shows the presence of only one

major daughter ion, 462 m/z, corresponding to the loss of the cytosine base.

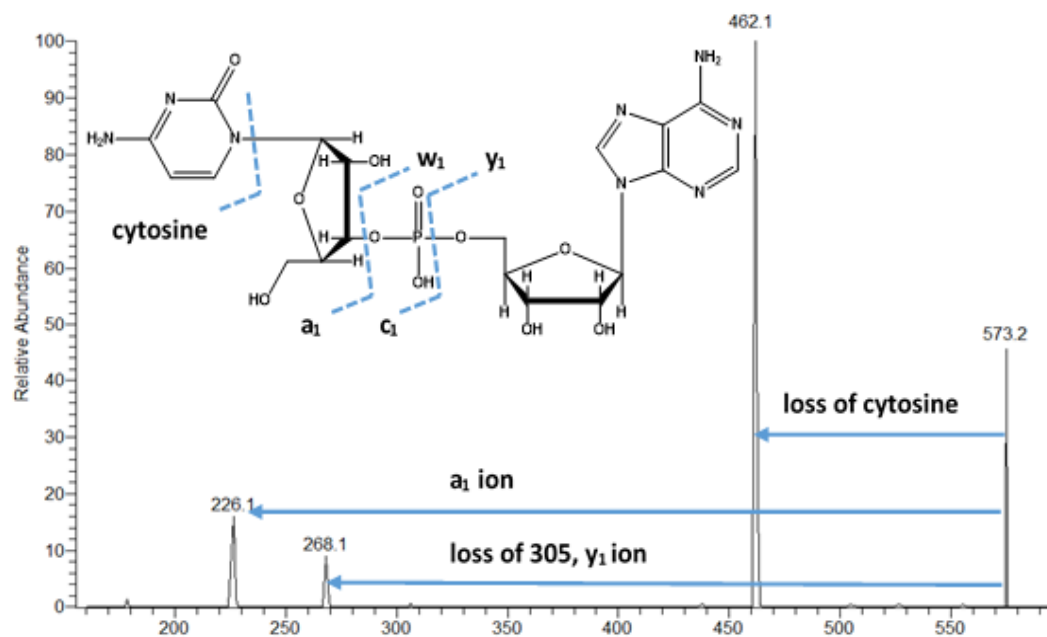


Figure 25: Mass fragmentation of 5', 3'-hydroxyl cytidine-adenosine.

In this spectrum the presence of the a<sub>1</sub> and y<sub>1</sub> ions were also observed, but to a lesser extent.

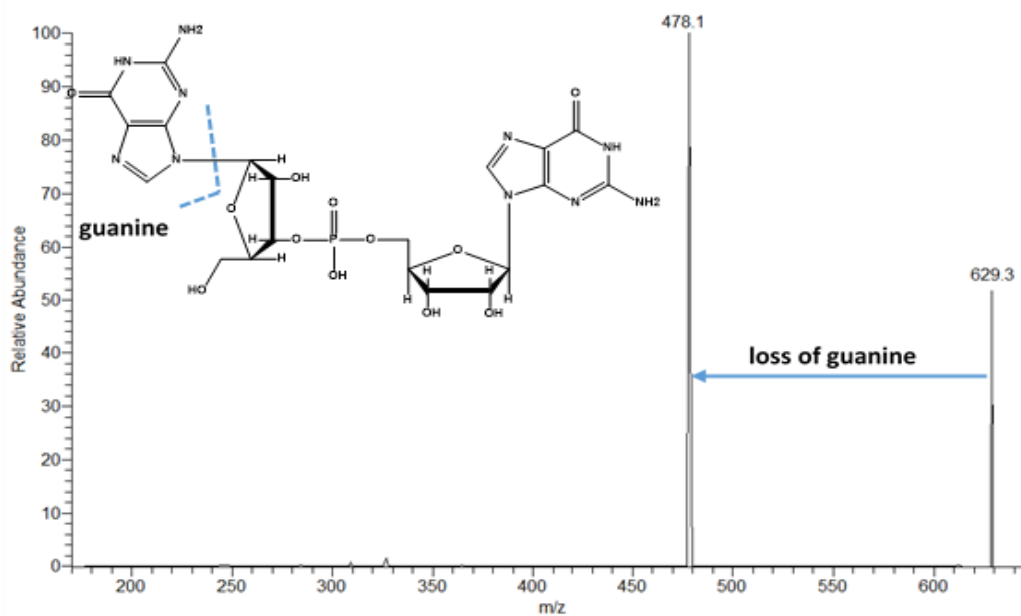
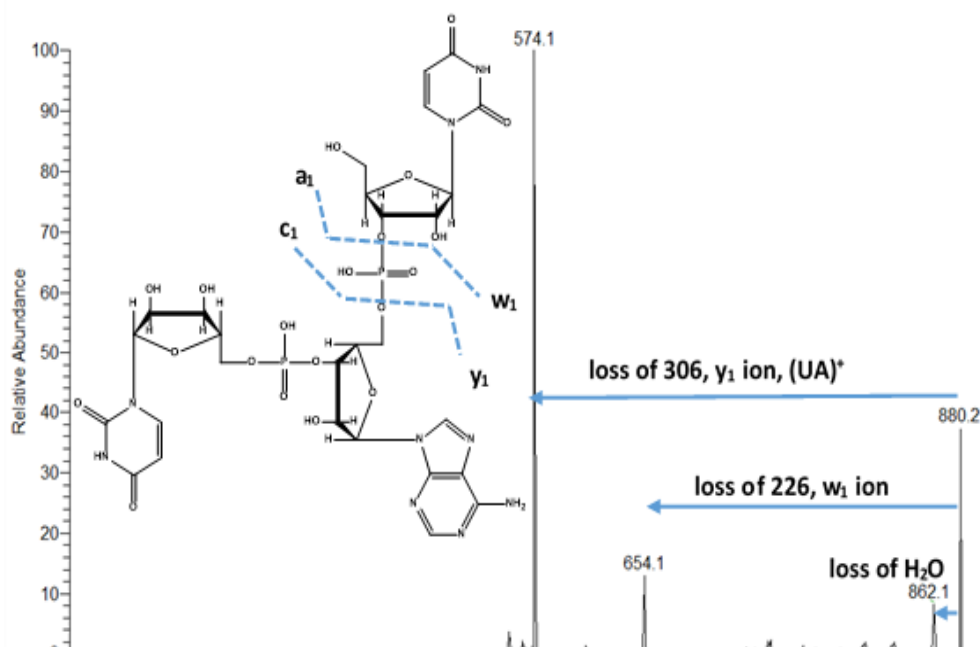


Figure 26: Mass fragmentation of 5', 3'-hydroxyl guanosine-guanosine.

Different major fragmentation pathways between CA and UA were not expected, but were welcomed as the parent ion masses are within 1 m/z of each other, 573 m/z versus 574 m/z, respectively. The primary daughter ion for CA was a loss of cytosine while the UA's primary daughter corresponded to a neutral loss of the  $a_1$  fragment. This slight differentiation increases the specificity of the MS/MS analysis of each species. The final di-nucleotide RNA oligomer analyzed was 5', 3'-hydroxyl guanosine-guanosine (GG). The fragmentation, shown in Figure 26, was very similar to CA. The primary fragmentation of GG is the loss of the base, guanine 151 m/z, and no other fragments were present in high abundance.

Our collaborators hypothesized di-nucleotide RNA oligomers were mostly responsible for the RNA transcription priming; however, analysis of tri-nucleotide RNA oligomers was also necessary, as a negative control. Two tri-nucleotide RNA oligomers



were evaluated for their fragmentation patterns. 5', 3'-hydroxyl uridine-adenosine-



uridine (UAU), 880 m/z, Figure 27, fragments to one major daughter ion, 574 m/z. Interestingly, this major daughter ion is the positively charged dinucleotide species 5', 3'-hydroxyl uridine-adenosine (UA<sup>+</sup>), or the y<sub>1</sub> ion. Other fragments result from the loss of a water, 862 m/z, and the formation of the w<sub>1</sub> ion, 654 m/z. The last RNA oligomer analyzed was 5', 3'-hydroxyl uridine-adenosine-adenosine (UAA), 903 m/z, Figure 28. The major fragment of UAA was also a positively charged dinucleotide species, 5', 3'-hydroxyl adenosine-adenosine, 597 m/z. The other observed fragment was a neutral loss, 267 m/z, to the c<sub>2</sub> ion. The results of the RNA oligomer mass spectra fragmentation patterns are summarized in Table 1. The data in the table shows the optimal parent-to-daughter ion transition for each species. These transitions were used in our MS/MS analysis of each species. When analyzing samples, the mass spectrometry would be specifically 'tuned', or optimized, for the transition corresponding to the nanoRNA chosen. We were able to track the specific transition using 'selected reaction monitoring' (SRM) which gave us increased specificity and sensitivity in our analysis.

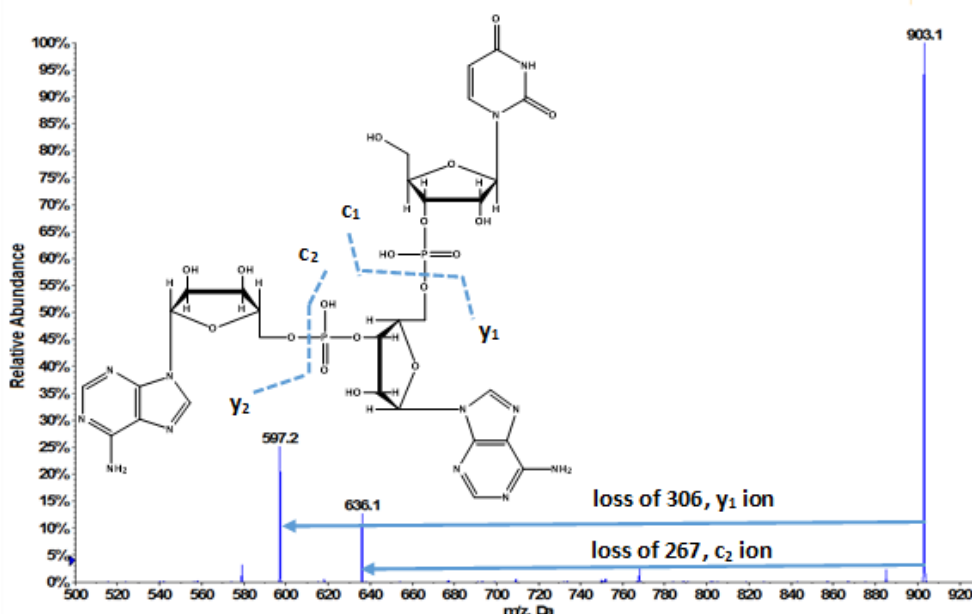


Figure 28: Mass fragmentation of 5', 3'-hydroxyl uridine-adenosine-adenosine

Table 1: Parent-to-daughter ion transitions for several nanoRNAs

RNA Oligomer	Parent Ion (M+1), m/z	Daughter Ion (M+1), m/z
5',3'-hydroxyl uridine-adenosine (UA)	574	348
5', 3'-hydroxyl cytidine-adenosine (CA)	573	462
5',3'-hydroxyl guanosine-guanosine (GG)	629	478
5',3'-hydroxyl uridine-adenosine-uridine (UAU)	880	574
5',3'-hydroxyl uridine-adenosine-adenosine (UAA)	903	597

### 3.3.2 Analysis of NanoRNAs in *Escherichia coli* Cells.

A tandem mass spectrometry method was developed for several nanoRNA species using the selected SRM transitions shown in Table 1. This method was compatible with

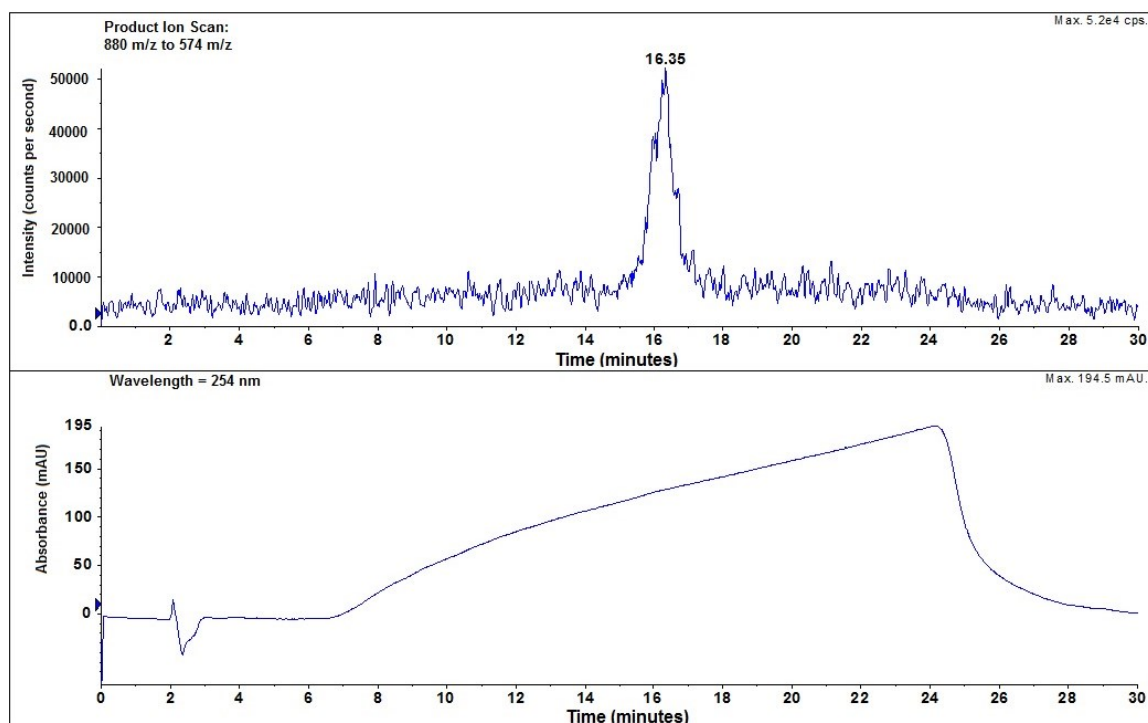


Figure 29: Overlay of product ion scan, 880 m/z to 574 m/z (top), and UV chromatogram, 254nm (bottom), for 75 fmoles UAU.

the HPLC method previously developed. Together, the HPLC-MS/MS method provided enough specificity and sensitivity to analyze nanoRNAs at a low level in *Escherichia coli* cells. In order to define the level of sensitivity which could be achieved using this method a series of controls (purchased RNA oligomers diluted to specific concentrations in diluent) were run prior to analyzing cell lysate samples. The lowest level observed was 75 fmole for 5', 3'-hydroxyl uridine-adenosine-uridine (UAU), with the MS/MS parameters optimized for this SRM transition, in the HPLC effluent. Figure 29 shows the mass and UV chromatographs of the 75 fmole control of UAU. As observed in the mass chromatograph (top), there is a signal corresponding to UAU at 16.35 minutes. Note, the difference in retention time compared to Chapter 2 was attributed to different instrumentation and age of the HPLC column. This signal had an acceptable detection limit with a signal-to-noise ratio greater than 3:1<sup>98</sup>. The UV chromatograph (bottom), at 254 nm, demonstrates the sensitivity difference between tandem MS and UV detection. The UV signal only contains the baseline, no UAU was observed.

After establishing the sensitivity level for UAU, *Escherichia coli* cell cultures were analyzed. To prove the existence of nanoRNAs in these cell cultures a study was performed with 'wild type' and a negative control culture, both grown to 'stationary phase' of cell growth. The negative control cell culture used in this study was grown with the expression of nanoRNase, *nrnB*. This oligoribonuclease is capable of degrading RNA oligomers 2+ mers in size, as discussed previously in this Chapter. All cell samples represent 25 mL of cell culture which, after work-up and sample preparation, results in 2.5 mL of cell culture per analysis by LC-MS/MS. For each culture type, wild type and *nrnB*, two sample preparations were analyzed. One sample preparation was prepared in

diluent alone while the other was spiked with 75 fmole/ $\mu$ L (750 fmole injected) of UAU.

The mass chromatographs are shown in Figure 30.

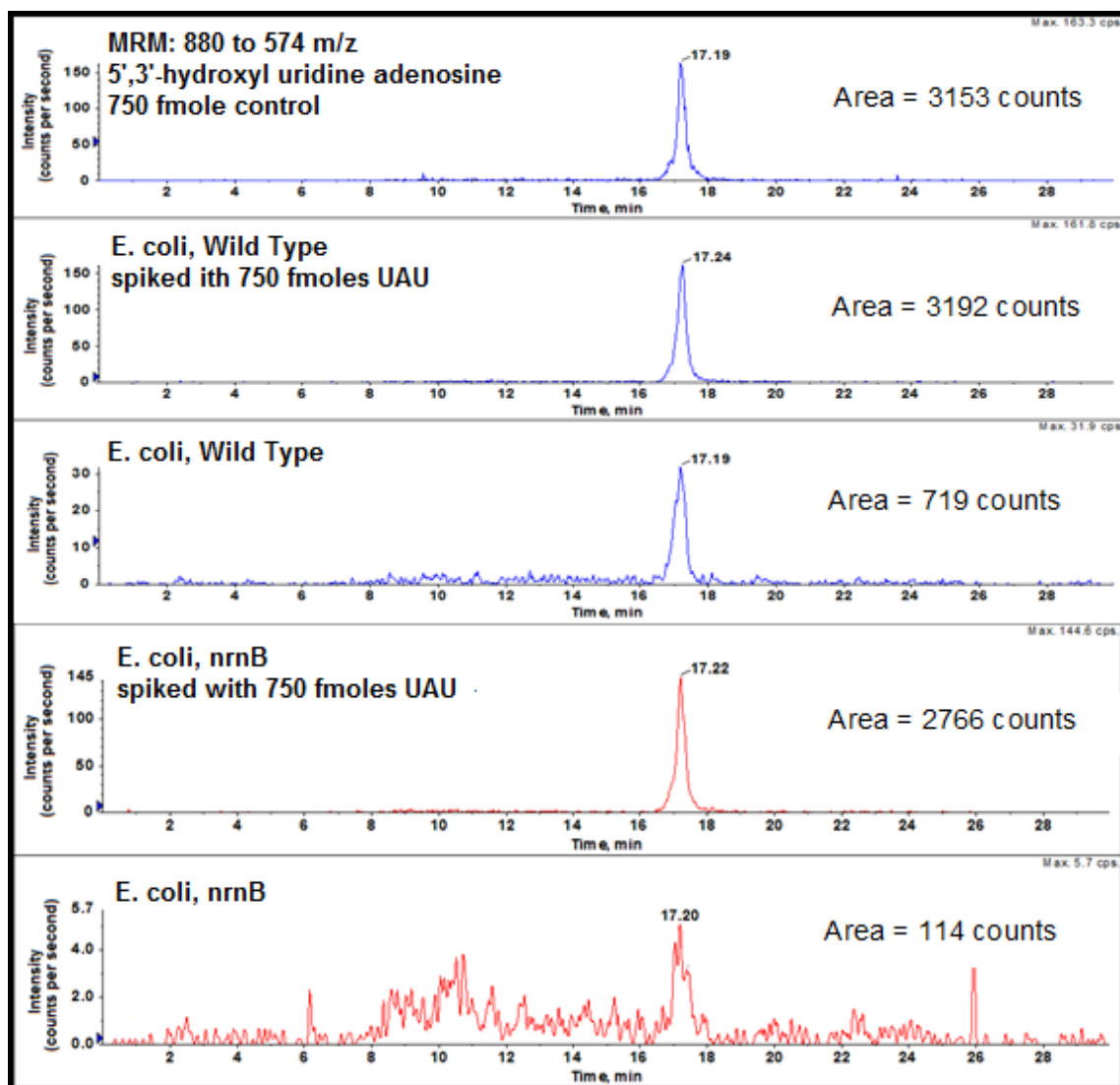


Figure 30: Comparison of mass chromatographs for wild type and *nrnB* active *E. coli* samples.

If you compare both un-spiked samples a significant difference in UAU signal area was observed for wild type and *nrnB*, 719 versus 114 counts, respectively. As expected, the wild type shows a greater signal corresponding to UAU than *nrnB* culture. Both of the UAU spiked samples show an increase in signal area compared to the un-spiked. Wild type un-spiked versus spiked area count was 719 versus 3192 and *nrnB* was 114 versus

2766, respectively. This doping gave us confidence we were analyzing UAU. When comparing the area increase in 750 fmole spiked samples versus the 750 fmole control (3153 area counts) we observed some ion suppression in the samples. The increase in signal of the spikes versus un-spiked were 2473 and 2652 for wild type and *nrnB*, respectively. When this difference is compared to the control, we observed ~20% ion suppression at this level<sup>99</sup>.

Next, the results were repeated to get a better idea of the absolute amount of UAU present in the cell cultures. A similar study was performed except 3 spikes were used per sample: 75, 300, and 750 fmoles UAU. Due to the observed ion suppression, standard addition calibration was performed using these levels to get a rough quantitation of UAU. Both wild type and *nrnB* cell extractions were analyzed. The results are summarized in Table 2.

*Table 2: UAU analysis (standard addition) in E. coli cell cultures: wild type and nrnB*

	<b>Wild Type (lot 38-5)</b>	<b>NrnB (lot 239-5)</b>
<b>UAU Amount (fmoles/culture)</b>	<b>1870</b>	<b>670</b>
Standard Addition (R <sup>2</sup> )	0.996	0.998

The quantitated amount of UAU was calculated using standard addition curve of the four preparations: 0, 75, 300, and 750 fmoles UAU spiked. The corresponding R<sup>2</sup> values of the standard addition linear regression curves demonstrated the linear response of UAU in these experiments. The amount calculated in the wild type and *nrnB* cultures correlate with the previous experiment qualitatively, more UAU was found in wild type versus *nrnB* cell cultures.

### 3.4 Conclusion

This research combined the HPLC method developed in Chapter 2 with tandem MS analysis. The fragmentation patterns of several nanoRNA species were studied. From those patterns, the major MS/MS fragmentation pathways, or parent-to-daughter ion pairs, were identified and used to develop a HPLC-MS/MS method. After determining the level of sensitivity, the method was used to successfully analyze UAU in two cell cultures, wild type and *nrnB*. This analysis was replicated and the absolute amount of UAU was calculated using standard addition analysis. These results qualitatively confirm the DNA sequencing experiments performed by our collaborators shown at the beginning of this Chapter.

## Chapter 4. Selection of *Escherichia coli* Cell Extraction Procedures and Sample Preparation Conditions for Routine Analysis

### 4.1 Introduction

In Chapters 2 and 3, an HPLC-MS/MS method was developed. This method was then used to successfully determine the amount of 5', 3'-hydroxyl uridine-adenosine-uridine in *Escherichia coli* cells after extraction. An attempt was made to quantitate the amount of UAU present in wild type and *nrnB* cell cultures using standard addition analysis. The results generated supported the qualitative hypothesis of our collaborators. However, absolute quantitation was not successful.

The HPLC-MS/MS method provided the sensitivity and specificity needed, analytically, to analyze *E. coli* cell cultures. However, it was determined the procedure for extracting the RNA oligomers from the *E. coli* cell cultures had major concerns. The conditions used for extraction were not translatable to other growth phases. Preparing comparable cell extracts of log and stationary growth phases would be problematic. Another concern with the current extraction procedure was the scalability of the extraction method. The cell volume needed to generate quantitative data over multiple growth phases was too large for our resources. The last major concern was the HPLC-MS/MS ion suppression discussed in Chapter 3. All these factors could have greatly affected the quality of the results. A different method of cell culture extraction was needed. Many different extraction procedures have been reported<sup>100,101,102</sup>. However, a

specific extraction procedure was necessary which was translatable to different conditions, scalable and reproducible.

In this research, experiments were performed in order to determine the optimal procedure to extract nanoRNAs from the bacterial cell cultures under various growth conditions. After several extraction procedures were evaluated, it was determined an additional sample extraction step was needed. A solid phase extraction (SPE) method was developed and implemented. Recovery experiments were performed to demonstrate the SPE method was efficient. A complete cell culture extraction procedure was evaluated in duplicate, with two cultures.

## 4.2 Experimental

All solvents used were HPLC grade. Water, formic acid (98.0%), triethylammonium acetate (~1.0 M in water), tris(hydroxymethyl)aminomethane (TRIS, 99.8%), sodium chloride, methanol and acetonitrile used were purchased from Sigma-Aldrich (USA). All mobile phases were prepared as described using a Fisher Scientific Accumet 950 pH meter, calibrated at time of use, to capture the pH. The RNA oligonucleotides: 5', 3'-hydroxyl uridine-adenosine (UA) and 5', 3'-hydroxyl uridine-adenosine-uridine (UAU) were received from our collaborator, Dr. Bryce Nickels, at a concentration of ~1mM. Controls were diluted to the specified concentrations using 1% formic acid in water/acetonitrile (50/50).

The cell cultures were grown and extracted as follows. Single colonies of *E. coli* MG1655, containing PlacUV5(-1T) reporter plasmid pBEN 493 and either empty expression vector (pPSV38) or NrnB-vsug expression vector (pSG239), were inoculated into 25 mL of LB broth (Miller formula; EMD Millipore) containing gentamycin (10



µg/mL) and chloramphenicol (25 µg/mL) in 125mL flasks with closures and shaken (220 RPM) at 37°C on a shaker overnight. In the morning, the cultures were diluted 1:100 into 200 mL of LB, in a 1000 mL flask. This culture was thoroughly mixed and grown over 23 hours on a shaker at 37°C. At 23 hours (5 hours for 'Log' samples), four 36 mL aliquots were taken and processed in four different ways as described in Table 3, to extract the nanoRNA oligonucleotides. Prior to analysis all four extraction lysates were concentrated through lyophilization. Samples were re-dissolved in 1% formic acid in water/acetonitrile (50/50) or nanoRNA spike solutions.

All analysis for the nanoRNA extraction experiments were performed on an Agilent 1100 HPLC connected to an AB Sciex 4000 Qtrap mass spectrometer. The liquid chromatography method used a Waters Altantis HILIC silica 3 µm column, 2.1 mm x 150 mm. The samples were separated using a gradient mobile phase consisting of acetonitrile (A) and 25 mM triethylammonium formate buffered to pH 2 in water (B). The gradient condition was: 0–2 min, 10% B; 2-20 min, 10-35% B; 20-21 min, 35-10% B; 21-35 min, 10% B. The effluent was analyzed using in-line mass spectrometry which was equipped with an electrospray ionization interface (ESI). Analytes were detected using ESI positive ionization MS/MS detection. Mass spectrometry analysis was carried out using selected reaction monitoring (SRM) mode with an isolation width set at 2. The transition observed was the parent ion at 880.0 m/z (M+1) fragmenting to 574 m/z with collision induced dissociation. ESI-MS conditions were as follows: drying gas N<sub>2</sub>; gas 1 flow rate of 40 arbitrary units; gas 2 flow rate of 20 arbitrary units; temperature, 400 °C; spray voltage, 5500V; and collision energy, 37. All instruments and data were controlled and captured using Analyst software v 1.5.2.

Solid phase extraction experiments were performed using 3cc SPE cartridges of Waters Sep-Pak C18, Oasis WAX, and Oasis MAX. The cartridges were attached to a 5cc syringe (BD). The specified solvents were passed through the cartridge using gravity or slight partial pressure (<1mL/minute). Fractions were collected in 3mL aliquots. All fractions were analyzed using the HPLC conditions above on a Waters Alliance 2695 HPLC system with a Waters 2996 Photodiode Array Detector, at 254nm. Data collection was performed by MassLynx software.

### **4.3 Results and Discussion**

#### ***4.3.1 E. coli Cell Culture NanoRNA Extraction Selection.***

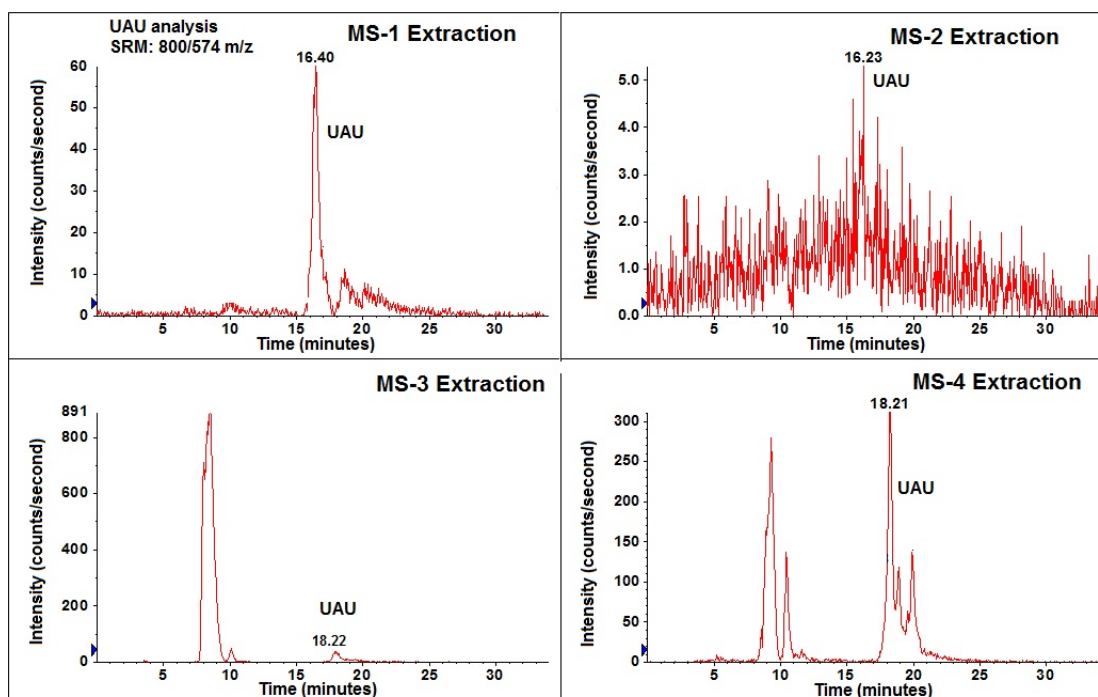
To improve the quality of the results, several extraction procedures were evaluated. All *Escherichia coli* cell cultures were initially grown the same. The cell culture then was split evenly and extracted in four different ways for oligonucleotides, Table 3, as single preparations. As displayed in the table, extraction labeled ‘MS-1’ was similar to the cell culture extraction performed in Chapter 2. The ‘MS-1’ culture was first quenched with ~10% formic acid, 4 mL of 100% formic acid was added to the 36 mL of cell culture. Then the RNA were precipitated with 100% ethanol. Followed by pelleting and re-dissolving in 1 mL of water. ‘MS-2’ through ‘MS-4’ involved pelleting the cells in the LB broth twice. Each time the culture was mixed thoroughly, centrifuged at 10,000g for 15 minutes, and the supernatant was discarded. Following pelleting ‘MS-2’ was re-suspended in 10% formic acid. The RNA were then precipitated with 100% ethanol, pelleted, and re-dissolved in 1 mL of water. ‘MS-3’, following pelleting, was simply re-suspended in 8 mL of 10% formic acid. ‘MS-4’ was re-suspended in a

different solvent, 40:40:20, acetonitrile: methanol: 0.1 M formic acid. The samples were prepared as previously described for analysis.

*Table 3: E. coli extraction methods for nanoRNAs.*

<b>Label</b>	<b>Procedure</b>
MS-1	<ol style="list-style-type: none"> <li>1. Culture quenched with 10% formic acid.</li> <li>2. RNA precipitated with ethanol.</li> <li>3. RNA pelleted.</li> <li>4. Re-dissolved in water.</li> </ol>
MS-2	<ol style="list-style-type: none"> <li>1. Cells pelleted.</li> <li>2. Pellet re-suspended in 10% formic acid.</li> <li>3. RNA precipitated with ethanol.</li> <li>4. RNA pelleted.</li> <li>5. Re-dissolved in water.</li> </ol>
MS-3	<ol style="list-style-type: none"> <li>1. Cells pelleted.</li> <li>2. Pellet re-suspended in 10% formic acid.</li> </ol>
MS-4	<ol style="list-style-type: none"> <li>1. Cells pelleted.</li> <li>2. RNA extracted with 40:40:20, acetonitrile:methanol:0.1M formic acid (MAF)</li> </ol>

The samples were analyzed using the HPLC-MS/MS method developed in Chapter 2 & 3. The results are summarized in Table 4 and MS chromatographs (un-spiked only) are shown in Figure 31. The major trend observed in the data was the difference in area counts of UAU in the ‘un-spiked’ sample extracts. The MS-4 sample extract resulted in a significantly larger response than the other extracts, 11520 versus 1796 and 2241, for MS-3 and MS-1, respectively. Although in the MS-4 extract, sample interference with the UAU peak was observed. The MS-1 and MS-3 extracts did not have any interference with UAU, but the response was significantly less. While the MS-2 extract did not have any response for UAU. The only deduction made from this analysis was the MS-2 extraction would not be suitable for analysis.



Further evaluation of the results in Table 4 revealed another concern. The table shows  
*Figure 31: LC-MS/MS chromatograms of UAU in E. coli cultures, evaluation of various extraction procedures.*

the ‘Difference’ in area between the un-spiked and the 22.5 pmole spiked sample extracts.

*Table 4: Results of UAU analysis in E. coli using various extraction procedures.*

HPLC-MS/MS Results (UAU)				
	Un-spiked Area (counts)	Spiked Area (counts)	Difference (spiked minus un-spiked)	Ion Suppression(-) / Enhancement(+) (%)
MS-1	2241	5730	3489	(-)44
MS-2	0	7439	7439	(+)20
MS-3	1796	2096	300	(-)91
MS-4	11520	14730	3210	(-)48
Control, 22.5 pmoles	NA	NA	6188	NA

Ideally, the ‘Difference’ should be within 15% (analytical error) of the response in the ‘Control, 22.5 pmoles’ results<sup>98</sup>. However, ‘MS-1’, ‘MS-3’ and ‘MS-4’ have

significantly lower values than expected. The ‘Ion Suppression/Enhancement’ percentage<sup>103</sup>, or % difference are detailed in the last column. These values demonstrate that in the presence of the cell lysates the ionization of UAU was suppressed, or enhanced, when compared to UAU in solvent alone. This result confirms that an internal standard approach must be taken when quantitating nanoRNA in *E. coli* cell extracts with these extraction procedures. Since only the ‘MS-2’ extraction procedure could be excluded with this data. Additional experiments were needed.

Next, the effect of the observed ion suppression on the linear response of UAU in the mass spectrometer was evaluated<sup>104</sup>. Since the ‘MS-4’ extraction procedure may best represent the *E. coli* samples quantitatively, with a significantly higher response, a set of additional samples were prepared with this procedure. Two *E. coli* cultures were prepared: wild type and *nrnB*. These two cultures were separated into four aliquots for standard addition analysis. The levels of UAU spiked for calibration were 0, 5, 10 and 15 pmoles. All solutions were analyzed using the HPLC-MS/MS method developed. The

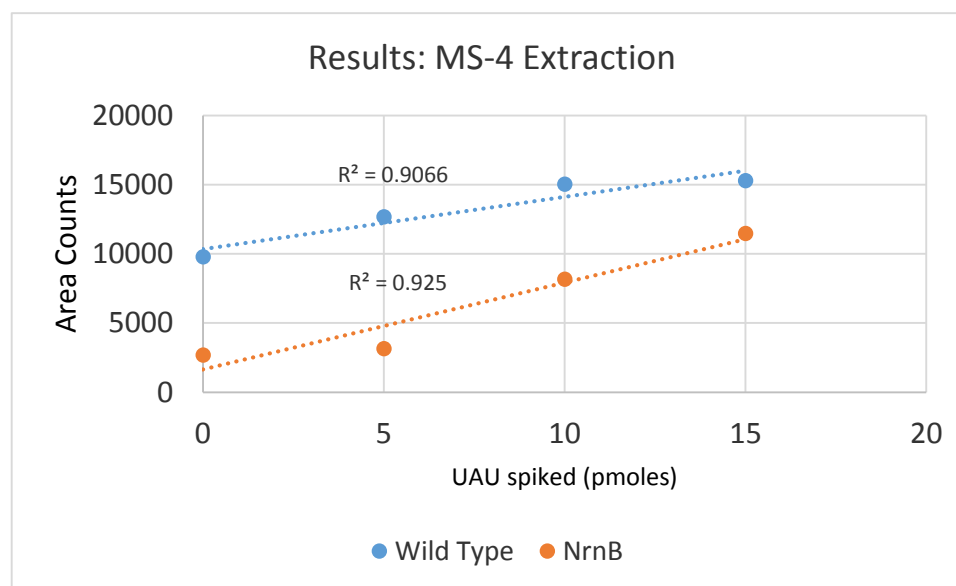


Figure 32: Standard addition linear regression for ‘MS-4’ extraction cell cultures.

results of the standard addition curves for wild type and nrnB are shown in Figure 32. The data shows there was more UAU in wild type compared to nrnB, qualitatively. However, the linear regression correlation coefficient ( $R^2$ ) of the standard addition curves were  $< 0.99$ . As previously shown, the 'MS-4' extraction procedure carries endogenous material to the analytical method. Some of which may interfere with the UAU mass spectrometer signal. This interference may cause the error seen in the standard addition curves in Figure 32. Although the 'MS-4' extraction procedure resulted in a large response, the quantitation of the sample extracts was not possible using the analytical method developed.

An analogous experiment was performed with samples extracted using the 'MS-1' procedure. The hypothesis was the 'MS-1' extraction procedure would alleviate the problem of endogenous material interfering in quantitation. The experimental conditions were similar to the previous study. Except the four samples analyzed were spiked according to 0, 5, 10 and 20 pmoles of UAU. The results of this experiment are found in

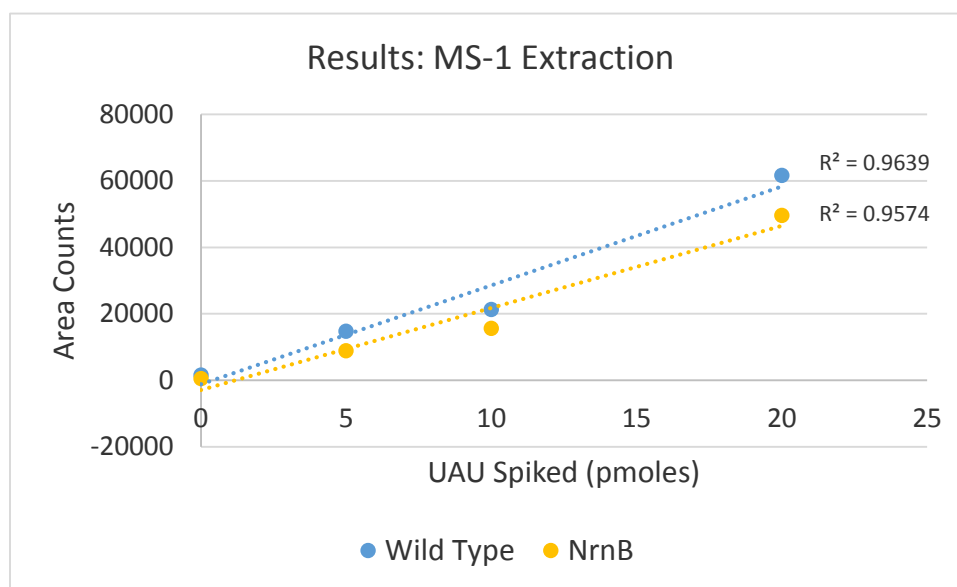


Figure 33: Standard addition linear regression for MS-1 extraction cell cultures.

Figure 33. For both wild type and nrnB *E. coli* cell extracts the standard addition curve

linear regression coefficient was  $<0.99$ . The observed results demonstrate the MS-1 extraction procedure also was not ideal for quantitative purposes. The final extraction procedure, 'MS-3', was evaluated next. However, given the unsuccessful trials of 'MS-1' and 'MS-4' extractions it was determined the cell cultures needed an additional processing step after extraction and before analysis. So prior to evaluating the MS-3 extraction samples a solid phase extraction method was developed.

#### ***4.3.2 Development of a Solid Phase Extraction Method.***

Solid-phase extraction (SPE) is a separation process by which compounds that are solvated are separated from other compounds in the solution according to their physical and chemical properties<sup>105</sup>. SPE utilizes the basic principles of chromatography to achieve separation. The stationary phase is the solid particles packed into the SPE cartridge/column. The mobile phase consists of solvents passed through the SPE cartridge/column to specifically elute desired and undesired compounds. Similar to HPLC method development the selection of a stationary phase is dictated by the compounds and the separation needed. The mobile phase is chosen based on the stationary phase and the compound's properties<sup>106</sup>.

The development of a SPE method began with selecting stationary phases based off of the properties of the nanoRNA oligomers. In our research, the primary oligonucleotides we were interested in isolating were 5', 3'-hydroxyl uridine-adenosine (UA) and 5', 3'-hydroxyl uridine-adenosine uridine (UAU). Based off of the structures of UA and UAU, in particular the phosphate backbone, the first SPE cartridges evaluated were anion exchange cartridges. It was hypothesized the positively charged groups on the SPE particles would interact with the negatively charged phosphate backbone<sup>107</sup>.

This retention would allow for the removal of some endogenous species in the *E. coli* cell extracts. The first type of stationary phase evaluated was a weak anion exchange cartridge, Waters Oasis WAX<sup>108</sup>. SPE procedures typically consists of 3-4 steps: sample loading, washing, and an elution step(s). In our development, 4+ steps were used to determine the robustness of the cartridges. For each step a fraction was collected and analyzed using HPLC-UV, at 254 nm. The conditions for the WAX column were optimized for isolation of UA and UAU. The UV chromatographs of the fractions collected are shown in Figure 34. Along with the fractions, a control solution of 100  $\mu$ M UA and UAU was overlaid for comparison. The steps used in this sequence were sample

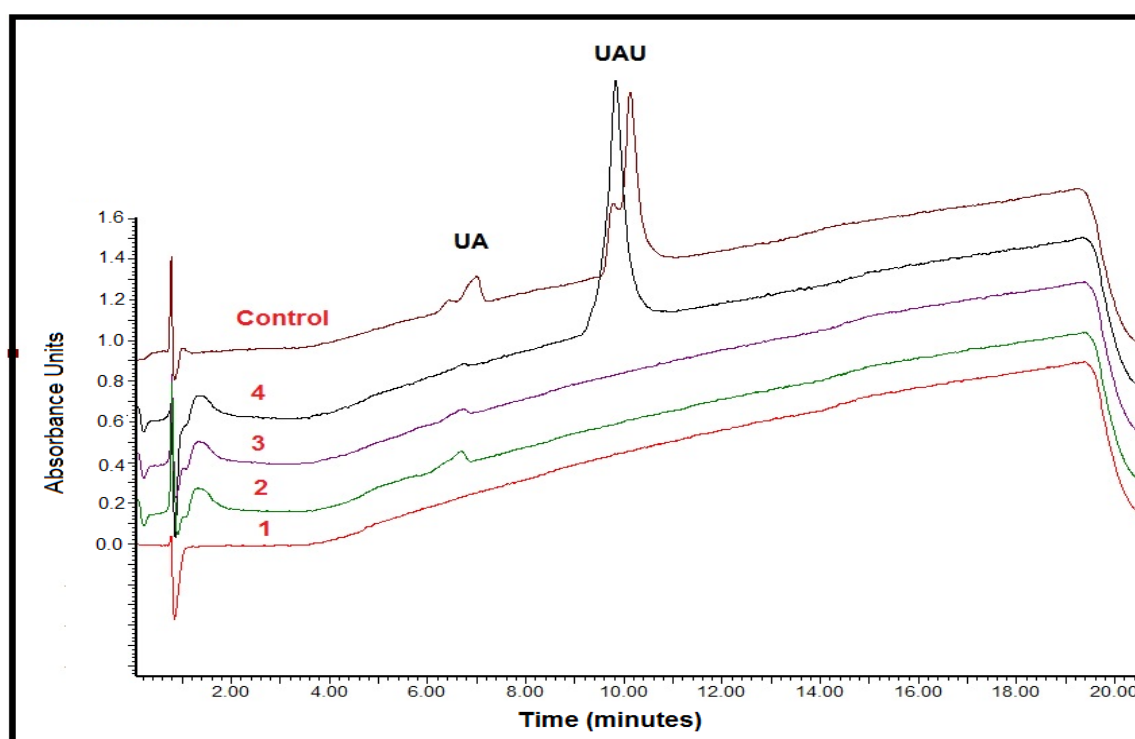


Figure 34: LC chromatographs of fractions collected from solid phase extraction of nanoRNAs with the Oasis WAX cartridge.

loading in 10% formic acid (1), washing with 10% formic acid (2), eluting with 30% acetonitrile (3) and eluting with 500mM ammonium acetate (4). The sample, 10 $\mu$ L of 100  $\mu$ M UA and UAU, was loaded in 10% formic acid because this was the solvent



composition expected from the MS-3 extraction procedure. The washing solvent was selected to simulate extra cell extraction solution being passed through the cartridge. The elution solvents (steps 3 and 4) were selected to see what attributes may cause UA and UAU to be retained, hydrophobicity or ion exchange. The results show UA starts to elute in the wash step (2) and continues eluting through each step. While UAU only elutes with ammonium acetate, through competing ionic interactions. Although this was promising for UAU, UA seems to have a very weak interaction with the cartridge.

Since UA did not interact strongly with the weak anion exchange cartridge the next cartridge evaluated was a strong anion exchange/mixed mode cartridge, Waters Oasis MAX<sup>109</sup>. The optimization of the conditions for this cartridge resulted in the same sequence of steps used for the WAX cartridge. Fractions were collected for each step and analyzed using HPLC-UV. The results, shown in Figure 35, were different from the

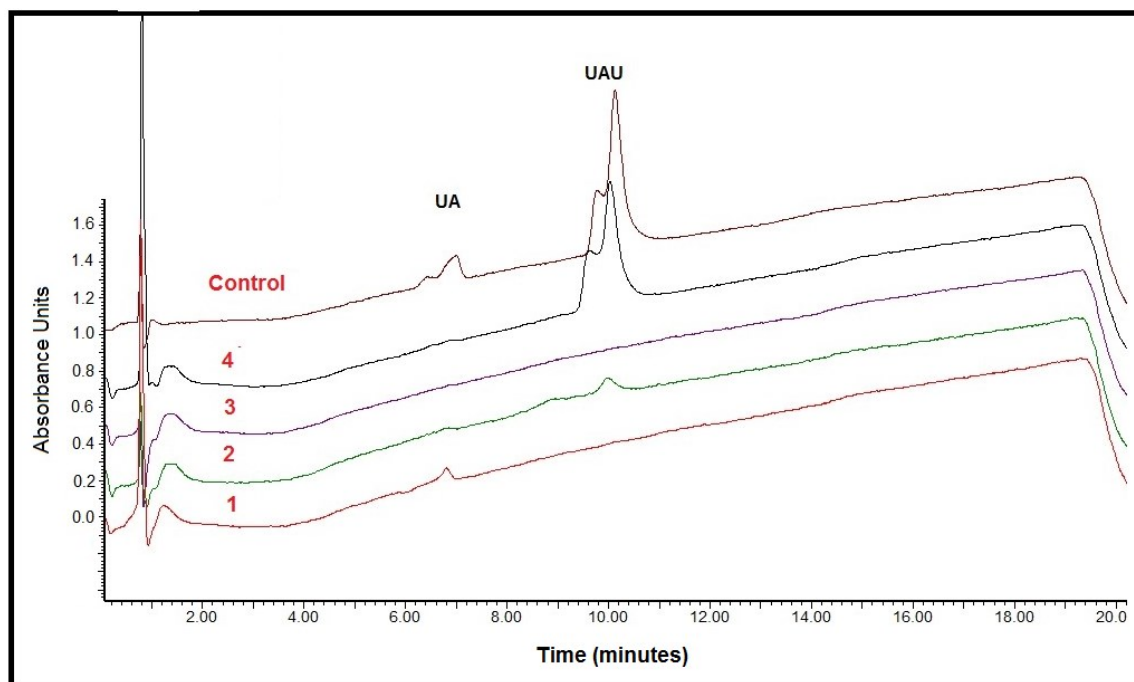
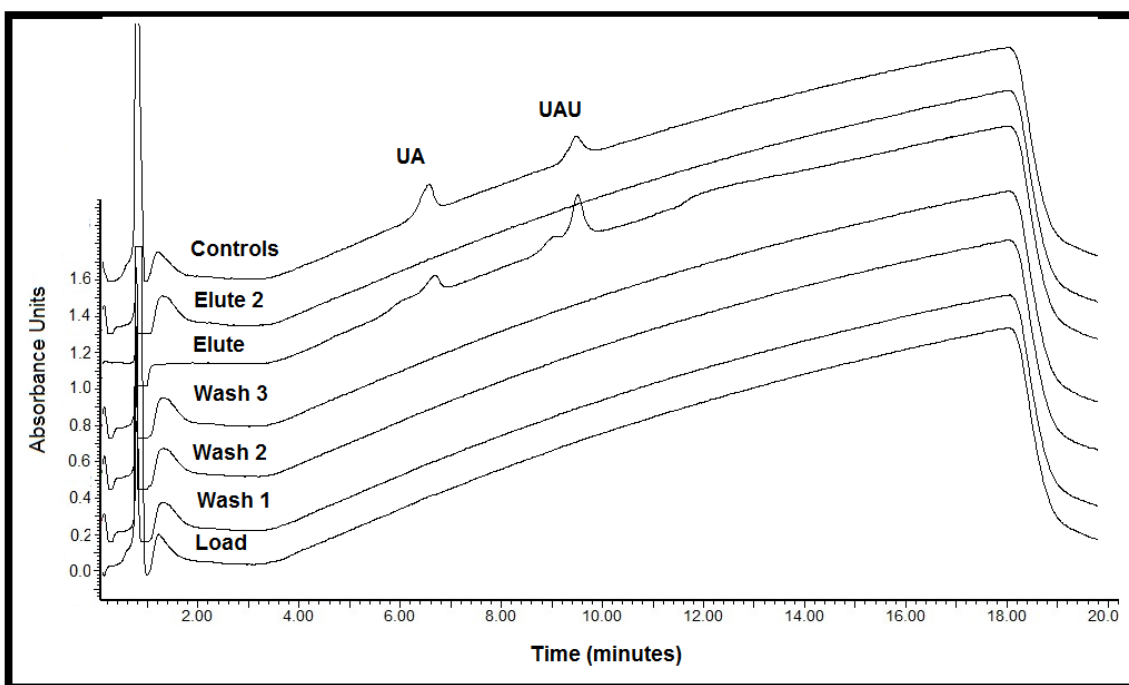


Figure 35: LC chromatographs of fractions collected from solid phase extraction of nanoRNAs with the MAX cartridge.

WAX cartridge and not expected. UA eluted from the cartridge during the load step (1)

which represents no interaction at all with the stationary phase. Also, UAU began eluting during the wash step (2) and completed eluting during the ammonium acetate step (4). Neither the WAX nor MAX anion exchange cartridges were capable of isolating both UA and UAU. Either the ionic interactions were too weak or the pH of the loading sample solution was too low for adequate interaction.

Next, it was proposed to use a reverse-phase cartridge to isolate UA and UAU. Although UA and UAU were not likely to be retained significantly without ion pairing reagent, the MS-3 extraction procedure results in a 100% aqueous sample solution. This solvent composition was ideal for reverse-phase where retention mechanism is hydrophobicity. The next cartridge evaluated was a reverse-phase C18 cartridge, Waters Sep-Pak C18<sup>110</sup>. The optimization was performed similarly to the anion-exchange



*Figure 36: LC chromatographs of fractions collected from solid phase extraction of nanoRNAs with the C18 cartridge.*

cartridges previously evaluated, except with different mobile phase solvents. The

optimal conditions for SPE of UA and UAU using the C18 cartridge were used to generate the fractions shown in Figure 36. This figure shows seven steps. Although, in practice, only three are used. The chromatographs shown are loading of 100uM UA and UAU in 10% formic acid (Load), washing with 10% formic acid 3 times (Wash 1-3), elution with 20% formic acid (Elute) and elution with acetonitrile (Elute 2). The results show retention of UA and UAU until the ‘Elute’ step. After loading, the samples were washed 3 times with 10% formic acid (‘Wash 1-3’) to demonstrate the strength of the hydrophobic interaction. Next, the RNA oligomers were effectively eluted using 20% acetonitrile (‘Elute’). To demonstrate all of the RNA oligomers were eluted previously, 100% acetonitrile was washed through the cartridge (‘Elute 2’).

Three different SPE cartridges were evaluated for isolating UA and UAU after extraction from *E. coli* cells using the MS-3 extraction procedure. The two anion exchange cartridges evaluated were inadequate at isolating both UA and UAU. The reverse phase cartridge successfully retained UA and UAU until the elution step. Going forward this SPE protocol was used previous to analyzing all *E. coli* cell culture extracts.

#### ***4.3.3 SPE Recovery of NanoRNAs from E. coli Cell Cultures.***

The solid phase extraction method was proven to isolate UA and UAU from a solution of 10% formic acid in water. Next, our goal was to demonstrate the SPE procedure was applicable to *E. coli* cell culture extract solutions. Experiments were performed to demonstrate the recovery of UA and UAU over the SPE process. For these experiments, four sample cultures were prepared (in duplicate) and subjected to the ‘MS-3’ extraction procedure previously detailed. The four cultures were wild type (stationary phase), *nrnB*, wild type (log phase), and wild type (acidified media). Two additional

negative control cultures were evaluated. The wild type (log phase) culture represents cells only grown over a 5 hour time-period versus 23 hours for wild type (stationary phase). This sample represents the exponential phase of growth which, as our collaborators proved, has fewer nanoRNAs present<sup>90</sup>. The other culture in this study was a wild type (acidified media). This culture was grown in media buffered to pH 5 which was expected to inhibit nanoRNA accumulation also.

The experiments were performed by subjecting each culture (in duplicate) to the extraction procedure ('MS 3'), separating the extract sample into 2 equivalent aliquots, spiking 1 aliquot with UA and UAU (5 pmoles/mL in diluent), performing SPE on both aliquots, lyophilizing both aliquots, re-dissolving the spiked aliquot in diluent and the unspiked in the spiking solution (5 pmoles/mL UA and UAU), and then analyzing each aliquot individually by HPLC-MS/MS for UA and UAU. For each cell culture, the peak area of the spiked before SPE and spiked after SPE samples were compared. A recovery percentage was calculated.

$$Recovery (\%) = \frac{Peak\ area\ (spiked\ before\ SPE)}{Peak\ area\ (spiked\ after\ SPE)} \times 100$$

The results of the recovery are summarized in Table 5. All cell culture recoveries were performed on duplicate sample preparations. Then the average and standard deviation of the recovery values were calculated for each RNA oligomer.

Table 5: Solid phase extraction recovery of nanoRNAs in *E. coli* cell culture extracts.

Cell Culture	Recovery (%)	
	UA	UAU
Wild Type, Stationary	100	93
	102	113
NrnB, Stationary	95	91
	81	103
Wild Type, Log	95	113
	99	122
Wild Type, Acidified Media	95	113
	99	122
<b>Average</b>	<b>95</b>	<b>109</b>
<b>Standard Deviation</b>	<b>9</b>	<b>12</b>

The results show the SPE recovery of UA was 95 % with a standard deviation of 9 % and the SPE recovery of UAU was 109 % with a standard deviation of 12 %. These results demonstrate full recovery<sup>111</sup> (within analytical error) of nanoRNAs over the SPE process. This SPE method would enable us to clean-up the samples without sacrificing yield or adding additional error.

After demonstrating recovery of the SPE method, the whole process (‘MS-3’ extraction procedure plus SPE) was evaluated using standard addition analysis. Similar to the evaluation of ‘MS-1’ and ‘MS-4’ procedures, two cultures of *E. coli* cell cultures (wild type and nrnB) were prepared, but in duplicate. The cultures were extracted for nanoRNAs using the ‘MS-3’ procedure. Then the extracts were subjected to the developed SPE protocol (only 1 wash step). Following SPE, the samples were lyophilized. Then the solid material was re-dissolved in diluent or spiking solutions of UAU. Samples were prepared at five levels: 0, 5, 10, 25, and 50 pmoles (per injection) spiked. All samples were analyzed using the HPLC-MS/MS method previously developed for monitoring UAU (880 to 574 m/z). The standard addition curves for the 1<sup>st</sup>

replicate of wild type and *nrnB* cultures are shown in Figure 37.

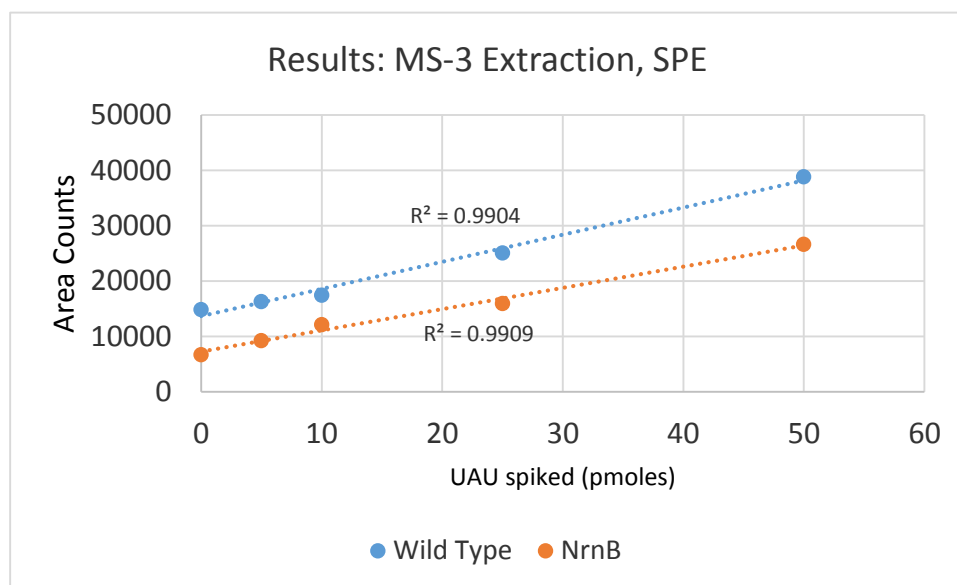


Figure 37: Standard addition linear regression for MS-3 extraction in *E. coli* cultures.

The linear regression coefficients ( $R^2$ ) are at an acceptable level,  $\geq 0.99$ . Also, the qualitative amount of UAU was larger in the wild type culture versus the *nrnB* culture. The concentration of UAU in the cell cultures calculated from the standard addition analysis for both replicates are found in Figure 38. For both replicates (analyzed on different days), the bar graph shows the same trend. However, the variability was significant. In wild type, the level was 3900 (fmoles/mL of cell culture) in the first replicate and 2800 (fmoles/mL of cell culture) in the second replicate. *NrnB* cultures had an even more significant variability with values of 800 (fmoles/mL of cell culture) and 1500 (fmoles/mL of cell culture). Despite the sample variability, these results were encouraging. We were able to successfully extract nanoRNAs and analyze them quantitatively.

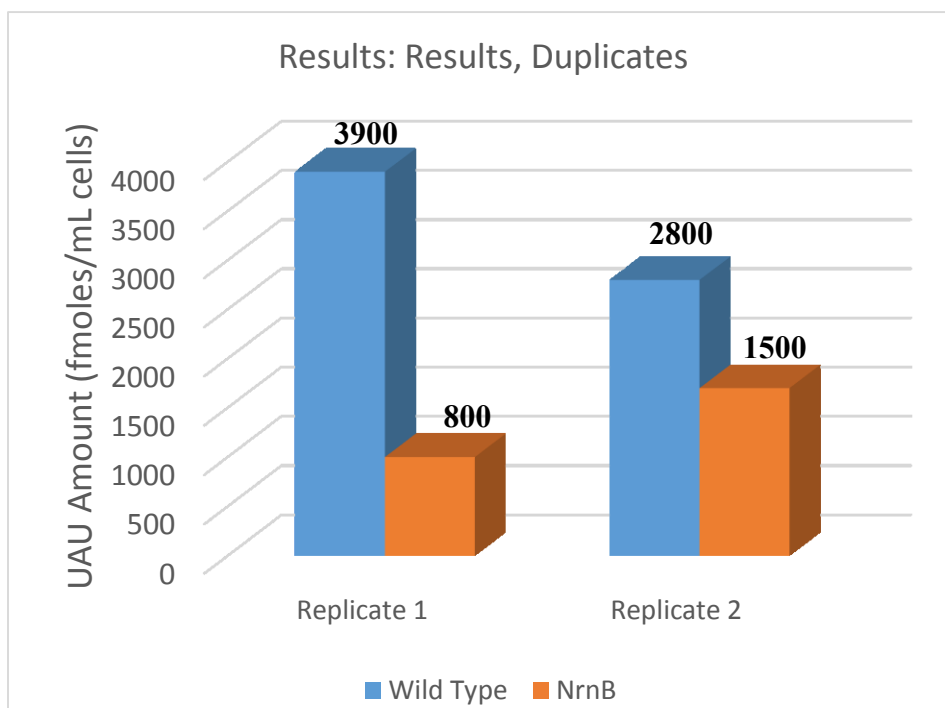


Figure 38: HPLC-MS/MS analysis of *E. coli* cell cultures for UAU (prepared in duplicate).

#### 4.4 Conclusions

In this research, the extraction of nanoRNA oligomers from *E. coli* cell cultures was evaluated. Four different procedures were performed on two cell culture types. One extraction procedure resulted in no analytical response for UAU in the mass spectrometer and was excluded as a possibility. The other three procedures were further evaluated for quantitative analysis using standard addition analysis. Two of those procedures yielded non-ideal ( $<0.99$ )

standard addition curves which could be attributed to the sample matrix and ion suppression. The final extraction procedure was not evaluated until another sample clean-up step was developed. A solid phase extraction method was developed which was demonstrated to have ‘full-recovery’. Using this additional clean-up step, the final

extraction procedure was evaluated and the results gave acceptable standard addition curves. The qualitative results also correlated with the observations made previously by our collaborators. From this research, a full sample preparation protocol has been optimized for analysis of nanoRNAs in *E. coli* cell cultures.



## Chapter 5. Validation of a HPLC-MS/MS Method for Quantitative Analysis of NanoRNAs in Escherichia coli Cell Cultures.

### 5.1 Introduction

Experiments performed previously focused on identifying several nanoRNA oligomers in *E. coli* cell cultures. These experiments involved developing a sensitive and specific HPLC-MS/MS method. This method was then used to optimize the RNA oligomer extraction procedure for *E. coli* cells. Finally, the optimized sample preparation procedure and HPLC-MS/MS method were used to qualitatively analyze the amount of a tri-nucleotide RNA oligomer in *E. coli* cell cultures, in vivo.

The research detailed in this chapter was focused on quantitating the absolute amount of two RNA oligomers in *E. coli*, in vivo. This research would further demonstrate nanoRNA mediated priming of transcription initiation in *E. coli*. The nanoRNA di-nucleotide, 5', 3'-hydroxyl uridine-adenosine, was determined to be the primary nanoRNA sequence responsible for nanoRNA-mediated transcription priming initiation<sup>90</sup>. In Figure 39, the results of high throughput put DNA sequencing of all nanoRNase-sensitive start site transcripts, in the stationary phase of *E. coli* growth, are shown. The DNA sequences with a -1/+1 TA promoter region (top) resulted in a shifted sequence ~18% in wild type (wt). While those sequences without a -1/+1 TA promoter sequence only showed shifting ~6% in wild type (wt). The -1/+1 TA promoter DNA sequence corresponds to priming by the nanoRNA of sequence UA. This experiment demonstrates UA was the nanoRNA responsible for the observed shifting of the resulting

RNA transcripts. Other experiments performed by our collaborators supported this hypothesis and excluded other possibilities.

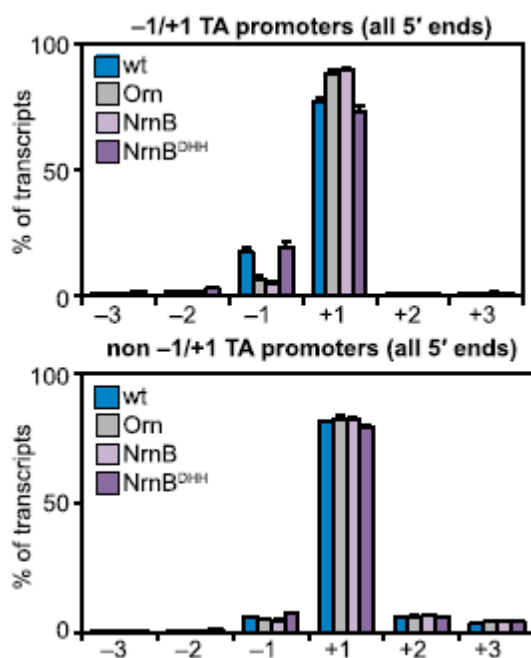


Figure 39: High throughput DNA sequencing, transcription start site shift summary<sup>90</sup>

The specific goal of the experiments performed in this research were to quantitate the absolute amount of UA and UAU (negative control) in *E. coli* cells under various physiological growth conditions. First, experiments were performed to demonstrate the quantitative ability of the HPLC-MS/MS method developed. Three mass spectrometer detectors were evaluated for this purpose. Next, a series of experiments were performed to demonstrate the levels needed for standard addition analysis of UA and UAU. Finally, absolute quantitation was performed and replicated.

## 5.2 Experimental

All solvents used were HPLC grade. Water, formic acid (98.0%), triethylammonium acetate (~1.0 M in water), and acetonitrile used were purchased from

Sigma-Aldrich (USA). All mobile phases were prepared as described using a Fisher Scientific Accumet 950 pH meter, calibrated at time of use, to measure the pH. The RNA oligonucleotides: 5', 3'-hydroxyl uridine-adenosine (UA) and 5', 3'-hydroxyl uridine-adenosine-uridine (UAU) were received from our collaborator, Dr. Bryce Nickels, at a concentration of ~1mM. Controls were diluted to the specified concentrations using 1% formic acid in water/acetonitrile (50/50).

The cell cultures were grown and extracted as follows by Dr. Seth Goldman. Single colonies of *E. coli* MG1655, containing PlacUV5(-1T) reporter plasmid pBEN 493 and either empty expression vector (pPSV38), NrnB-vsvg expression vector (pSG239), or EcOrn-vsvg expression vector (pSG243) were inoculated into 25 mL of LB broth (Miller formula; EMD Millipore) containing gentamycin (10 µg/mL) and chloramphenicol (25 µg/mL) in 125mL flasks with closures and shaken (220 RPM) at 37°C on a shaker overnight. In the morning, the cultures were diluted 1:100 into 200 mL of LB media, in a 1000 mL flask. Or diluted 1:100 in 25 mL of LB media in 125 mL flasks. This culture was thoroughly mixed and grown over 23 hours (or 5 hours for log phase) on a shaker at 37°C. At 23 hours (5 hours for log samples), the cells were harvested by centrifugation twice over, collecting the pellet. Then the pellets were re-suspended in 10% (v/v) formic acid and vigorously shaken for 60 minutes. Followed by centrifugation. Supernatants were further clarified by vacuum filtration. The optimized solid phase extraction procedure (described in Chapter 4) was used to further 'clean-up' the lysates. All cell lysates were lyophilized and re-suspended at a concentration equivalent to 10 mL of cell media per injection with or without spikes of UA and UAU.

All analysis of *E. coli* cell cultures was performed on a Thermo Surveyor HPLC with a Thermo Finnigan LTQ mass spectrometer. The liquid chromatography method used a Waters Altantis HILIC silica 3  $\mu\text{m}$  column, 2.1 mm x 150 mm. The samples were separated using a gradient mobile phase consisting of acetonitrile (A) and 25 mM triethylammonium formate buffered to pH 2 in water (B). The gradient condition was: 0–2 min, 10% B; 2–20 min, 10–35% B; 20–21 min, 35–10% B; 21–35 min, 10% B. The effluent was analyzed using in-line mass spectrometry which was equipped with an electrospray ionization interface (ESI). Peaks were detected using positive ionization mode with MS/MS detection. Mass spectrometry analysis was carried out using selected reaction monitoring (SRM) mode with an isolation width set at 2 m/z. ESI-MS/MS conditions were optimized for the specific RNA oligomer being analyzed prior to analysis. Data collection was performed by XCalibur software.

### **5.3 Results and Discussion**

#### ***5.3.1 HPLC-MS/MS Method Validation Experiments.***

Experiments were performed to demonstrate the quantitative ability of the HPLC-MS/MS method developed. These validation experiments were performed and the results were weighted against Food and Drug Administration (FDA)<sup>111</sup> and International Conference on Harmonisation (ICH) guidelines<sup>98</sup>. These guidelines define specifications a quantitative analytical method should meet. The validation experiments were performed on three different mass spectrometers: AB Sciex 4000 Qtrap (Agilent 1100 HPLC), Thermo Finnigan LCQ (Waters Alliance HPLC), and Thermo Finnigan LTQ (Thermo Surveyor HPLC). All three detectors were tested for injection reproducibility.

The LTQ mass spectrometer was further evaluated for a linear range of detection and limit-of-detection/limit-of-quantitation values were calculated.

The Thermo Finnigan LTQ mass spectrometer is a quadrupole linear ion trap mass spectrometer, as previously discussed in Chapter 1. Validation experiments performed on this detector were injection repeatability (3 levels) and linearity. These experiments used purified, commercially available, nanoRNAs which were prepared to the concentrations specified in 1% formic acid in water/acetonitrile, 50/50. Analysis was performed only on the single reaction monitoring mode using the transitions previously determined (Chapter 3): 574 m/z to 348 m/z (UA) and 880 m/z to 574 m/z (UAU). Mass spectrometer conditions were optimized specifically for each species prior to analysis.

The linear ranges for UA and UAU were evaluated from the ‘visual’ detection limit (3:1, signal-to-noise<sup>98</sup>), 0.5 pmoles/ $\mu$ L, to a level higher than any response seen in the *E. coli* samples, 20 pmoles/ $\mu$ L. The results of the average response, of duplicate injections, for each level are summarized in Table 6. The linear regression analysis (calibration curves) for both UA and UAU are shown in Figure 40.

*Table 6: Thermo Finnigan LTQ linearity raw data.*

<b>Thermo Finnigan LTQ Linearity</b>		
Concentration (pmoles/ $\mu$ L)	UA Average Response (counts)	UAU Average Response (counts)
0.5	1819	212
1	3291	395
2.5	9978	1319
5	16924	2941
10	32823	6493
20	70773	13528

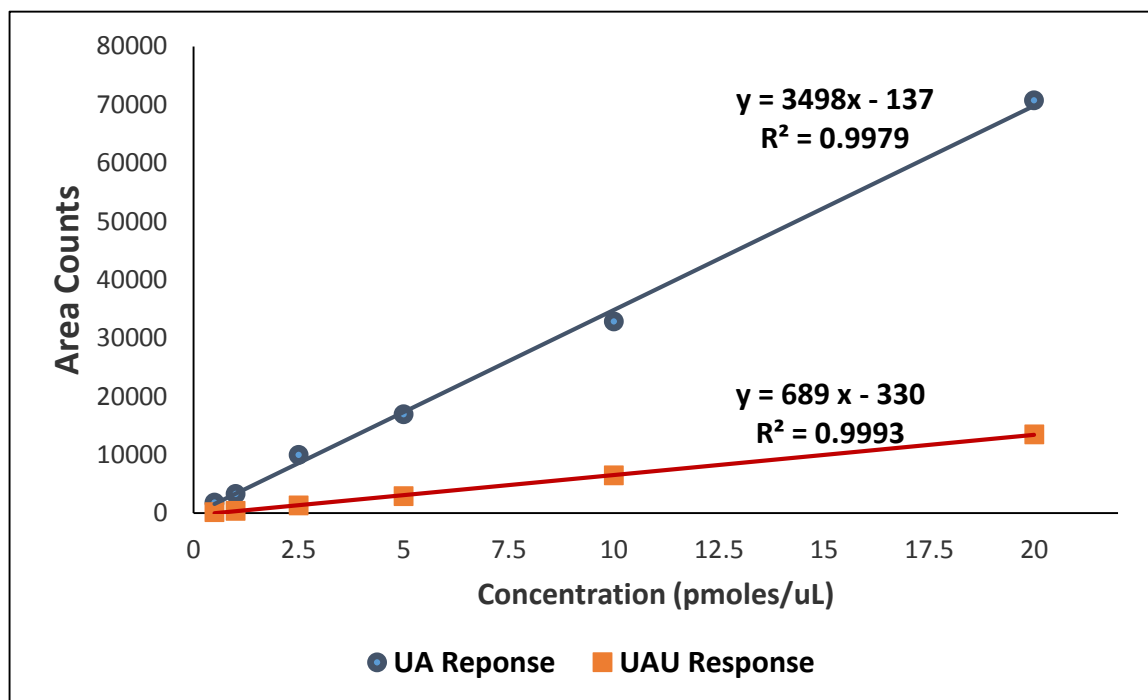


Figure 40: Thermo Finnigan LTQ linear regression results.

The results demonstrate a linear response for both UA and UAU over the range, 0.5 – 20 pmoles/ $\mu$ L, with both linear regression coefficients  $>0.995$ . The response for UA was greater than UAU under the conditions analyzed. As seen in Table 6, the 0.5 pmoles/ $\mu$ L response was 1819 counts for UA versus 212 counts for UAU. Also, the slope of the linear regression curve for UA was steeper (larger) than that of UAU, 3498 versus 689, respectively.

The reproducibility of the method was also evaluated for injection repeatability. On the LTQ system, injection repeatability was tested at 3 different levels with 8 injections at each level. From this analysis, the % coefficient of variation and the limit-of-detection/limit-of quantitation were calculated for both UA and UAU. The results are in Table 7.

Table 7: Reproducibility and limit-of-detection/limit-of-quantitation analysis for the LTQ system.

Concentration (pmoles/ $\mu$ L)	CV (%)		LOD/LOQ (pmoles/ $\mu$ L)	
	UA	UAU	UA	UAU
0.5	14.9%	17.8%		
1	5.3%	12.3%	0.2/0.8	0.2/0.6
2.5	8.4%	10.3%		

LOD: Limit of detection,  $3\sigma/\text{slope}$  LOQ: Limit of quantitation,  $10\sigma/\text{slope}$  CV = coefficient of variation,  $\sigma$  is the standard deviation of the lowest standard

The % coefficient of variance (% CV) was calculated as the ratio of the standard deviation to the mean multiplied by 100. This value represents the precision of the whole HPLC-MS/MS analytical procedure. Around the detection limit, 0.5 pmoles/ $\mu$ L, the values are ~15-18 % for UA and UAU. Using the ‘FDA Guidance for Industry Bioanalytical Method Validation’<sup>111</sup> as our reference the % CV values meet the 20% criteria for the lower limit of quantitation (LLOQ). At the two higher levels, 1 and 2.5 pmoles/ $\mu$ L, all % CV values are also acceptable, or  $\leq 15\%$ . The limit-of-quantitation (LOQ) and limit-of-detection (LOD) were calculated according to the International Conference on Harmonisation (ICH) guidelines<sup>98</sup>. The LOD for UA and UAU was calculated to be the same, 0.2 pmoles/ $\mu$ L. The LOQ was determined to be a little lower for UAU than UA at 0.6 pmoles/ $\mu$ L versus 0.8 pmoles/ $\mu$ L, respectively. The results of these validation experiments for the Thermo Finnigan LTQ system provided confidence in the quantitative ability of our analytical procedure.

Throughout our research, other types of mass spectrometers were utilized. In Tables 8 and 9, the injection repeatability results of a Thermo Finnigan LCQ system and AB Sciex 4000 Qtrap system are summarized, respectively. The LCQ system, a quadrupole ion trap, was also run using selected reaction monitoring mode for analysis of

UAU. Due to the instrument configuration, the direct flow of HPLC eluent goes directly into the heated capillary, high ion suppression was observed with this mass spectrometer. The lowest level of response, detection limit, for UAU observed was 5 pmoles/ $\mu$ L and the quantitation limit was considered 20 pmoles / $\mu$ L. Table 8 shows the results of the injection repeatability at the ‘visual’ quantitation limits (s/n ratio, 10:1).

*Table 8: Injection repeatability on the LCQ system.*

<b>Concentration: 20 pmoles/<math>\mu</math>L</b>	
<b>Replicate</b>	<b>UAU Response (Counts)</b>
1	1055071
2	1103488
3	1346297
4	1142593
5	1407470
Average	1210984
Standard Deviation	156091
% CV	12.9%

The % CV at the quantitation limit was acceptable ( $\leq 20\%$ ) and was comparable to the % CV at the quantitation limit for UAU in the LTQ mass spectrometer. The other mass spectrometer tested for injection repeatability was the AB Sciex 4000 Qtrap. The quantitation limit of this mass detector was the lowest at  $\sim 0.075$  pmoles/ $\mu$ L (75 fmoles/ $\mu$ L). The injection repeatability was also the most precise, see Table 9. The Qtrap had a % CV of 2.46 % at the quantitation limit for UAU compared to  $\sim 12\%$  for the LCQ and LTQ at the corresponding quantitation limits.



Table 9: Injection Repeatability on the Qtrap system.

Concentration: 75 fmoles/ $\mu$ L	
Replicate	UAU Response (Counts)
1	3153
2	3109
3	3111
4	3159
5	3211
6	3317
7	3263
Average	3189
Standard Deviation	78.6
% CV	2.46%

### 5.3.2 Preliminary Quantitative *E. coli* Cell Culture Analysis.

A preliminary analysis of *E. coli* cell cultures was performed to demonstrate sample reproducibility using the HPLC-LTQ system as this was the most sensitive instrument available to us at the time. In this study, triplicate cell cultures were prepared, at a 200 mL cell media volume, for two types of cell culture media. The media types used were unbuffered Luria Broth (LB) and pH 5 buffered Luria Broth. Altogether, six cultures (3 unbuffered and 3 buffered) were extracted using the optimized extraction procedure (Chapter 3), ‘cleaned up’ using SPE, concentrated by lyophilization and re-dissolved in diluent. After re-dissolving in diluent, the unbuffered wild type replicates were split into two solutions. One solution was left ‘as is’ and the other was diluted 2x in diluent. These diluted, unbuffered wild type replicates were prepared to evaluate the cell concentration effect on the analytical method and results. Standard addition quantitation was used. So each replicate (9 in total) was prepared to contain aliquots of 0, 10k, 25k,

50k and 100k fmoles/injection of UA and UAU. All the aliquots were analyzed using the developed HPLC-MS/MS method. The results of this study are in Table 10.

*Table 10: Preliminary analysis of E. coli cell cultures (in triplicate).*

Cell Culture	RNA Oligo	Calculated Amount (fmoles/mL cell media)			Average	% CV
		1	2	3		
Wild Type	UA	3500	4400	7500	<b>5100</b>	<b>41</b>
	UAU	1800	3700	2300	<b>2600</b>	<b>38</b>
Wild Type 2x diluted analysis	UA	5000	4200	9400	<b>6200</b>	<b>45</b>
	UAU	2400	2000	<1000	<b>2200</b>	<b>13</b>
Wild Type buffered pH 5	UA	4500	7300	6000	<b>5900</b>	<b>24</b>
	UAU	<500	<500	<500	<b>&lt;500</b>	<b>NA</b>

As expected for all 3 cell culture samples the amount of UA was higher than UAU. For example, the average value for the ‘Wild Type’ of UA was 5100 fmoles/mL cell media versus 2600 fmoles/mL cell media for UAU. This trend supports the hypothesis UA di-nucleotide was more responsible for the transcription initiation priming than UAU given the higher concentration. The high level of UA in the ‘Wild Type buffered pH 5’ replicates was not expected. The UA average value in ‘Wild Type buffered pH 5’ was within analytical error (+/- 20%) of the other cell culture samples at 5900 fmoles/mL cell media. The ‘Wild Type buffered pH 5’ sample was expected to have a lower level of both UA and UAU than the unbuffered samples due to the pH effect on cell growth<sup>112</sup>. The other unexpected observation of this study was the significant % CV values, sample precision. The analytical precision was already established to be less than 20% during the validation studies on this system. The sample precision for the unbuffered wild type samples was around 40% as shown in the table. The ‘Wild Type buffered pH 5’ sample had a more reasonable sample precision at 25 % CV. Overall, the

results of this study demonstrated the quantitative ability of the developed HPLC-MS/MS method and defined the level of UA and UAU expected in the wild type samples.

However, the sample precision was not ideal.

A second preliminary analysis of *E. coli* cell cultures was performed to address the sample precision. In this study, three different cell cultures were prepared in triplicate. The three cultures prepared were wild type, *nrnB*, and *orn*. The oligoribonucleases, *nrnB* and *orn*, were used as negative controls as previously discussed. To address the high sample variability in the previous study, the cultures were prepared in smaller volumes and pooled. For each replicate, 8 cultures of 25 mL of cell media were grown independently to stationary phase (23 hours) and then pooled prior to extraction. All replicates were extracted, ‘cleaned-up’ by SPE, concentrated and re-constituted the same as the previous study. No diluted wild type extraction was prepared. The same standard addition levels were used as the previous study. The raw data was analyzed the same, except a ‘Total Error (%)’ was also calculated.

To better define the error in our analysis, the average variance between the calculated amount (back-calculated from the standard addition equation) and the spiked amount of all 5 injections was calculated for each replicate. The equation used was:

$$Average\ Variance = \sqrt{\left( \frac{\sum_{injections} (Spiked\ Amount - Calculated\ Amount)^2}{\#\ of\ injections} \right)}$$

This average variance of each replicate was then averaged over the 3 replicates. Then the combined average variance was summed with the coefficient of variation (between replicates) to get a ‘Total Error’. Finally, the ‘Total Error’ was expressed as a ratio to the average calculated value and multiplied by 100 to give the ‘Total Error (%)’.

The results of the second preliminary analysis are shown in Table 11. The results were as expected. Overall, UA had significantly higher amounts than UAU, in the wild type, 8500 fmoles/mL cell media versus 1200 fmoles/mL cell media, respectively. Also, the ‘Wild Type’ cell culture had more nanoRNA present than the cultures which contained nrnB and orn. These oligoribonucleases were expected to degrade the nanoRNAs and the results support this.

*Table 11: Second preliminary analysis of various cell cultures (in triplicate).*

Cell Culture	RNA Oligo	Calculated Amount (fmoles/mL cell media)			Average	CV (%)	Total Error (%)
		1	2	3			
Wild Type	UA	9600	8900	10100*	<b>9500</b>	<b>6</b>	<b>8</b>
	UAU	<1000	<1000	1700	<b>1200</b>	<b>33</b>	<b>58</b>
Nrnb	UA	<2500**	<1000	<1000	<b>&lt;2500</b>	<b>NA</b>	<b>NA</b>
	UAU	<1000	<1000	<1000	<b>&lt;1000</b>	<b>NA</b>	<b>NA</b>
Orn	UA	3700	2800	4500**	<b>3700</b>	<b>23</b>	<b>28</b>
	UAU	<1000	<1000	<1000	<b>&lt;1000</b>	<b>NA</b>	<b>NA</b>

\*Quantitation only performed with 3 injections \*\*Quantitation only performed with 4 injections, quantitation limit defined as 2500 fmoles/mL

No nanoRNAs were present above the quantitation limit, 1000 fmoles/mL cell media, for the nrnB culture. The orn culture had ~60% less UA than the wild type culture. Another observation was the sample precision in this study was greatly improved compared to the previous study. For UA in ‘Wild Type’ the %CV was 6% versus ~40% for ‘Wild Type’ in the previous study (Table 10). The only concern with the data in this study was the UA ion suppression and its effect on the quantitation limit.

As footnoted in Table 11, three of the UA calculated amounts were derived using fewer injections (typically 5) due to concerns over the quantitation limit. The lower level

standard addition responses (10 and 25 pmoles/injection) could not be distinguished from the un-spiked response. Figure 41, shows the standard addition curves for the 3 replicates

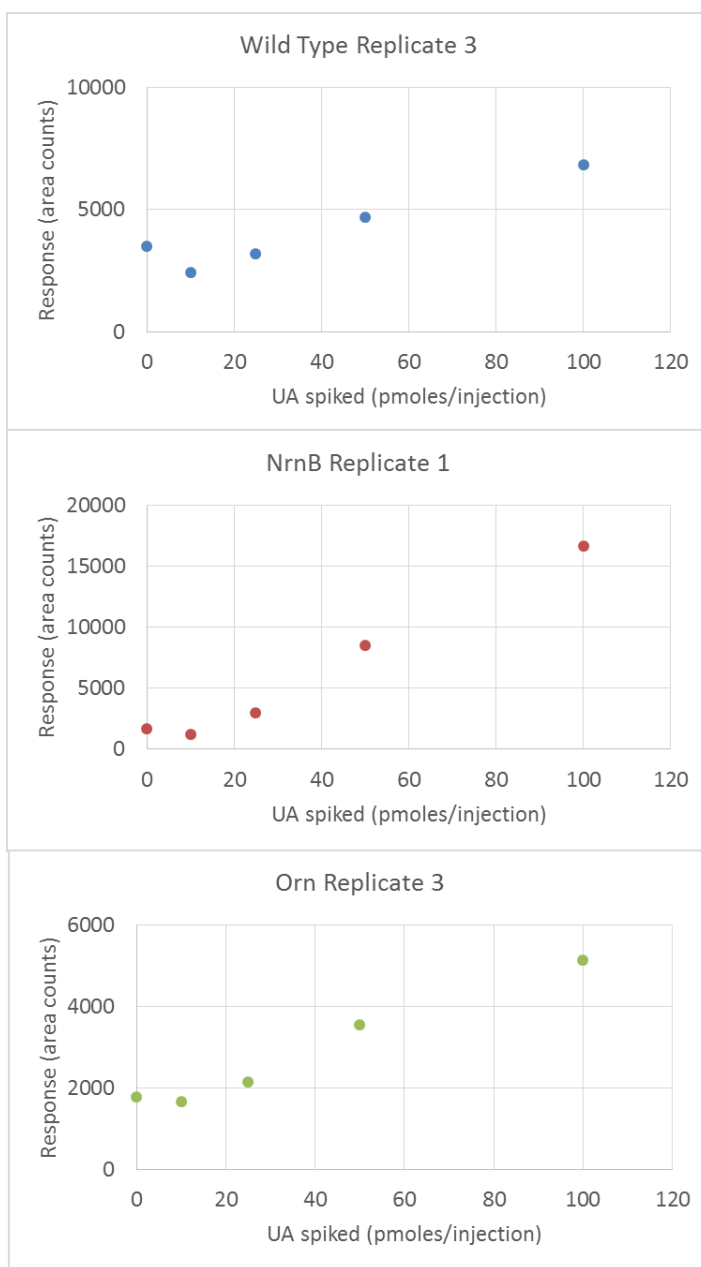


*Figure 41: Second preliminary analysis standard addition curves for E. coli cell cultures.*

in this study where the addition of UA at the lower level(s) appears to be in the noise due to ion suppression. As observed in 'Wild Type Replicate 3' the 10 pmoles/injection and 25 pmoles/injection standards could not be used in the analysis. For 'NrnB Replicate 1'

and ‘Orn Replicate 3’, the 10 pmoles/injection standard could not be used. The significance of this was the uncertainty ion suppression adds to the analysis. This uncertainty in the LOQ was taken into consideration for future analysis.

### **5.3.3 *Quantitative Analysis of NanoRNAs in E. coli Cell Cultures***

Following the two preliminary studies performed on the HPLC-LTQ system, a more comprehensive experiment was set-up. To fully demonstrate the presence of nanoRNAs, in particular UA, in cells during nanoRNA-mediated transcription initiation priming several conditions needed to be compared. This study compared 4 different cell cultures prepared in triplicate. The cultures prepared were wild type grown to stationary phase (23 hours), wild type grown to log phase (5 hours), *nrnB* active grown to stationary phase (23 hours), and wild type in acidified media grown to stationary phase (23 hours). All cultures were grown in 25 mL cell media batches. For all stationary phase replicates, 8 batches were pooled to make one replicate. For the log phase replicates, 24 batches were pooled to make one replicate. After pooling, all replicates were extracted, underwent solid phase extraction, concentrated by lyophilization, and re-constituted in diluent. For each replicate, five aliquots were prepared to contain standard addition levels of UA and UAU at 0, 10k, 25k, 50k and 100k fmoles/injection.

Figure 42, compares all the stationary phase cultures in fmoles/mL cell media for each stationary phase cell culture along with error bars. The error bars are the ‘Total

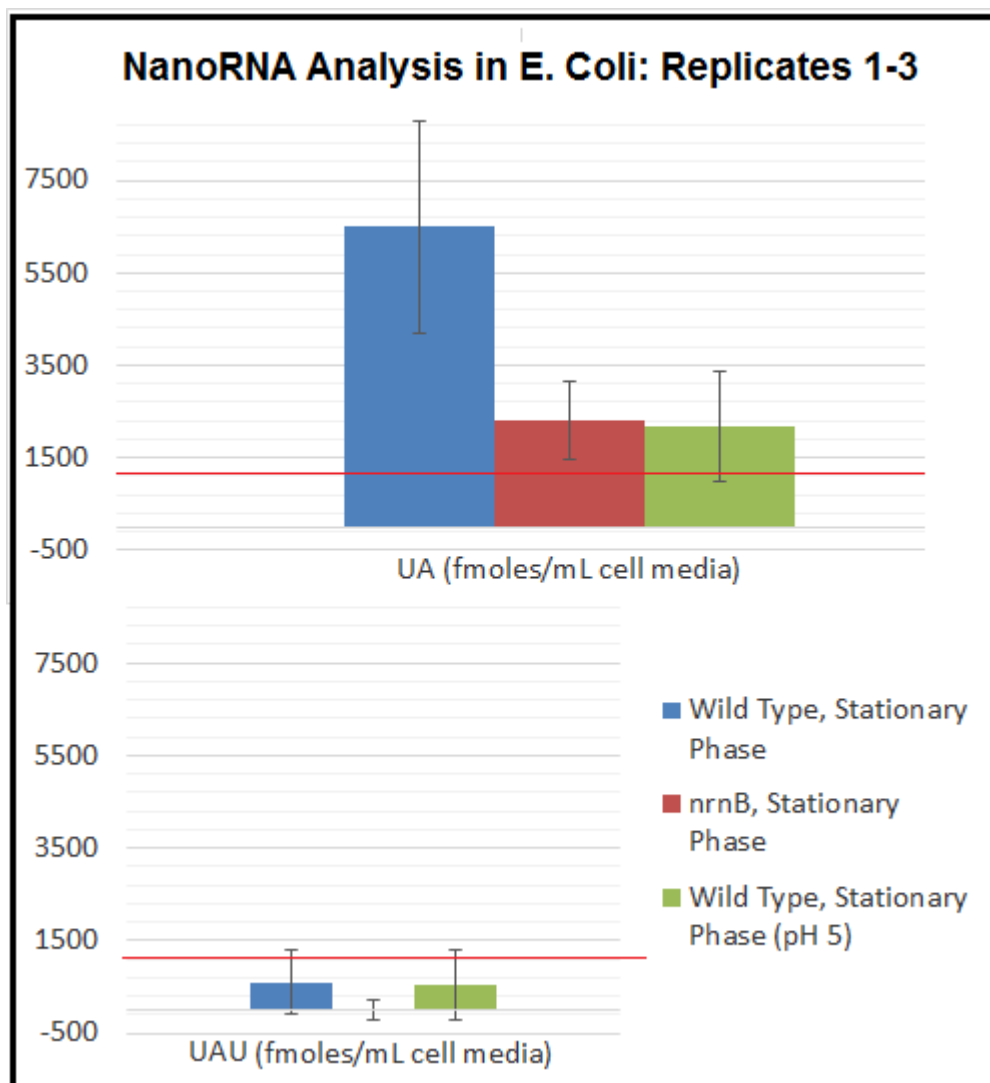


Figure 42: NanoRNA quantitation results of 'Analysis 1' stationary phase cultures.

Error' calculated as described previously. The results confirm the hypothesis of UA being more prevalent than UAU in all stationary phase cultures. The average amount of UAU was below the quantitation limit (1000 fmoles/mL cell media) in all cultures. Also, the results demonstrate higher levels of UA in the 'Wild Type, Stationary Phase' versus the 'nrnB, Stationary Phase' and 'Wild Type, Stationary Phase (pH 5)'. In Figure 43, the stationary phase cultures are compared to the log phase by plotting the pmoles/OD, where 1 OD/mL represents  $\sim 1 \times 10^9$  cells<sup>113</sup>. For this comparison, the optical density of the cell

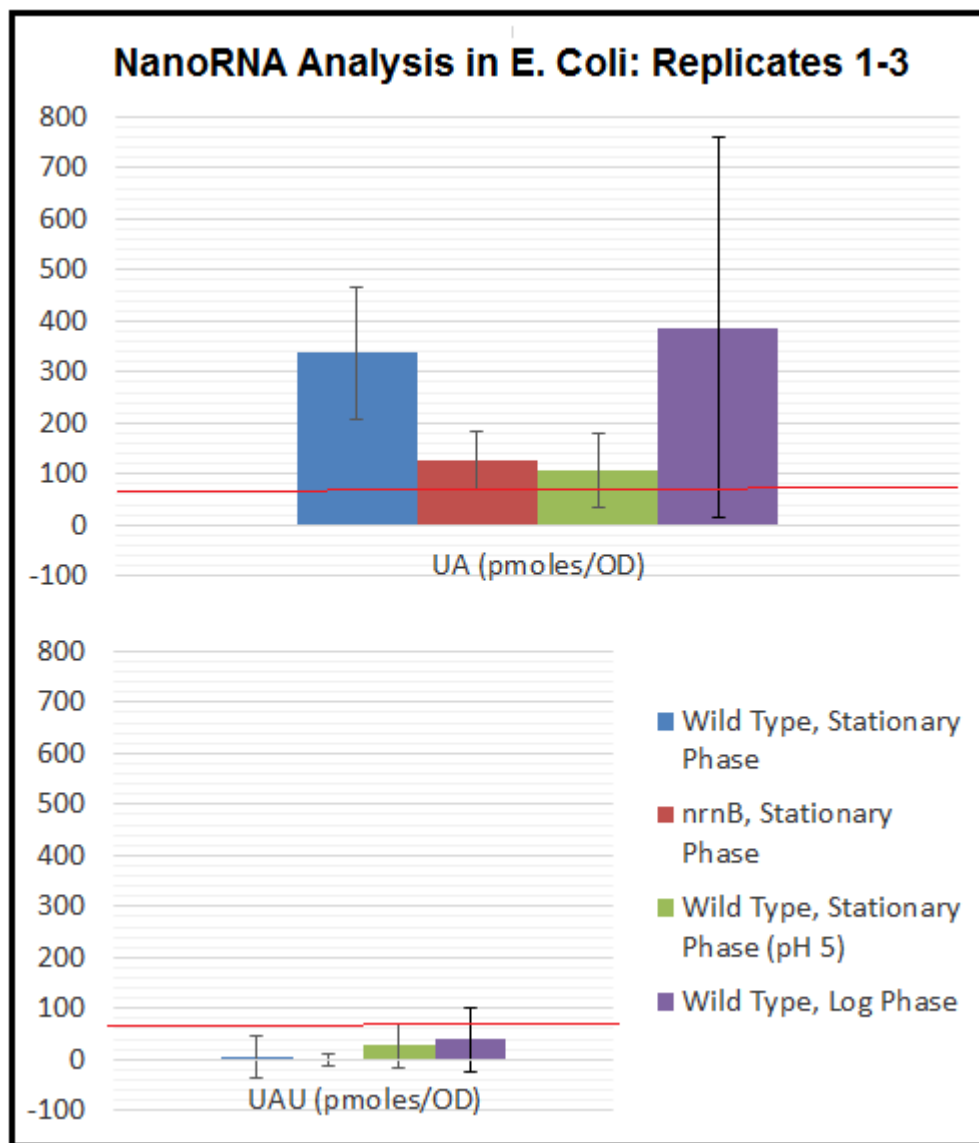


Figure 43: NanoRNA quantitation results, Analysis 1, log vs. stationary phase.

cultures, at 600 nm, was factored into the calculated amounts. This was necessary as the log phase has significantly less cells per volume of cell media. As the results show, the trends for the stationary phase cultures were the same as the OD values were similar. The comparison of the wild type log phase and stationary phase cultures revealed a qualitative trend which was unexpected. It was hypothesized in log phase primarily nucleotide triphosphates are responsible for transcription initiation priming so the level of



nanoRNAs should be less in log phase than stationary phase<sup>90</sup>. This was not the trend observed; however, the significant error associated with the log phase culture analysis makes this result inconclusive.

The results of this quantitative analysis (Analysis 1, replicates 1-3) demonstrated the expected trends with the exception of the log phase culture. The only concern with the results was the amount of ‘Total Error’ (Table 12). The % CV between the replicates was between 35% - 50% for UA. For UAU all results were below the quantitation limit. This error was mostly attributed to the sample precision as the ‘Total Error (%)’ was similar

*Table 12: Summary of ‘Analysis 1’ results.*

<b>Analysis 1 (Replicates 1-3): Results</b>				
<b>Cell Culture</b>	<b>RNA Oligo</b>	<b>Average Amount (fmol/mL cell media)</b>	<b>CV (%)</b>	<b>Total Error (%)</b>
Wild Type, Stationary Phase	UA	6500	35	35
	UAU	<1000	NA	NA
nrnB, Stationary Phase	UA	2300	36	36
	UAU	<1000	NA	NA
Wild Type, Stationary Phase (pH 5)	UA	2200	50	55
	UAU	<1000	NA	NA

(+/- 10%) to the % CV in all cultures. To address the error an additional 3 replicates of each culture were prepared identically and analyzed by HPLC-MS/MS, ‘Analysis 2’. The rationale behind this experiment was to generate additional data points for each culture and reduce the error in the sample precision.

In the second analysis (Analysis 2, replicates 4-6), the same four cultures were prepared and analyzed exactly the same way. The analysis of these replicates did not

proceed as expected. In Table 13, the standard addition linear regression coefficients of determination ( $R^2$ ) are shown for each cell culture replicate and nanoRNA. Values determined to be acceptable were  $\geq 0.98$  and are in bold typeface. As observed, only the

Table 13: 'Analysis 2' standard addition linear regression  $R^2$  values

Cell Culture	Replicate	$R^2$	
		UA	UAU
Wild Type, Stationary Phase	4	0.90	<b>0.98</b>
	5	0.88	0.95
	6	0.88	<b>1.00</b>
Wild Type, Log Phase	4	0.69	<b>0.99</b>
	5	0.18	<b>0.99</b>
	6	0.76	0.74
NrnB, Stationary Phase	4	0.77	<b>0.99</b>
	5	0.33	<b>0.99</b>
	6	0.83	0.85
Wild Type, Stationary Phase, pH 5	4	<b>1.00</b>	<b>1.00</b>
	5	<b>1.00</b>	<b>0.99</b>
	6	<b>0.98</b>	<b>1.00</b>

'Wild Type, Stationary Phase, pH 5' culture had acceptable  $R^2$  values for both UA and UAU. All the other UA results were not acceptable. More replicates had acceptable  $R^2$  values for UAU; however, given the corresponding UA values had  $R^2 < 0.90$ , these results

Table 14: Control Injections of 'Analysis 2'

Control Injections: 10 pmoles/injection			
Replicate	RNA Oligo	Average Response (counts)	% CV
4	UA	755	6
	UAU	124	7
5	UA	938	4
	UAU	372	6
6	UA	862	6
	UAU	343	15
Combined (interday)	UA	852	11
	UAU	280	48

were not used. To evaluate the cause of this error the control solutions were analyzed. Control solutions of UA and UAU were analyzed before, during and after the samples ( $n = 3$ ), each day (1 set per day over 3 days). This was routinely done to ensure the instrument was running efficiently. The % CV values for each day (each replicate) are shown in Table 14. All precision values (UA and UAU) were 15 % CV or less intraday. The inter-day precision value of UA was also below 15% CV. The inter-day precision of UAU was a higher at 48%, but each sample replicate was finished within the day (intraday) and this error was unlikely to account for the observed standard addition error (Table 13). Due to the lack of sample, troubleshooting this error further was not possible. Only the analysis of 'Wild Type, Stationary Phase, pH 5' culture from 'Analysis 2' could be combined with the results from 'Analysis 1' (replicates 1-3).

Due to the unacceptable results in 'Analysis 2' (replicates 4-6), third set of triplicate samples, Analysis 3 (replicates 7-9,) were prepared for the 'Wild Type, Stationary Phase', 'Wild Type, Log Phase' and the 'NrnB, Stationary Phase' cultures. The cultures were prepared and analyzed as previously described. For this analysis all reagents used were newly purchased. The error seen in 'Analysis 2' may have been caused by reagent contamination and this would eliminate that possibility. Again some of the results yielded a non-linear standard addition curve. The 'Wild Type, Log Phase' replicates 7-9 results were not used. The results of the other two cultures are in Table 15. The standard addition curves for these replicates/samples in this table were acceptable. As observed, 'Analysis 3' for 'Wild Type, Stationary Phase' had significantly higher

Table 15: Summarized results of 'Analysis 3'

Analysis 3 (Replicates 7-9): Results			
Cell Culture	RNA Oligo	Calculated Amount (fmoles/mL cell media)	Total Error (%)
Wild Type, Stationary Phase	UA	18300	36
	UAU	2067	67
NrnB, Stationary Phase	UA	7900	8
	UAU	<1000	NA

values of UA and UAU than 'Analysis 1' (Table 12). The same observation was made for the 'nrnB, Stationary Phase' culture. However, the error (Total Error %) remained at or below the level achieved previously (~35% or less) for UA. UAU error could not be compared. The cause of these higher values was not determined.

Table 16: Summarize results: Quantitation of nanoRNAs in *E. coli* cell cultures.

Combined Analysis (6 replicates): Results			
Cell Culture	RNA Oligo	Average Amount (fmoles/mL cell media)	Total Error (%)
Wild Type, Stationary Phase	UA	12400	63
	UAU	1600	69
NrnB, Stationary Phase	UA	5100	64
	UAU	1000	23
Wild Type, Stationary Phase (pH 5)	UA	2200	43
	UAU	1100	43

The combined the results of Analysis 1, 2, and 3 yields 6 replicates for each 'Wild Type, Stationary Phase', 'Wild Type, Stationary Phase (pH 5)' and the 'NrnB, Stationary Phase' cultures. The combined results are shown in Table 16 and Figure 44. The 'Total Error (%)' for UA was high for all 3 cultures, 43% - 64 %. A lot of this error was from the difference between the preparation of the different analysis groups 1, 2, and 3. The error in each analysis, previously discussed, was significantly lower for UA than the combined error. UAU in all cultures was found to be near or below the quantitation limit of the method and always lower than the UA amount. The error in the UAU analysis

ranged from 23% to 69%. Since the level of UAU was near the LOQ, this high level of error was expected. Figure 44, displays the trends which were hypothesized. The

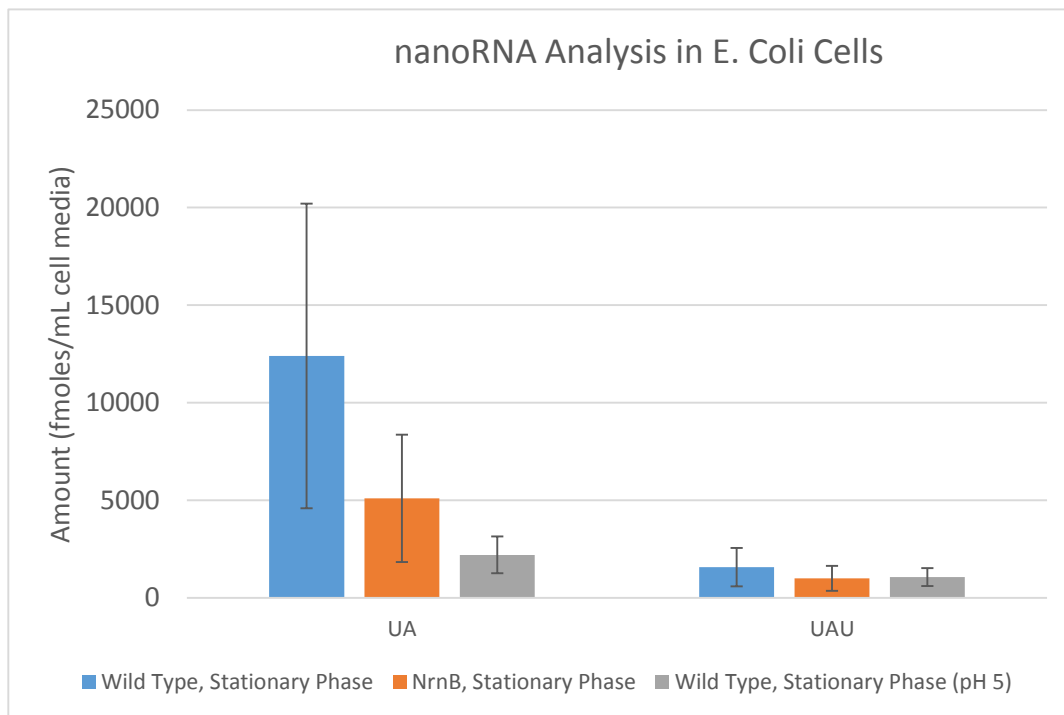


Figure 44: Summarized results: Quantitation of nanoRNAs in *E. coli* cell cultures.

amount of UA in the ‘Wild Type, Stationary Phase’ culture was the highest of all the cultures evaluated. Also, the amount of UAU was statistically less than UA in all cultures. However, the error in the analysis, shown by the error bars, was significant and concerning.

## 5.4 Conclusions

In this research, validation studies were successfully performed on multiple systems which demonstrated the quantitative ability of the developed HPLC-MS/MS method. This method was then used to perform preliminary analysis of various *E. coli* cell cultures and optimize the experimental set-up. This preliminary analysis gave

confidence in the procedures developed. Finally, three sets of samples were analyzed which generated quantitative data for three cell cultures. The quantitative results were compared to our hypotheses and supported them<sup>99</sup>. However, the error of the combined analysis was larger than desired. The research demonstrates the ability to quantitate nanoRNAs in *E. coli* cells.

## Chapter 6. Development of a Protocol for the Isolation, Purification and Identification of a Colonic Epithelial Protein

### 6.1 Introduction

Over 25 years ago a novel monoclonal antibody, mAb Das-1, was generated<sup>21</sup> by hybridoma technology. A little over 10 years later a specific antigen of mAb Das-1 was found in colon epithelial cells<sup>25</sup>, appropriately named the colon epithelial protein (CEP). Since CEP's discovery very little information has been gathered on the structure of CEP. However, it has been observed in precancerous and cancerous conditions. More specifically, CEP was tracked to various pre-cancerous conditions of the upper GI tract such as Barrett's epithelium (BE)<sup>26</sup>, gastric intestinal metaplasia (GIM)<sup>27</sup>, intraductal papillary mucinous neoplasm (IPMN)<sup>28</sup>, and the respective cancerous conditions. The expression of CEP in these clinical conditions have been found to be highly sensitive (80–100%) and specific (90-100%). Defining the significance of CEP.

One of the first studies of CEP itself was investigating its origin by examining fetal tissue<sup>25</sup>. Using tissue from 7-24 weeks old human fetuses, mAb Das-1 reacted with cells in organs arising from the pharyngeal cleft (thymus) and the primitive gut (oral cavity, pharynx, lung, esophagus, stomach, biliary tree, pancreas, liver, colon). In adult tissues, however, mAb Das-1 reactivity was restricted to the colon and biliary epithelium, keratinocytes, and ciliary body. This led to the belief CEP is an oncofetal protein. Following this important discovery, more studies were performed which identified CEP as a membrane-associated protein<sup>24</sup> and determined its molecular weight to be more than 200 kDa<sup>23</sup>. Through these discoveries, a protocol was developed to isolate CEP rich

colon cell supernatant. However, attempts to purify and characterize CEP by affinity methods have been unsuccessful. Although, these studies have provided greater understanding of its binding properties. And its binding with lectins, in particular, led to the hypothesis CEP is a glycoprotein<sup>114</sup>. Using this prior knowledge of CEP, the goal was to isolate and purify CEP from rich colon cell supernatant. Once purified sufficiently, the structural properties of the protein could be studied.

The research detailed in this chapter focused on the development a protein isolation strategy to purify CEP. The strategy used several chromatography methods to sequentially purify CEP. Throughout the isolation, the presence of CEP could only be tracked using enzyme-linked immunosorbent assays (ELISA) and western blot analysis due to the lack of structural knowledge. A three step isolation protocol was developed. First, CEP was purified based on size using gel filtration/size exclusion chromatography. Next, the isolated material from gel filtration was further purified using strong anion exchange chromatography. Last, the purified material from the first two steps was even further purified using hydrophobic interaction chromatography.

## **6.2 Experimental**

All solvents used were HPLC grade and reagents were of high purity (>95%). Water, sodium phosphate, sodium chloride, tris(hydroxymethyl)aminomethane (TRIS, 99.8%), hydrochloric acid, and ammonium sulfate were purchased from Sigma-Aldrich (USA). All mobile phases were prepared as described using a Fisher Scientific Accumet 950 pH meter, calibrated at time of use, to capture the pH. Protein molecular weight markers were purchased from Sigma-Aldrich as a kit (PN: MWGF1000). Marker solutions were prepared by dilution in water to ~2-3mg/mL. Colon cell supernatant was



received from Dr. Xin Geng as a solution of ~0.5mg/mL material in water. The concentration was kept equivalent throughout the purification at ~3mg/mL of the original mass.

All HPLC method development and analysis was performed on a Waters 2695 Alliance HPLC with a Waters 2996 Photodiode Array Detector (PDA). The liquid chromatography method for gel filtration used an Agilent Zorbax GF-250 6  $\mu$ m column, 4.6 mm x 250 mm. The samples were separated using an isocratic sequence. The mobile phase consisted of 50 mM Na<sub>2</sub>HPO<sub>4</sub> and 150 mM NaCl buffered to pH ~7, run over 60 minutes. The strong anion exchange method used a Sepax Proteomix SAX-NP3, 4.6 mm x 150 mm, 3 micron particle size column. The separation was achieved using gradient elution. The mobile phases consisted of 20 mM Tris-HCl buffered to pH 8 (A) and 'A' with 1M NaCl (B). The gradient condition was: 0–2 min, 0% B; 2–43 min, 0–100% B; 43–45 min., 100% B. The hydrophobic interaction chromatography method used a Thermo (Dionex) ProPac HIC-10, 4.6 x 100 mm column. The separation was achieved using gradient elution. The mobile phases consisted of 0.1 M sodium phosphate buffered to pH 7 (A) and 'A' with 2M ammonium sulfate (B). The gradient condition was: 0–2 min, 100% B; 2–43 min, 100–0% B; 43–45 min., 0% B. For all methods, fractions were collected and pooled manually.

De-salting, after strong anion exchange chromatography, was performed using the manufacturer protocol. The cartridges used were Zeba Spin Desalting Columns, 40K MWCO, 0.5mL sample size, purchased from Pierce. The de-salting after hydrophobic interaction chromatography was also performed according to manufacturer instructions using Amicon Ultra-4 50k NMWL molecular sieves, purchased from EMD Millipore.

All immunoassays were performed by Dr. Xin Geng at Robert Wood Johnson Medical School according to previously developed protocols<sup>28</sup>.

## **6.3 Results and Discussion**

### ***6.3.1 Size Exclusion/Gel Filtration Isolation***

Due to the lack of prior structural knowledge of CEP. The first isolation step performed was size exclusion/gel filtration chromatography. As previously discussed in Chapter 1, gel filtration chromatography separates molecules based on their effective size. The effective size of a molecule can be correlated to the molecular weight in molecules of a similar class. Since we know CEP is a protein of ~200 kDa molecular weight, gel filtration chromatography was the optimal method to begin with.

For this separation an analytical scale chromatography column was used. The column used was a Zorbax GF-250 column. This column contains wide-pore (150 angstrom), small particle-diameter silica spheres and is optimized for the size separation of water-soluble macromolecules having molecular weights up to 400 kDa, with the most linear separation range being between 10-250 kDa. The HPLC conditions were optimized using molecular weight protein markers. The mobile phase was buffered to maintain protein stability through the analysis. The developed method was initially used to capture the chromatographs of 7 protein molecular weight markers, as shown in Figure 45. The overlaid chromatographs, detected at 280 nm, show some resolution between the molecular weight markers. Although many of the markers are not baseline resolved from each other. The methodology of chromatographic gel filtration was not expected to have high separation efficiency<sup>115</sup>.

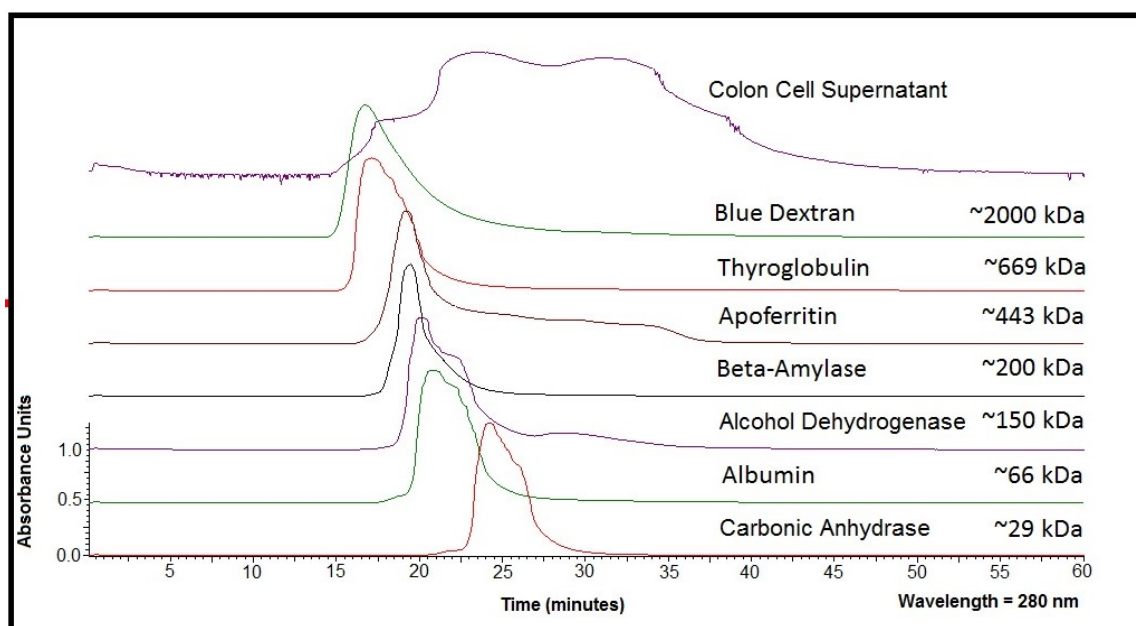


Figure 45: Gel filtration chromatographic overlay of protein molecular weight markers and colon cell supernatant.

Once the protein marker retention times were established an experiment was set-up to run the colon cell supernatant using the developed method. In this experiment, 50  $\mu$ L of  $\sim$ 3 mg/mL solution of colon cell supernatant was run using the developed method. Fractions were taken in 1 minute intervals, up to 30 minutes. The UV chromatograph of this run is shown in Figure 45. These fractions were analyzed for CEP using a sandwich ELISA immunoassay<sup>28</sup>. This immunoassay uses reactivity with the novel monoclonal antibody, mAb Das-1, to track the presence of CEP. The results of this analysis are shown in Figure 46. This bar graph shows the measured optical density (OD), at 600 nm, versus the elution time of the fractions collected. Also, shown are the OD of controls, positive and negative. From this study, it was concluded CEP elutes over a large time-frame,  $\sim$ 13-30 minutes. While the chromatograph of the protein markers (Figure 45) insinuate CEP was expected to elute primarily from 17-25 minutes. This difference may have been caused by CEP being over-concentrated during this analysis.

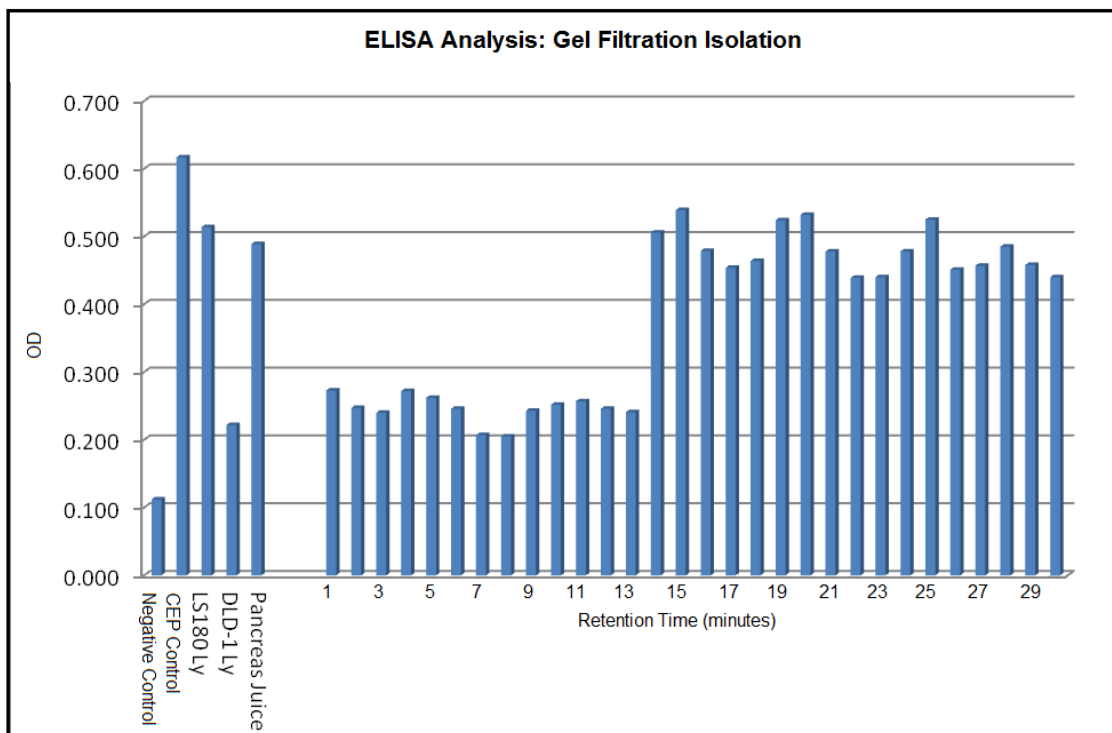


Figure 46: ELISA analysis of gel filtration fractions from separation of colon cell supernatant.

Another possibility is that several proteins in the supernatant have affinity for mAb Das-1. These results were positive. CEP was effectively retained, eluted, and tracked by ELISA throughout isolation by gel filtration. More colon cell supernatant was fractionated using the gel filtration method. Two major fractions were collected iteratively and pooled: a primary fraction (13-20 minutes) and a secondary fraction (20-27 minutes). These fractions were then concentrated by lyophilization.

### 6.3.2 Strong Anion Exchange Isolation

The next isolation step performed was an ion exchange chromatography method. In particular, an anion exchange chromatography method was developed to further isolate the purified fractions from gel filtration. Anion exchange chromatography separates proteins based on the overall surface charge differences<sup>73</sup>. The anion exchange chromatography column evaluated was a strong anion exchange column which consists

of non-porous silica particles with quaternary ammonium groups attached, Proteomix SAX NP3. In this separation it was expected that proteins with a more anionic surface character to interact more strongly to the particle surface. An increasing sodium chloride gradient would be used to elute the proteins. The elution order should correspond to the strength of this electrostatic interaction.<sup>116</sup>

Initially, a method was developed which utilized a sodium chloride gradient up to 500 mM. This method was buffered using 2-amino-2-hydroxymethyl-propane-1, 3-diol ("tris") hydrochloride to pH 8.

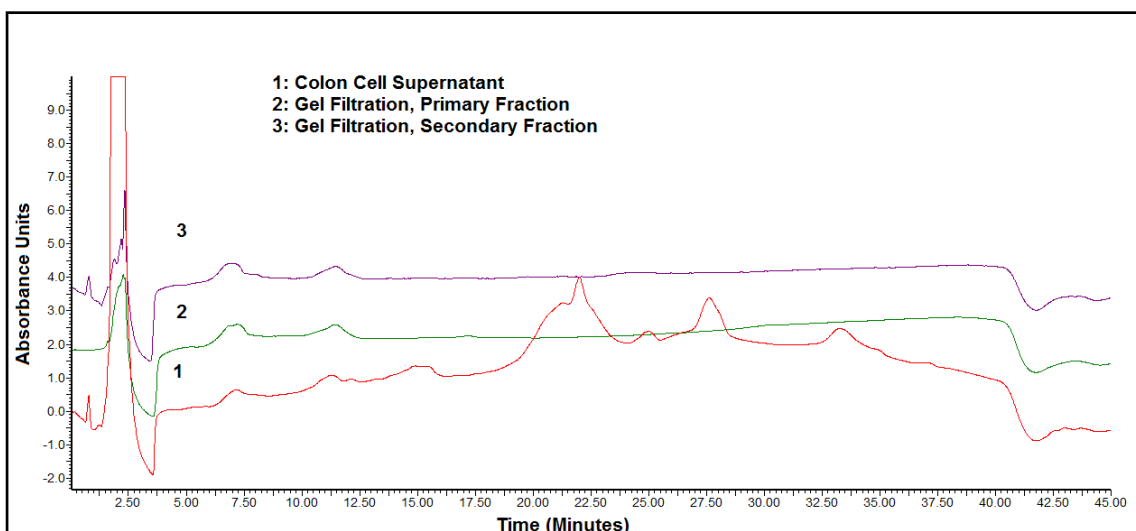


Figure 47: HPLC-UV chromatographs, at 280nm, of a strong anion exchange method separating 'gel filtration fractions' and colon cell supernatant.

The overlaid chromatographs of the colon cell supernatant and the isolated fractions from gel filtration are shown in Figure 47. These chromatographs demonstrate separation of various endogenous material in the colon cell samples. As many peaks are observed over the entirety of the run, 5-40 minutes. Comparing the colon cell supernatant (1) to the primary and secondary gel filtration pooled fractions (2 & 3) demonstrates the effectiveness of the previous, gel filtration, procedure. The gel filtration fractions were

visually ‘cleaner’ than the original cell supernatant sample. To determine the elution time of CEP, fractions were collected throughout the 3 chromatography runs in Figure 47. These fractions were de-salted and then analyzed by the developed ELISA immunoassay. The ELISA results are shown in Figure 48.

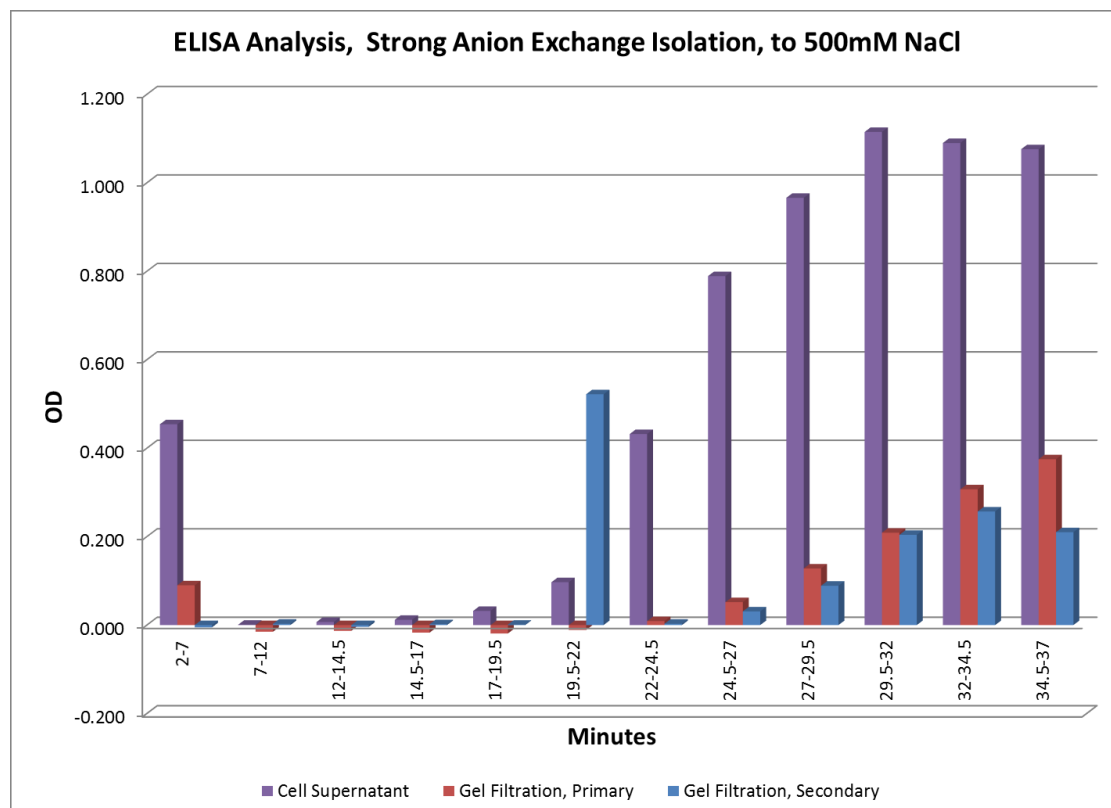


Figure 48: ELISA analysis of strong anion exchange (up to 500mM NaCl) fractions from separation of colon cell supernatant and gel filtration pooled samples.

The OD appears to increase in the primary and secondary fractions around 25 minutes and continues through 37 minutes. This increase correlates to the presence of CEP. These results demonstrate CEP was well retained using this method. However, the method needed to be optimized. It cannot be determined from the results in Figure 48 whether all the CEP was eluted during the chromatography run since the OD never returns to a baseline value over time.

To make sure all of the CEP retained was eluted during the analysis, the salt gradient was changed. The gradient was modified to go up to a 1M concentration of sodium chloride over ~40 minutes. This steeper gradient was expected to fully elute CEP and possibly provide better separation efficiency. A protein marker, alcohol dehydrogenase, was analyzed prior to the colon cell supernatant. An overlaid chromatograph of colon cell supernatant, alcohol dehydrogenase and water are shown in Figure 49.

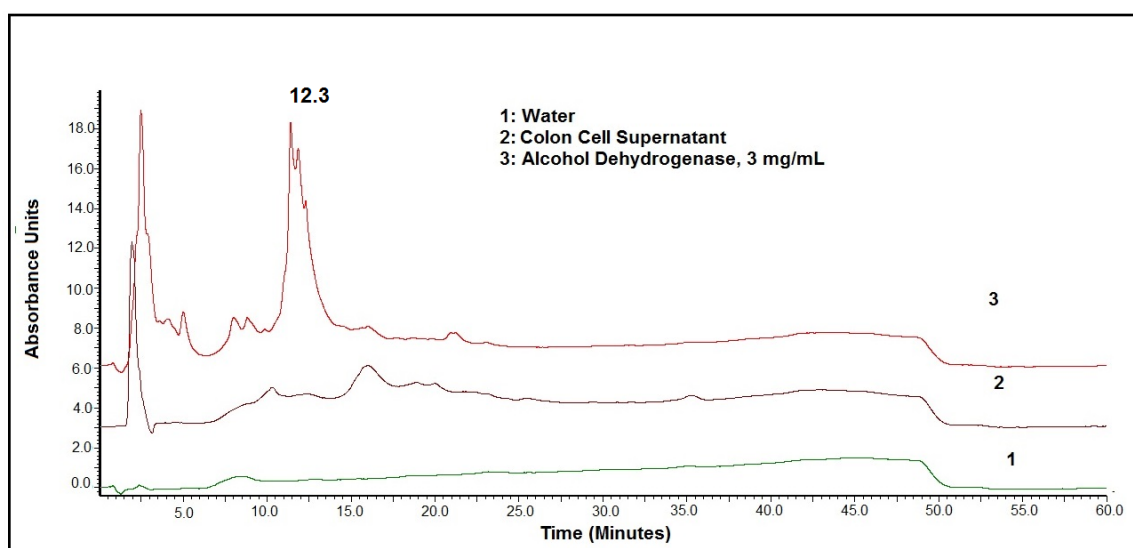


Figure 49: HPLC-UV chromatographs, at 280nm, of a strong anion exchange method (up to 1M NaCl) separating alcohol dehydrogenase and colon cell supernatant.

As observed alcohol dehydrogenase elutes at 12.3 minutes. This retention would be used later to track where CEP retains, relatively, over multiple runs. The chromatograph also shows separation of endogenous material in the colon cell supernatant, compared to the water control, as was demonstrated in Figure 47. Using this optimized method the colon cell supernatant, gel filtration (primary fraction), gel filtration (secondary fraction), and a 2x diluted gel filtration (secondary fraction) were fractionated in 2 to 3 minute intervals from 10 – 45 minutes. These fractions were de-salted and analyzed by the ELISA

immunoassay. The results are shown in Figure 50.

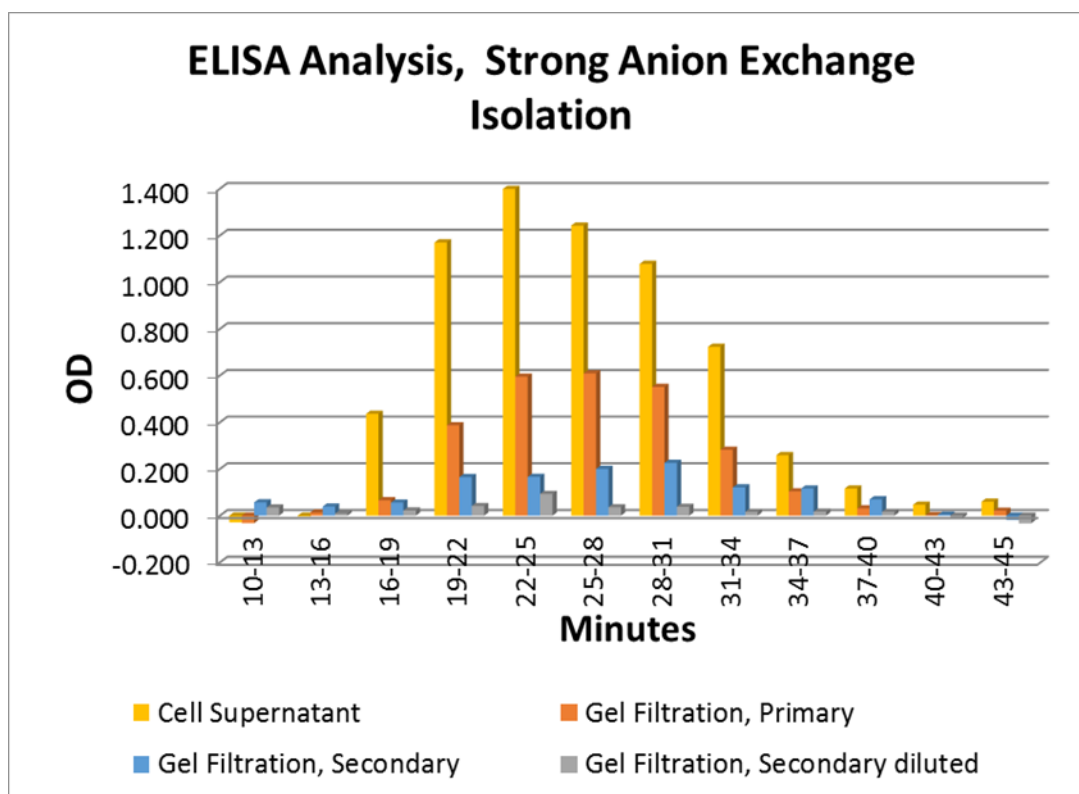
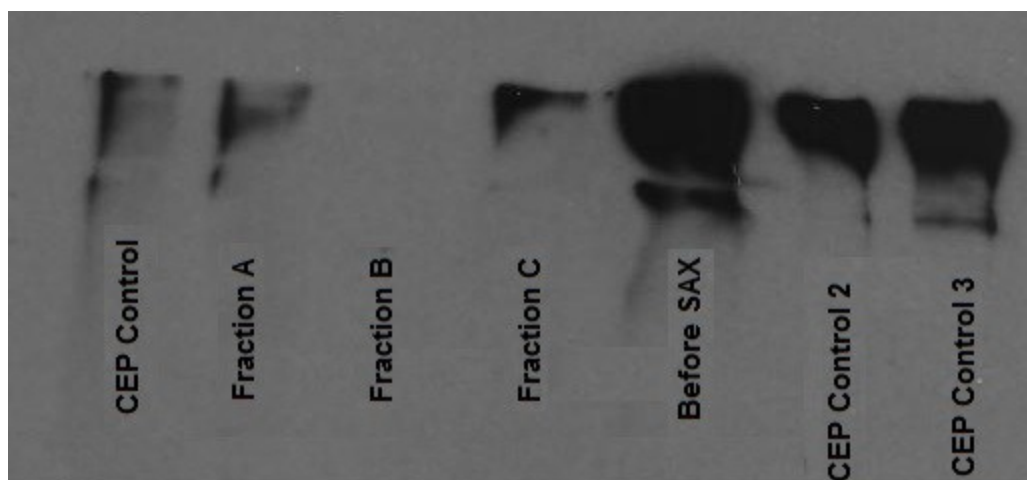


Figure 50: ELISA analysis of strong anion exchange (up to 1mM NaCl) fractions from separation of colon cell supernatant and gel filtration pooled samples.

As observed in the ELISA results, CEP was fully eluted using the optimized SAX method. The results indicate CEP was most prevalent between 19 and 31 minutes, according to the ‘Gel Filtration, Primary’ fraction. Following these results, the remaining ‘gel filtration, primary fraction’ sample was fractionated using the developed SAX method. Fractions were collected and pooled corresponding to the following retention time groups: 19-23 minutes (C), 23-27 minutes (A), and 27-31 minutes (B). These fractions were then analyzed by western blot analysis<sup>115</sup>. The results, shown in Figure 51, demonstrate fraction A and C have a positive assay for CEP while fraction B does





*Figure 51: Western blot analysis of the pooled fractions after strong anion exchange analysis (A, B, & C) compared to 'Before SAX' and controls.*

not. Although fraction B had a positive ELISA, western blot analysis is more specific for CEP. Western blot requires both molecular weight and affinity correlation for a positive CEP identification. Another observation (Figure 51), is the difference in the blot size between the 'Before SAX' and after, A & C. These fractions were kept at a constant concentration; yet, 'Before SAX' has a more obscure blot. This was noted.

Further analysis of the same isolated fractions was performed by silver staining<sup>117</sup>. CEP, being a glycoprotein, was not expected to undergo staining by the silver staining method used<sup>118</sup>. Silver staining was performed to determine the purity of the fractions collected, Figure 52. The three isolated fractions and the colon cell supernatant were analyzed at the same protein concentration. The figure indicates where CEP would be found if it underwent staining.

The results demonstrate some purification of CEP has been achieved in fractions A and C, through two steps of isolation. In these fractions, there was significantly less material

observed in silver staining versus the colon cell supernatant.

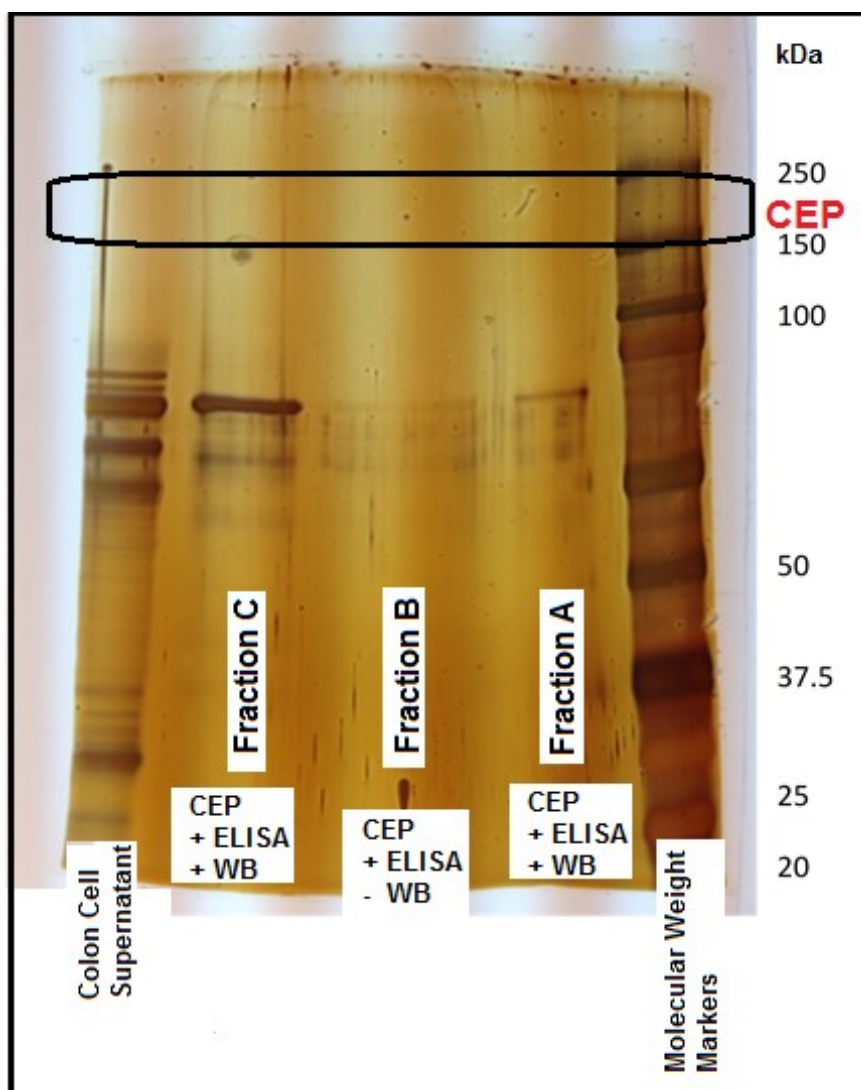


Figure 52: Silver staining after two isolation steps (A, B, & C) compared to the original colon cell supernatant.

### 6.3.3 *Hydrophobic Interaction Chromatography Isolation*

The final isolation method developed was a hydrophobic interaction chromatography (HIC) method. HIC separates biomolecules in a decreasing salt gradient, based on differences in surface hydrophobicity<sup>77-78</sup>. This method preserves the biological activity of proteins unlike another hydrophobic separation method, reverse-

phase chromatography. The HIC separation mechanism is complementary to gel filtration and ion-exchange chromatography. In this separation, the high salt concentration de-solvates the hydrophobic groups on the surface of proteins. The more surface hydrophobicity a protein has, the more de-solvation occurs, and the greater the interaction with the hydrophobic particle surface. As the salt concentration is decreased the proteins will elute in increasing order of hydrophobicity. With the most hydrophobic eluting later.

A Dionex ProPac HIC-10 column with 5  $\mu\text{m}$  spherical silica gel particles, with a 300 angstrom pore size, was used. The developed method was buffered to pH 8 with a 100 mM sodium phosphate buffer. A decreasing ammonium sulfate gradient, 2M – 0M, was used to elute the proteins. Initially, six protein markers were used to evaluate the separation efficiency of the method. Figure 53 shows an overlaid chromatograph of the

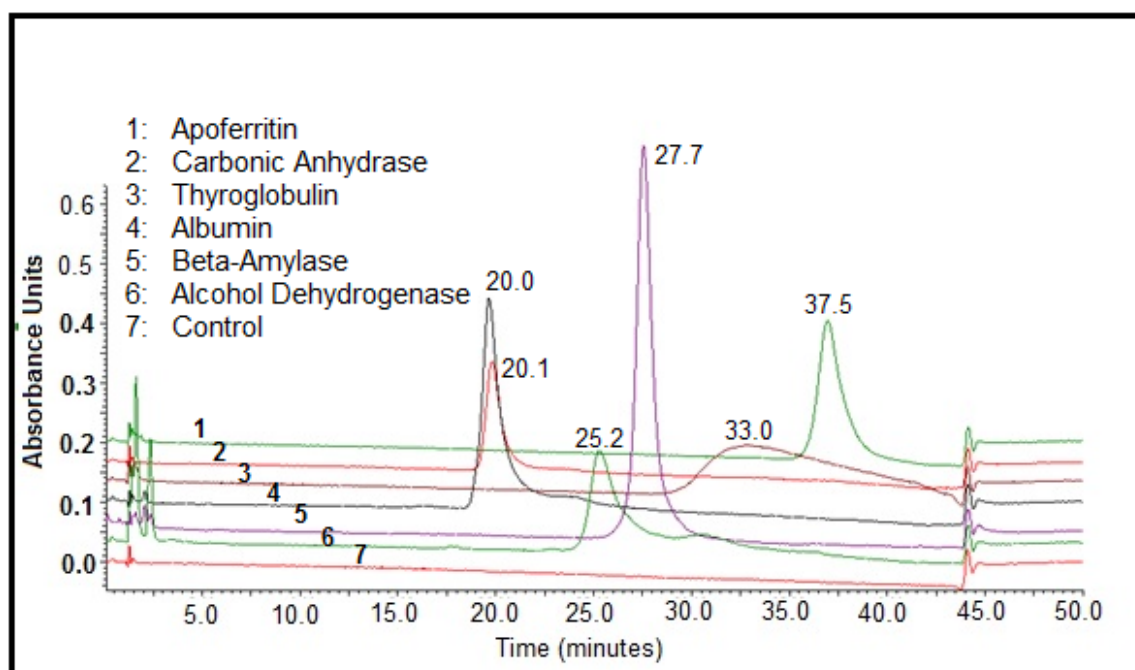


Figure 53: Overlaid chromatographs of protein markers separated by hydrophobic interaction chromatography, at 280 nm.

protein markers with a control (blank). As observed, the protein markers are separated

over a 25 minute range. The peak widths of several markers are less than 3 minutes, which demonstrates good efficiency ( $N > 700$ ) for several markers. The isolated fraction 'A' sample (Figure 51 & 52), processed through gel filtration and SAX, was analyzed using the developed HIC method. Fractions were collected in 2 minute intervals. These fractions were concentrated and de-salted using molecular sieve cartridges. The concentrated solutions were analyzed by sandwich ELISA. The results are in Figure

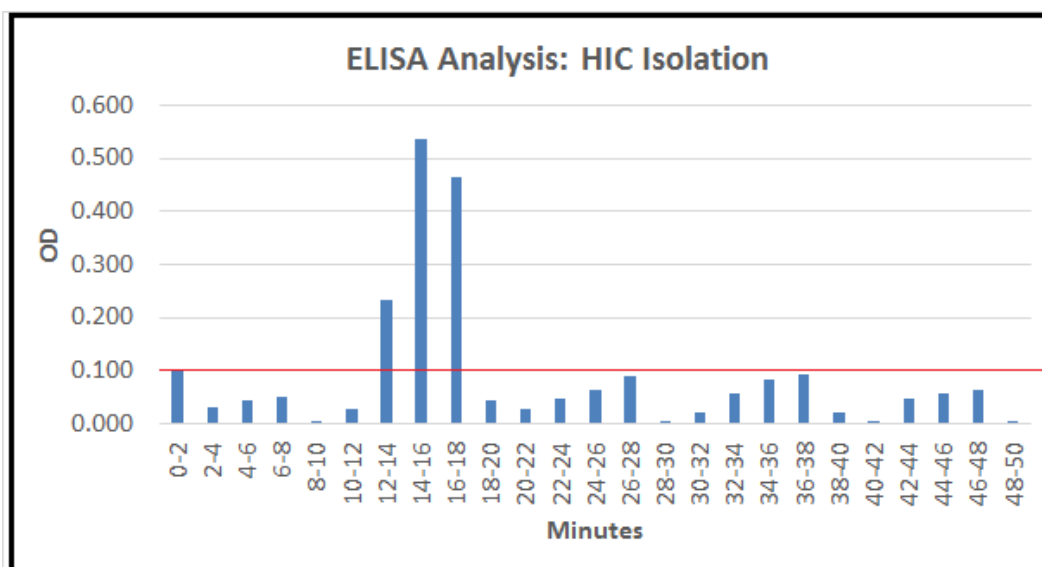


Figure 54: ELISA analysis of hydrophobic interaction chromatography fractions from separation of isolated fraction 'A' (CEP after two steps).

54. The red line in the bar graph represents the baseline, or the highest level of a negative control. As observed, CEP was isolated and elutes from 12-18 minutes. This earlier elution was expected. CEP previously demonstrated behavior of a glycoprotein. Glycoproteins are proteins with an oligosaccharide side chain(s) attached to a polypeptide<sup>119</sup>. The oligosaccharide group(s) can increase the hydrophilicity of the protein. If CEP is more hydrophilic than the protein markers the earlier elution would be explained. The HIC method of isolation was successful. CEP was again retained and fully eluted. Also, CEP was baseline resolved from the marker proteins.

## **6.4 Conclusion**

In this research, a three step isolation procedure was developed to purify an unknown colon epithelial protein from colon cell supernatant. The procedure effectively isolated CEP by size, overall surface charge (pI) and hydrophobicity. Throughout the procedure the presence of CEP was successfully tracked by a specific ELISA immunoassay. Western blot analysis was used to confirm the presence of CEP. Silver staining confirmed the isolated sample had less endogenous material. This procedure will be used to further research the properties and structural identity of CEP.

## REFERENCES

- 1 Watson, J. D., Crick F.H.C. *Nature* **1953**, 737-738.
- 2 Prados, J., et al. *BioDrugs* **2013**, 27, 317-327.
- 3 "Craig C. Mello - Facts". *Nobelprize.org*. Nobel Media AB 2013. Web.  
30 May 014.  
<[http://www.nobelprize.org/nobel\\_prizes/medicine/laureates/2006/mello-facts.html](http://www.nobelprize.org/nobel_prizes/medicine/laureates/2006/mello-facts.html)>
- 4 "Andrew Z. Fire - Biographical". *Nobelprize.org*. Nobel Media AB  
2013. Web. 30 May 2014.  
<[http://www.nobelprize.org/nobel\\_prizes/medicine/laureates/2006/fire-bio.html](http://www.nobelprize.org/nobel_prizes/medicine/laureates/2006/fire-bio.html)>
- 5 Huang, Y., et al. *Mol. Biol.* **2013**, 47, 465-475.
- 6 Muers, M. *Nat. Rev. Genet.* **2011**, 12, 742-743.
- 7 Maden, B. *Progr. Nucleic Acid Res. Mol. Bio.* **1990**, 39, 241-303.
- 8 Eddy, S.R. *Nat. Rev. Genet.* **2001**, 2, 919-929.
- 9 Mattick, J.S., Makunin, I.V. *Hum. Mol. Genet.* **2006**, 15, R17-R29.
- 10 Hinkle, D.C., Chamberlin, M.J. *J. Mol. Biol.* **1972**, 70, 157-185.
- 11 Murakami, K.S., et al. *Science* **2002**, 296, 1285-1290.
- 12 Goldman, S.R., Ebright, R.H., Nickels, B.E. *Science* **2009**, 324, 927-928.
- 13 Korzheva, N., et al. *Science* **2000**, 289, 619-625.
- 14 Lodish, H., Berk, A., Zipursky, S.L., et al. *Molecular Cell Biology*. 4th edition. New York: W. H. Freeman; **2000**. Section 11.1, Transcription Termination.
- 15 Richardson, J.P. *Biochim. Biophys. Acta.* **2002**, 1577, 251-260.
- 16 Nickels, B.E., Dove, S.L. *J. Mol. Biol.* **2011**, 412, 772-781.
- 17 Mechold, U., et al. *Nucleic Acids Res.* **2007**, 35, 4552-4561.
- 18 Whisstock, J.C., Lesk, A.M. *Quarterly Rev. of Biophys.* **2003**, 36, 307-340.
- 19 Alberts, B., Johnson, A., Lewis, J., et al. *Molecular Biology of the Cell*. 4th edition. New York: Garland Science; **2002**. Protein Function.
- 20 Davis, A.C., Roux, R.H., and Shulman, M.J. *Eur. J. Immunol.* **1988**, 18, 1001-1008.
- 21 Das, K.M., et al. *J. Immunol.* **1987**, 139, 77-84.
- 22 Marks, M., et al. *Gastroenterology* **1998**, 114, A1032.
- 23 Das, K.M. *Journal of Gastroenterology and Hepatology* 2004, 19, S290-S294.
- 24 Kesari, K. V., et al. *Clin. Exp. Immunol.* **1999**, 118, 219-227.
- 25 Badve, S., et al. *Pathobiology* **2000**, 68, 76-86.
- 26 Griffel, L.H., Amenta, P.S., Das, K.M. *Dig. Dis. Sci.* **2000**, 45, 40-48.
- 27 Mirza, Z. K., et al. *Gut* **2003**, 52, 807-812.
- 28 Das, K.K., et al. *Gut* **2013**, gutjnl-2013.
- 29 Barnes, J., ed. *High performance liquid chromatography*. Vol. 33. John Wiley & Sons, **1992**.

- 30 Lough, W.J., Wainer, I.W. eds. *High performance liquid chromatography: fundamental principles and practice*. CRC Press, 1995.
- 31 Ertürk, S., et al. *J. Pharm. Biomed. Anal.* **2003**, 33, 1017-1023.
- 32 Schafer, W.A., et al. *Org. Process Res. Dev.* **2007**, 11, 870-876.
- 33 Fett, J.W., et al. *Biochem.* **1985**, 24, 5480-5486.
- 34 Folta-Stogniew, E., Williams, K. *J. Biomol. Tech.* **1999**, 10, 51.
- 35 Barnes, J., ed. *High performance liquid chromatography*. Vol. 33. John Wiley & Sons, 1992.
- 36 Snyder, L.R., Kirkland, J.J., Glajch, J.L. *Practical HPLC method development*. John Wiley & Sons, 2012.
- 37 Pav, J.W., Rowland, L.S., Korpalski, D.J. *J. Pharm. Biomed. Anal.* **1999**, 20, 91-98.
- 38 Tessier, F., et al. *Int. J. Vitamin Nutrition Res.* **1995**, 66, 166-170.
- 39 Romani, A., et al. *Chromatographia* **1994**, 39, 35-39.
- 40 Helbock, H.J., et al. *Proc. Natl. Acad. Sci. U.S.A* **1998**, 95, 288-293.
- 41 Inagaki, S., Min, J.Z., Toyo'oka T. *Biomed. Chromatogr.* **2007**, 21, 338-342.
- 42 Wilson, I.D., et al. *J. Chromatogr., B* **2005**, 817, 67-76.
- 43 Fenn, J.B., et al. *Mass Spectrometry Reviews* **1990**, 9, 37-70.
- 44 Zubarev, R.A., Makarov, A. *Anal. Chem.* **2013**, 85, 5288-5296.
- 45 Wiley, W. C., McLaren, I.H. *Review of Scientific Instruments* **2004**, 26, 1150-1157.
- 46 Wilm, M.S., Mann, M. *Int. J. Mass Spectrom. Ion Proc.* **1994**, 136, 167-180.
- 47 "University of Bristol" Web. 30 May 2014  
<<http://www.chm.bris.ac.uk/ms/theory/esi-ionisation.html>>
- 48 Kebarle, P. *J. Mass Spectrom.* **2000**, 35, 804-817.
- 49 Fenn, J.B., et al. *Science* **1989**, 246, 64-71.
- 50 Apffel, A., et al. *Anal. Chem.* **1997**, 69, 1320-1325.
- 51 Beck, J. L., et al. *Mass Spectrom. Rev.* **2001**, 20, 61-87.
- 52 Steinwedel, H. U.S. Patent No. 2,939,952. 7 Jun. 1960.
- 53 Dawson, P. H. *Mass Spectrom. Rev.* **1986**, 5, 1-37.
- 54 Hager, J.W. *Rapid Commun. Mass Spectrom.* **2002**, 16, 512-526.
- 55 Prentice, B.M., et al. *Int. J. Mass Spectrom.* **2011**, 306, 114-122.
- 56 LoBrutto, R., Kazakevich, Y. *HPLC Pharm. Scientists* **2007**, 139-239.
- 57 Snyder, L.R., Kirkland, J.J., Glajch, J.L. *Practical HPLC method development*. John Wiley & Sons, 2012.
- 58 Guidance, Reviewer. *Center for Drug Evaluation and Research, Food and Drug Administration* **1994**, 669-671.
- 59 Alpert, A.J. *J. Chromatogr. A* **1990**, 499, 177-196.
- 60 Ikegami, T., et al *J. Chromatogr. A* **2008**, 1184, 474-503.
- 61 Buszewski, B., Noga, S. *Anal. Bioanal. Chem.* **2012**, 402, 231-247.
- 62 Liu, Y., Vailaya, A. *HPLC Pharm. Scientists* **2007**, 241-261.
- 63 Molnar, I., Horváth, C.S. *Clin. Chem.* **1976**, 22, 1497-1502.
- 64 Weiss, J. *Ion Chromatography*. John Wiley & Sons, 2008.

- 65 Hemström, P., Irgum, K. *J. Sep. Sci.* **2006**, 29, 1784-1821.
- 66 Snyder, L.R., Kirkland, J.J., Dolan, J.W. *Introduction to modern liquid chromatography*. John Wiley & Sons, 2011.
- 67 Dizdaroglu, M., & Hermes, W. *J. Chromatogr. A* **1979**, 171, 321-330.
- 68 McGinnis, A. C., Cummings, B. S., & Bartlett, M. G. *Anal. Chim. Acta* **2013**, 799, 57-67.
- 69 Gilar, M., Fountain, K. J., Budman, Y., Neue, U. D., Yardley, K. R., Rainville, P. D., & Gebler, J. C. *J. Chromatogr., A* **2002**, 958(1), 167-182.
- 70 Lindqvist, B., Storgårds, T. *Nature* **1955**, 511-512.
- 71 Hong, P., Koza, S., Bouvier, E.S.P. *J. Liquid Chromatogr. & Related Tech.* **2012**, 35, 2923-2950.
- 72 Margolis, S. *J. Lipid Res.* **1967**, 8, 501-507.
- 73 Peterson, E.A., Sober, H.A. *J. Am. Chem. Soc.* **1956**, 78, 751-755.
- 74 Yamamoto, S., Ishihara, T. *J. Chromatogr. A* **1999**, 852, 31-36.
- 75 Thayer, J. R., et al. *Anal. Biochem.* **2005**, 338, 39-47.
- 76 Hallgren, E., et al. *J. Chromatogr. A* **2000**, 877, 13-24.
- 77 Nair, A. J. *Principles of biotechnology*. Laxmi Publications, 2008.
- 78 Heinitz, Maxine L., et al. *J. Chromatogr. A* **1998**, 443, 173-182.
- 79 McCue, J.T. *Methods Enzymol.* **2009**, 463, 405-414.
- 80 Louris, J.N., et al. *Anal. Chem.* **1987**, 59, 1677-1685.
- 81 Ni, J., et al. *Anal. Chem.* **1996**, 68, 1989-1999.
- 82 McLuckey, S.A., Vaidyanathan, G., Habibi-Goudarzi, S. *J. Mass Spectrom.* **1995**, 30, 1222-1229.
- 83 Apffel, A., et al. *Anal. Chem.* **1997**, 69, 1320-1325.
- 84 Acharya, S. *Some Aspects of Physicochemical Properties of DNA and RNA*. (2006).
- 85 Sannes-Lowery, K.A., et al. *Journal of the American Society for Mass Spectrometry* 8.1 (1997): 90-95.
- 86 McLuckey, S.A., Van Berker, G.J., Glish, G.L. *J. Am. Soc. Mass Spectrom.* **1992**, 3, 60-70.
- 87 Goldman, S.R., et al. *Mol. Cell* **2011**, 42, 817-825.
- 88 Datta, A. K., Niyogi, K. *J. Bio. Chem.* **1975**, 250, 7313-7319.
- 89 Campbell, E.A., et al. *Cell* **2001**, 104, 901-912.
- 90 Vvedenskaya, I.O., et al. *Genes Dev.* **2012**, 13, 1498-1507.
- 91 Gilar, Martin. *Anal. Biochem.* **2001**, 298, 196-206.
- 92 Fang, M., et al. *Nucleic Acids Res.* **2009**, 37, 5114-5125.
- 93 Srivastav, R., et al. *Nucleic Acids Res.* **2014**, 425.
- 94 Yamana, Kazushige, et al. *Angew. Chem.* **2001**, 113, 1138-1140.
- 95 Bajad, S.U., et al. *J. Chromatogr. A* **2006**, 1125, 76-88.
- 96 Wu, J., McLuckey, S.A. *Int. J. Mass Spectrom.* **2004**, 237, 197-241.
- 97 Boschenok, J., Sheil, M.M. *Rapid Commun. Mass Spectrom.* **1996**, 10, 144-149.
- 98 ICH Harmonised Tripartite Guideline. Validation of Analytical Procedures: Text and Methodology; 2005, ICHQ2(R1).



- 99 Annesley, T. M. *Clin. Chem.* **2003**, *49*, 1041-1044.
- 100 Mandeles, S., Kammen, H.O. *Anal. Biochem.* **1966**, *17*, 540-544.
- 101 Yanes, O., et al. *Anal. Chem.* **2011**, *83*, 2152-2161.
- 102 Simm, R., et al. *Anal. Biochem.* **2009**, *386*, 53-58.
- 103 Jessome, L. L., Volmer, D. A. *LCGC N. Am.* **2006**, *24*, 498-510
- 104 Van Eeckhaut, A., et al. *J. Chromatogr. B* **2009**, *877*, 2198-2207.
- 105 Thurman, E.M., Mills, M.S.. *Solid-phase extraction: principles and practice*. Vol. 16. New York: Wiley, 1998.
- 106 Fritz, J.S. *Analytical solid-phase extraction*. New York: Wiley-Vch, 1999.
- 107 Gilar, M., Bouvier, E.S.P. *J. Chromatogr. A* **2000**, *890*, 167-177.
- 108 Llorca, M., et al. *J. Chromatogr. A* **2009**, *1216*, 7195-7204.
- 109 Fontanals, N., Marcé, R.M., Borrull, F. *J. Chromatogr. A* **2007**, *1152*, 14-31.
- 110 Beier, R.C., Greenblatt, G.A. *J. Liquid Chromatogr.* **1981**, *4*, 515-524.
- 111 FDA Guidance for Industry Bioanalytical Method Validation; U.S. Department of Health and Human Services, 2001.  
<http://www.fda.gov/cder/guidance/index.htm>.
- 112 Small, P. et al. *J. Bacteriol.* **1994**, *176*, 1729-1737.
- 113 Sezonov, G., Joseleau-Petit, D., D'Ari, R.. *J. Bacteriol.* **2007**, *189*, 8746-8749.
- 114 Work by Dr. Xin Geng. Robert Wood Johnson Medical School.
- 115 Kato, Y., et al. *J. Chromatogr. A* **1980**, *190*, 297-303.
- 116 Pfeiffer, G., et al. *Biomed. Chromatogr.* **1990**, *4*, 193-199.
- 117 Merril, C.R., Goldman, D., Van Keuren, M.L..*Methods Enzymol.* **1983**, *96*, 230-239.
- 118 Sasse, J., Gallagher, S.R. *Curr. Prot. Mol. Biol.* **2003**, *10*, 6.
- 119 Toor, B., et al. *Throm. Res.* **1982**, *26*, 317-328.